From sea to land: Characterization and shoreline analysis of an Arctic paraglacial coastal system undergoing forced regression, Arviat, Nunavut

by

© Benjamin Bagnall

A thesis submitted to the

School of Graduate Studies

in partial fulfillment of the requirements for the degree of

Master of Science

Geography Department

Memorial University of Newfoundland

October 2021

St John's, Newfoundland

ABSTRACT

This study assesses the form, materials, and evolution of a paraglacial Arctic coastline undergoing forced regression. It is based on the analysis of field and remote-sensing data within the municipal boundary of Arviat, Nunavut, western Hudson Bay. Arviat is part of an extensive emergent glacial and marine sedimentary plain. Discrete reaches of the municipal foreshore and backshore are characterized by form and material. Analysis of historical shoreline change confirmed that shoreline advance was more prevalent than retreat within the study area between 1960 and 2011. However, shoreline retreat was also observed despite forced regression conditions, particularly around the east-facing portion of the headland. The principle forcing agent for shoreline change is interpreted as forced regression, but coastal dynamics are also playing a role in shoreline evolution. This study contributes to the understanding of coastal evolution in a forced regression environment and the characterization of an understudied Canadian Arctic coastal environment.

ACKNOWLEDGEMENTS

I would first like to thank my supervisors, Dr. Don Forbes and Dr. Trevor Bell. Thank you for your dedication and perseverance throughout this process. I am grateful for the opportunity, your guidance, and the many lessons learned working with you.

Thank you to the residents of Arviat, and, in particular, to Shirley Tagalik and the members of the Arviat Wellness Centre for their generosity and hospitality throughout the project. To Bob Chapple and the Government of Nunavut Lands and Planning Office (Community and Government Services), and 3vGeomatics for the ideas and data shared. To Johnathan Carter, Robert Deering, Jonathan Roger, Andrew Kuksuk and Ancilla Irkok for their assistance in the field.

I would also like to acknowledge funding support from ArcticNet, the Northern Scientific Training Program, Memorial University, the Canadian Northern Economic Development Agency and the Government of Nunavut. As well, thanks to the Nunavut Research Institute, Arctic College, and the Arviat Wellness Centre for logistical support.

Finally, to my family, thank you for your boundless love and support. I will always strive to remember and follow the example you have given of who one should strive to be. After all, it is more beautiful, more good, and more just to remember the best of life.

TABLE OF CONTENTS

LIST OF FIGURES

LIST OF ABBREVIATIONS

DEM	digital elevation model
dGPS	differential Global Positioning System
GIA	glacial isostatic adjustment
GMSL	global mean sea level
HWL	high-water line
LGM	Last Glacial Maximum
RSL	relative sea level

LIST OF APPENDICES

CO-AUTHORSHIP STATEMENT

I am lead author on all components of the thesis. Dr. Donald Forbes and Dr. Trevor Bell, my supervisors, provided invaluable input and guidance throughout the entire research and writing process.

As part of the production of this thesis, I performed a literature review to discern knowledge gaps in our understanding of the Arviat environment and regions which share its underlying conditions. From that point, I outlined the research objectives and led two field seasons to acquire relevant data for addressing these knowledge gaps. I then analyzed and synthesized this data and linked it to the knowledge gaps and research questions during the writing process. This thesis is the culmination of those efforts. My supervisors helped guide my understanding of the opportunities for scientific work in the region, form the available data and field work results into a scientific story, secure funding for the project, and they provided input throughout the writing process.

CHAPTER 1: INTRODUCTION

1.1 Research context

The key forcing agent underlying assumptions of regional and local shoreline advance and diminishing coastal hazard exposure in the central Canadian Arctic is falling relative sea level (RSL; Hart and Long, 1996; Shaw et al., 1998a). As opposed to generalized global mean sea level (GMSL) change (Church et al., 2013), RSL change refers to sea level change relative to the local land surface, which can diverge from GMSL trends depending on local variables.

RSL change is the product of both terrestrial and marine factors, impacted by either changing water levels, vertical crustal (or land surface) motion, or both. RSL change naturally impacts the position of the local shoreline through time and space. A coastal environment undergoing rising RSL will experience local shoreline retreat inland over sufficient time scales, a process called ‘marine transgression’. A shoreline advancing seaward due to falling RSL, on the other hand, is undergoing a process known as ‘forced regression’ (Fig 1.1; Curray, 1964; Posamentier et al., 1992; Catuneanu, 2002). This is not to be confused with shorelines which advance seaward due to prograding sedimentary deposits, known as ‘marine regression’.

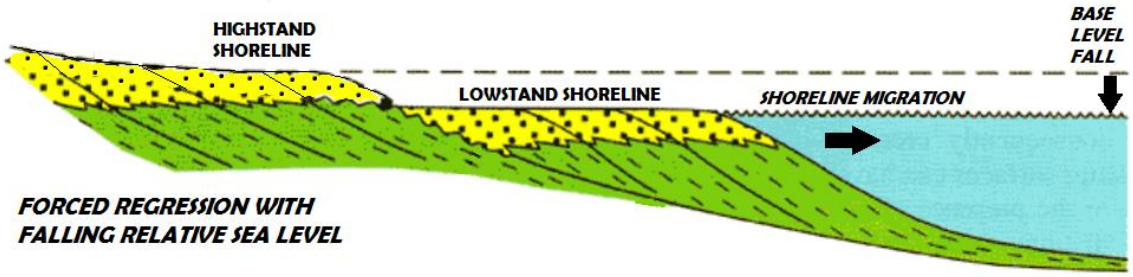

Figure 1.1: Forced regression, the migration of the shoreline seaward due to base level fall (modified from Posamentier et al., 1992).

Falling RSL is the most important potential mitigating factor for coastal processes related to recent record lows in circum-Arctic sea-ice extent, thickness and duration, and stronger, more persistent wave action (Comiso et al., 2008; Lantuit and Pollard, 2008; Forbes, 2011a; Asplin et al., 2012). These trends combined with warming-induced permafrost thaw and ground-ice volume reduction underlie increases in circum-Arctic and Canadian Arctic shoreline erosion rates, flood risk and subsequent hazard exposure in northern communities (Forbes, 2011a; Lantuit et al., 2011). However, when the coastal environment is undergoing forced regression at a sufficient rate, these trends can be reversed on local and regional scales (Shaw et al., 1998a).

The principal driver of RSL change in Arctic environments is the recent glacial history of the region (Shaw et al., 1998a; James et al., 2014). Although GMSL has risen approximately 92 mm between 1960 and 2010 (Church et al., 2013), many areas in Canada are still experiencing RSL fall due to the extent of glacio-isostatic depression under continental ice sheets up to 3 km thick during last glacial maximum (LGM; Simon

et al., 2011). The subsequent isostatic adjustment, causing uplift that continues today, drives the migration of the wave base downslope, abandoning the nearshore to the foreshore and the foreshore to the backshore with sufficient time.

In those places where ice thickness was greatest, as was the case in the central Canadian Arctic (Dyke, 2004), forced regression has played a key role in recent landscape and coastal evolution (Boisson and Allard, 2020). The stratigraphic succession in forced regression is typically deeper marine units overlain by shallow-marine deposits overlain by coastal facies. For example, in the Lac Saint-Jean region of eastern Quebec, Nutz et al. (2015) documented a stratigraphic succession from glaciomarine to marine to shallow-marine sediments, the shallowing marine units interpreted primarily as the result of forced regression due to glacioisostatic uplift. In eastern Hudson Bay, Fraser et al. (2005) observed a more complicated stratigraphy of downstepping wedges of coarser deposits unconformably overlying finer marine units, in a forced-regressive setting with excess accommodation space, which is the space available for sediment deposition. The unconformity was interpreted as the base of wave erosion and re-working. Such sedimentary sequences are consistent with existing models of forced regression (Posamentier et al., 1992).

The forced regression conditions of the central Canadian Arctic coincide with extensive paraglacial coastal environments (Forbes and Syvitski, 1994). In general, paraglacial environments are defined by a shift from deglacial sediment abundance to postglacial scarcity as the sediment is re-worked by nonglacial processes (Forbes, 2011b). Within a

coastal environment, reworking of glacigenic sediment can be initiated through changes in sea level and shoreline migration. The deglacial landforms which frame these paraglacial environments are largely a product of the most recent and final flow trend of glacial ice, either flow-parallel or -perpendicular depending on the landform and process in question (Benn and Evans, 2010). As a result, the shorelines produced often have a high fractal dimension (Boisson and Allard, 2020). In the context of forced regression, these paraglacial sediment sources are continuously activated by the downslope migration of the wave base over time. This continuous activation of novel paraglacial sediment sources has the potential to further mitigate coastal vulnerability in these environments.

Through the next century, as GMSL accelerates (IPCC, 2021), the regions of James Bay, Hudson Bay, Foxe Basin, Hudson Strait and northern areas of the Canadian Arctic Archipelago are all expected to persist as forced regression environments due to continuous isostatic uplift outpacing regional sea level rise (James et al., 2021). In principle, forced regression is synonymous with shoreline advance (Posamentier et al., 1992). However, erosion and shoreline retreat have been documented in unconsolidated forced regression environments (e.g. Ruz and Beaulieu, 1998). It is possible that rates of sediment removal and shoreline erosion can outstrip the rate at which the shoreline is abandoned due to RSL fall, even in areas of rapid glacioisostatic uplift.

It is largely due to our understanding of the principles of forced regression that much of the Arctic coastal zone is hypothesized to be at relatively low risk of hazard exposure moving forward (Shaw et al., 1998b; Lemmen and Warren, 2016). These assumptions

require testing at local temporal and spatial scales suitable for engineering and planning (Wright and Tom, 1994; Forbes et al., 2014). This information is particularly important for the many coastal communities in the Arctic otherwise bearing the brunt of the effects of regional environmental change (Ford et al., 2010).

One of the least studied coastal environments in Canada is the western coast of Hudson Bay, where RSL fall is expected to mitigate the negative impacts of eustatic sea level rise on a decadal timescale (James et al., 2011). This knowledge gap exists even though several communities are located along the coast of western Hudson Bay, one of which (Churchill, MB) contains one of the few Arctic seaports in Canada. There is little published information on the region's coastal forms and the trends and rates of local shoreline change. Without an understanding of how the coastline has behaved in the recent past, or an inventory of the landforms shaping the current coastline, the assumption that relative sea level fall will sufficiently reduce local and regional coastal sensitivity remains untested. This study seeks to begin to address this knowledge gap through an inventory of the coastal forms and materials within the municipal boundary of Arviat, Nunavut, and a survey of historical shoreline change surrounding the townsite. The research findings underpin an assessment of the processes which factor into the ongoing evolution of this emergent Arctic coastal environment.

1.2 Study area

The hamlet of Arviat is situated on the western coast of Hudson Bay. It is part of an extensive emergent sedimentary plain found roughly 90 km north of the treeline and underlain by continuous permafrost (Brown et al., 2001), a layer of ground that remains at or below 0^{o}C for two or more years (van Everdingen, 1998). It is the most southerly community in Nunavut, connected to surrounding communities by boat in the summer, sea-ice in the winter, and by plane year-round. The nearest neighbouring communities are Whale Cove and Rankin Inlet, located 100 km and 215 km, respectively, to the north in Nunavut, and Churchill, 260 km to the south in Manitoba.

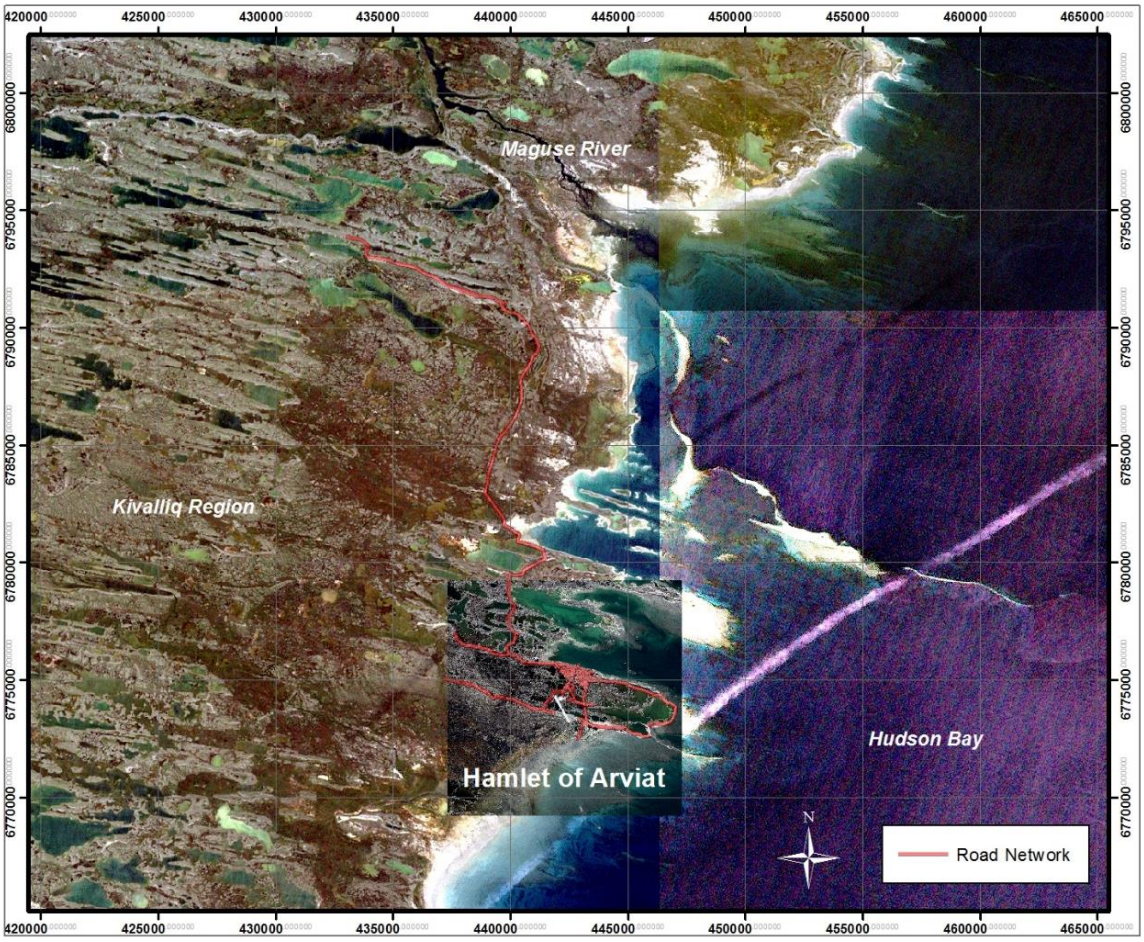

Figure 1.2: Hamlet of Arviat, Kivalliq Region, Nunavut, located on a prominent point extending east into Hudson Bay (contains material ©Digital Globe, 2011).

During the LGM, a thick cover of glacial ice overlay western Hudson Bay and the local Arviat environment (Dyke, 2004). This was part of the Keewatin ice dome, a primary dispersal centre of the Laurentide Ice Sheet covering northeastern North America (Clark et al., 2009). The general regional trend of ice movement during the Wisconsinan glaciation was a shift from southwesterly ice flow during glacial onset, to various degrees

of southeasterly ice flow at LGM, and finally to easterly flow during deglaciation (McMartin et al., 2004).

Maximum regional ice depth and extent occurred approximately 26.5 cal ka BP (Clark et al., 2009). The ice sheet slowly began to collapse and retreat towards a shifting central ice divide, located approximately 650 km west of Arviat, in the modern Kivalliq region of Nunavut. Approximately 17 cal ka BP, this process of ice retreat accelerated as the climate continued to warm (Dyke et al., 2002). Glaciofluvial activity was locally intense during this time of ice-sheet thinning, warming and receding, the prominent eskers framing the local Arviat shoreline and landscape being the primary evidence of this activity (Arsenault et al., 1981). Evidence for retreating glacial margins is provided by recessional moraines where, within the larger trend of glacial retreat, glacial sediment was dumped in N-S aligned ridges during interludes of margin stasis and possible re-advance (Shilts et al., 1976).

Approximately 10 cal ka BP, ice retreat accelerated still further due to the opening of Hudson Strait and the subsequent incursion of the marine environment (Dyke, 2004). The incipient Tyrrell Sea further buoyed the thinning and shrinking Keewatin Ice Dome and created shifting tidewater glacial margins along the paleo-shoreline. Further inland, the regional ice divide began a pattern of migration towards the southeast until the ice sheet disappeared around 7 cal ka BP (Dyke, 2004). Arviat and the surrounding area then

emerged from an offshore marine environment to the terrestrial environment of today through crustal uplift and forced regression (Simon et al., 2014).

1.3 Materials and Methods

A combination of data acquisition via field surveys and observations and data analysis using ArcGIS software, remote sensing data, and digital topography, was used to characterize the Arviat coastal environment and shoreline behaviour.

The form and material of the backshore (supratidal) and foreshore (intertidal) zones was documented, organized, and stored within a Coastal Information System maintained by the Geological Survey of Canada (Sherin and Edwardson, 1996; Couture et al., 2015). The classification used was based on field data obtained through the shoreline surveys mentioned above, as well as field observations of the municipal shoreline. These data and observations were combined in turn with analysis of remote sensing imagery, which provided complete shoreline characterization within the municipal boundary. These observations and classifications were combined to subdivide a subset of the Arviat shoreline, centred around the peninsula underlying the modern community, into quasi-homogenous reaches.

The calculation of shoreline change rates was undertaken using the Digital Shoreline Analysis Software (DSAS) add-on to ArcGIS v10 (Thieler et al., 2009). Comparing the historical 1960 shoreline with the quasi-modern 2011 shoreline positions, rates and direction of shoreline position change were obtained.

Differential geographic positioning system (dGPS) surveys were used to obtain precise shore-normal and shore parallel profiles from which to base observations and analysis. These surveys were completed in August 2014 during low tide. Transects were prioritized from comparing remote sensing imagery according to both areas of shoreline change and with an eye for representative sites from all distinct coastal environments present. Shore-parallel beach berm and edge-of-vegetation transects were also completed, marking the limit of active coastal processes.

The degree to which calculated shoreline position change diverged from the shoreline position change predicted by RSL change alone was used to determine the relative extent that coastal dynamics factor into shoreline evolution. RSL change between 1960 and 2011 was transposed onto the shore normal survey profiles obtained on-site and used to generate planform shoreline change predicted by RSL alone (forced regression). These results were then compared to the actual shoreline position change calculated above to determine the extent to which sediment was added or removed from the shoreline.

Longer term historical shoreline change was simulated using a digital elevation model (DEM) courtesy of 3vGeomatics® (Vancouver, BC) and the local RSL curve (Simon et al., 2014), the local evolution of sea level height over time. Although this historical shoreline change could not take historic coastal dynamics into account, it is illustrative of the evolutionary process which the Arviat shoreline has undergone over the last 1 ka.

1.4 Thesis Outline

The thesis contains a central manuscript (Chapter 2), supplemented by the preceding introduction (Chapter 1) and a concluding chapter (Chapter 3). The manuscript is presented as a thesis chapter, but it contains the principal components of a standard journal paper.

The manuscript chapter (Chapter 2) elaborates on the processes and findings of the scientific study of an Arctic emergent paraglacial sedimentary plain. This study finds that while the principles of forced regression explain much of the coastal evolution of the region, local shoreline dynamics still play an important role in local shore-zone evolution and, in some areas, override expected shoreline advance due to forced regression.

Chapter 3 summarizes the results of the study and considers ways in which the research has contributed to our scientific understanding of forced regression environments, as well as ways the research could be supplemented or improved moving forward.

1.5 References

Arsenault, L., Aylsworth, J.M., Cunningham, C.M., Kettles, I.M. & Shilts, W.W. (1981). Surficial geology, Eskimo Point, District of Keewatin; Geological Survey of Canada, Preliminary Map 8-1980, scale 1:125 000.

Asplin, M.G., Galley, R., Barber, D.G., & Prinsenberg, S. (2012). Fracture of summer perennial sea ice by ocean swell as a result of Arctic storms. *Journal of Geophysical Research: Oceans*, 117(C6).

Benn, D.I., & Evans, D.J.A. (2010). *Glaciers and Glaciation*. 802 pp. Arnold, London, U.K.

Brown, J., Ferrians, O.J., Jr., Heginbottom, J.A. & Melnikov, E.S. (2001). Circum-Arctic map of permafrost and ground ice conditions. National Snow and Ice Data Center, digital media, URL - gsg.uottawa.ca/data/open/svgmetadata/circum-arctic.pdf

Church, J.A., Clark, P.U., Cazenave, A., Gregory, J.M., Jevrejeva, S., Levermann, A., Merrifield, M.A., Milne, M.A., Nerem, R.S., Nunn, P.D., Payne, A.J., Pfeffer, W.T., Stammer, D., & Unnikrishnan, A.S. (2013). Sea level change. *Climate change*, pp. 1137-1216.

Catuneanu, O. (2002). Sequence stratigraphy of clastic systems: concepts, merits, and pitfalls. *Journal of African Earth Sciences*, 35(1), 1-43.

Clark, P.U., Dyke, A.S., Shakun, J.D., Carlson, A.E., Clark, J., Wohlfarth, B., Mitrovica, J.X., Hostetler, S.W., & Mccabe, A.M. (2009). The Last Glacial Maximum. *Science*, 325, 710-4.

Comiso, J.C., Parkinson, C.L., Gersten, R., & Stock, L. (2008). Accelerated decline in the Arctic sea ice cover. *Geophysical Research Letters*, 35(1), LO1703.

Curray, J.R. (1964). Transgressions and regressions. In: R.L. Miller (ed.) *Papers in Marine Geology:* New York, Macmillan, pp. 175-203.

Dyke, A. S. (2004). An outline of North American deglaciation with emphasis on central and northern Canada. In Gibbard, P.L. & Ehlers, P. (eds.) *Quaternary Glaciations: Extent and Chronology*, Amsterdam, Boston, pp. 373-424.

Dyke, A.S., Andrews, J.T., Clark, P.U., England, J.H., Miller, G.H., Shaw, J., & Veillette, J.J. (2002). The Laurentide and Innuitian ice sheets during the last glacial maximum. *Quaternary Science Reviews*, 21(1–3), 9-31.

Fraser, C., Hill, P., & Allard, M. (2005). Morphology and facies architecture of a falling sea level strandplain, Umiujaq, Hudson Bay, Canada. *Sedimentology*, 52(1), 141-160.

Forbes, D.L. (editor). (2011a). State of the Arctic Coast 2010 – Scientific Review and Outlook. International Arctic Science Committee, Land-Ocean Interactions in the Coastal Zone, Arctic Monitoring and Assessment Programme, International Permafrost Association. Helmholtz- Zentrum, Geesthacht, Germany, 178 p. http://arcticcoasts.org

Forbes, D.L. (2011b) Glaciated Coasts. In: Wolanski E. and McLusky D.S. (eds.) *Treatise on Estuarine and Coastal Science*, Vol 3, pp. 223–243. Waltham: Academic Press.

Forbes, D.L., Bell, T., James, T.S., & Simon, K.M. (2014). Reconnaissance assessment of landscape hazards and potential impacts of future climate change in Arviat, southern Nunavut. *Summary of Activities 2013*, Canada-Nunavut Geoscience Office, pp. 183–192.

Ford, J.D., Bell, T., & St-Hilaire-Gravel, D. (2010). Vulnerability of community infrastructure to climate change in Nunavut: a case study from Arctic Bay. In Community Adaptation and Vulnerability in Arctic Regions (G.K. Hovelsrud & Barry Smit, Eds.). Springer, Dordrecht, 107-130.

Hart, B.S., & Long, B.F. (1996). Forced regressions and lowstand deltas: Holocene Canadian examples. *Journal of Sedimentary Research*, 66(4).

IPCC, (2021): *Climate Change 2021: The Physical Science Basis. Contribution of Working Group I to the Sixth Assessment Report of the Intergovernmental Panel on Climate Change* [Masson-Delmotte, V., P. Zhai, A. Pirani, S.L. Connors, C. Péan, S. Berger, N. Caud, Y. Chen, L. Goldfarb, M.I. Gomis, M. Huang, K. Leitzell, E. Lonnoy, J.B.R. Matthews, T.K. Maycock, T. Waterfield, O. Yelekçi, R. Yu, and B. Zhou (eds.)]. Cambridge University Press. In Press.

James, T.S., Henton, J.A., Leonard, L.J., Darlington, A., Forbes, D.L., & Craymer, M., (2014). Relative Sea level Projections in Canada and the Adjacent Mainland United States; Geological Survey of Canada, Open File 7737, 72 p. doi:10.4095/295574

James, T.S., Robin, C., Henton, J.A. and Craymer, M. (2021). Relative sea-level projections for Canada based on the IPCC Fifth Assessment Report and the NAD83v70VG national crustal velocity model. Geological Survey of Canada, Open File 8764, 1 zip file, https://doi.org/10.4095/327878

Lantuit, H., & Pollard, W. H. (2008). Fifty years of coastal erosion and retrogressive thaw slump activity on Herschel Island, southern Beaufort Sea, Yukon Territory, Canada. *Geomorphology*, 95(1), 84-102.

Lantuit, H., Overduin, P.P., Couture, N., Wetterich, S., Aré, F., Atkinson, D., Brown, J., Cherkashov, G., Drozdov, D., Forbes, D.L., Graves-Gaylord, A., Grigoriev, M., Hubberten, H.W., Jordan, J., Jorgensen. T., Ødegård, R.S., Ogorodov, S., Pollard, W.H., Rachold, V., Sedenko, S., Solomon, S., Steenhuisen, F., Streletskaya, I & Vasiliev, A. (2012). The Arctic Coastal Dynamics database: A new classification scheme and statistics on Arctic permafrost coastlines. *Estuaries and Coasts*, 35(2), 383-400.

Lemmen, D.S. & Warren, F.J. (2016). Synthesis. In Lemmen, D. S., Warren, F. J., James, T. S. & Mercer Clarke, C. S. L. (eds.) *Canada's Marine Coasts in a Changing Climate*, Government of Canada, Ottawa, ON, 17-26

McMartin, I., Henderson, P.J., Roy, A., Richard, P., Wolfe, S., & Plouffe, A. (2004). Evidence from Keewatin (Central Nunavut) for Paleo-Ice Divide Migration. *Géographie Physique Et Quaternaire*, 58(2-3), 163-186.

Mitrovica, J.X., Gomez, N., Morrow, E., Hay, C., Latychev, K., & Tamisiea, M.E. (2011). On the robustness of predictions of sea level fingerprints. *Geophysical Journal International*, 187(2), 729-742.

Nutz, A., Ghienne, J., Schuster, M., Dietrich, P., Roquin, C., Hay, M., Bouchette, F., & Cousineau, P. (2015). Forced regressive deposits of a deglaciation sequence: Example from the Late Quaternary succession in the Lake Saint-Jean basin (Québec, Canada). *Sedimentology*, 62(6), 1573-1610.

Posamentier, H.W., Allen, G.P., James, D.P., & Tesson, M. (1992). Forced regressions in a sequence stratigraphic framework: concepts, examples, and exploration significance (1). *AAPG Bulletin*, 76(11), 1687-1709.

Ruz, M-H., & Beaulieu, N. (1998). Érosion littorale le long d'une côte en émersion rapide: Détroit de Manitounuk, Canada. *Annales De Géographie*, 107(600), 160-178.

Shaw, J., Taylor, R.B. Forbes, D.L., Ruz, M-H., & Solomon, S. (1998a). Sensitivity of the Coasts of Canada to Sea-Level Rise. Geological Survey of Canada, Bulletin 505, 79 p. +map.

Shaw, J., Taylor, R.B., Solomon, S., Christian, H.A., & Forbes, D.L. (1998b). Potential impacts of global sea-level rise on Canadian coasts. *The Canadian Geographer/Le Géographe canadien*, 42(4), 365-379.

Shilts, W.W., Kettles, I.M. & Arsenault, L. (1976). Surficial geology, southeast Keewatin; Geological Survey of Canada, Open File 356, 28 p

Simon, K.M., James, T.S., Forbes, D.L., Telka, A.M., Dyke, A.S., & Henton, J.A. (2014). A relative sea-level history for Arviat, Nunavut, and implications for Laurentide Ice Sheet thickness west of Hudson Bay. *Quaternary Research*, 82(1), 185-197.

Van Everdingen, R.O. (1998). *Multi-language glossary of permafrost and related ground-ice terms*. Arctic Institute of North America, University of Calgary.

Wright, L.D. & Thom, B.G. (1977). Coastal depositional landforms: a morphodynamic approach. *Progress in Physical Geography*, 1(3), 412-459.

CHAPTER 2: PARAGLACIAL SHORELINE ADJUSTMENT UNDER FORCED REGRESSION: A CASE STUDY FROM ARVIAT, NUNAVUT

Abstract

This study assesses the multitemporal stability of an Arctic coastline undergoing forced regression driven by glacial isostatic crustal uplift. The coastal environment of Arviat, Nunavut, on the west coast of Hudson Bay, is part of an emergent Arctic glacial and marine sedimentary plain. The topography and sedimentology of the emerging paraglacial shoreline, including a peninsula with shallow basins between prominent esker ridges projecting seaward, play an important role in the geomorphological development of the coast. Discrete reaches of the foreshore and backshore are characterized according to form and material. The coastal environment is dominated by tidal flats, sand and gravel beaches, and sand and gravel supratidal ridges. These classifications are supported by coastal topographic surveys at 19 locations. On the decadal scale, analysis of shoreline change since 1960 was completed using air photographs and satellite imagery, confirming the prevalence of shoreline seaward advance driven by falling relative sea level. On the centennial scale, shoreline adjustment is considered over the past 1000 years using regional sea-level change imposed on a digital elevation model. Retreat was observed locally, particularly around the east-facing headland, and coastal reworking of glacigenic deposits has formed spits and dunes along the southern shore. This is among the first studies to explicitly consider the geomorphic response to paraglacial sediment remobilization on an emergent coast. The rate of local sea-level lowering (land emergence) may slow substantially in coming decades as climate change drives

accelerated global sea-level rise. This, combined with a reduction in annual sea ice, may lead to more energetic net wave action at the coast. In this situation, the Arviat coast may exhibit more widespread shoreline retreat.

2.1 Introduction

The circum-Arctic coast has witnessed record lows in sea-ice extent, thickness and duration, stronger and more persistent wave action, and coastal destabilization linked to permafrost thaw, ground-ice melt and subsurface volume loss since the turn of the century (Comiso et al., 2008; Lantuit and Pollard, 2008; Forbes, 2011a; Asplin et al., 2012). These widespread trends fuel enhanced shoreline erosion rates and increased flood risk and hazard exposure in northern communities (Forbes, 2011a; Lantuit et al., 2012). In some regions, however, factors such as local sea-level lowering and abundant paraglacial sediment sources may mitigate these adverse changes on local scales, particularly in areas of rapid coastal uplift (Shaw et al., 1998a). Whether the assumptions that underlie such expectations of reduced shoreline retreat and hazard exposure have been appropriately tested is an important question for northern communities and researchers.

Relative sea level (RSL) change is the change of base level on the local scale relative to the land surface and may not always be consistent with global mean sea level (GMSL) change. Falling relative sea level (RSL) is one of the key factors underlying assumptions of shoreline advance and, thus, diminishing local and regional coastal hazard exposure in

regions such as northwest Russia, Norway, and northern Greenland (Fig 2.1; Hart and Long, 1996; Shaw et al., 1998a; Møller et al., 2002; Sanjuame and Tolgensbakk, 2009; Mason, 2010). The principal driver of RSL change in Arctic environments is the regional glacial history and associated glacio-isostatic adjustment (GIA; Simon et al., 2014). This imprint factors into several processes, including global mean and regional sea level change, gravitational fingerprinting resulting from mass changes in regional ice sheets (e.g. Greenland; Mitrovica et al., 2011) and vertical crustal motion resulting from the changing ice load (James et al., 2014, 2021; Robin et al., 2020), with a relaxation scale of thousads of years.

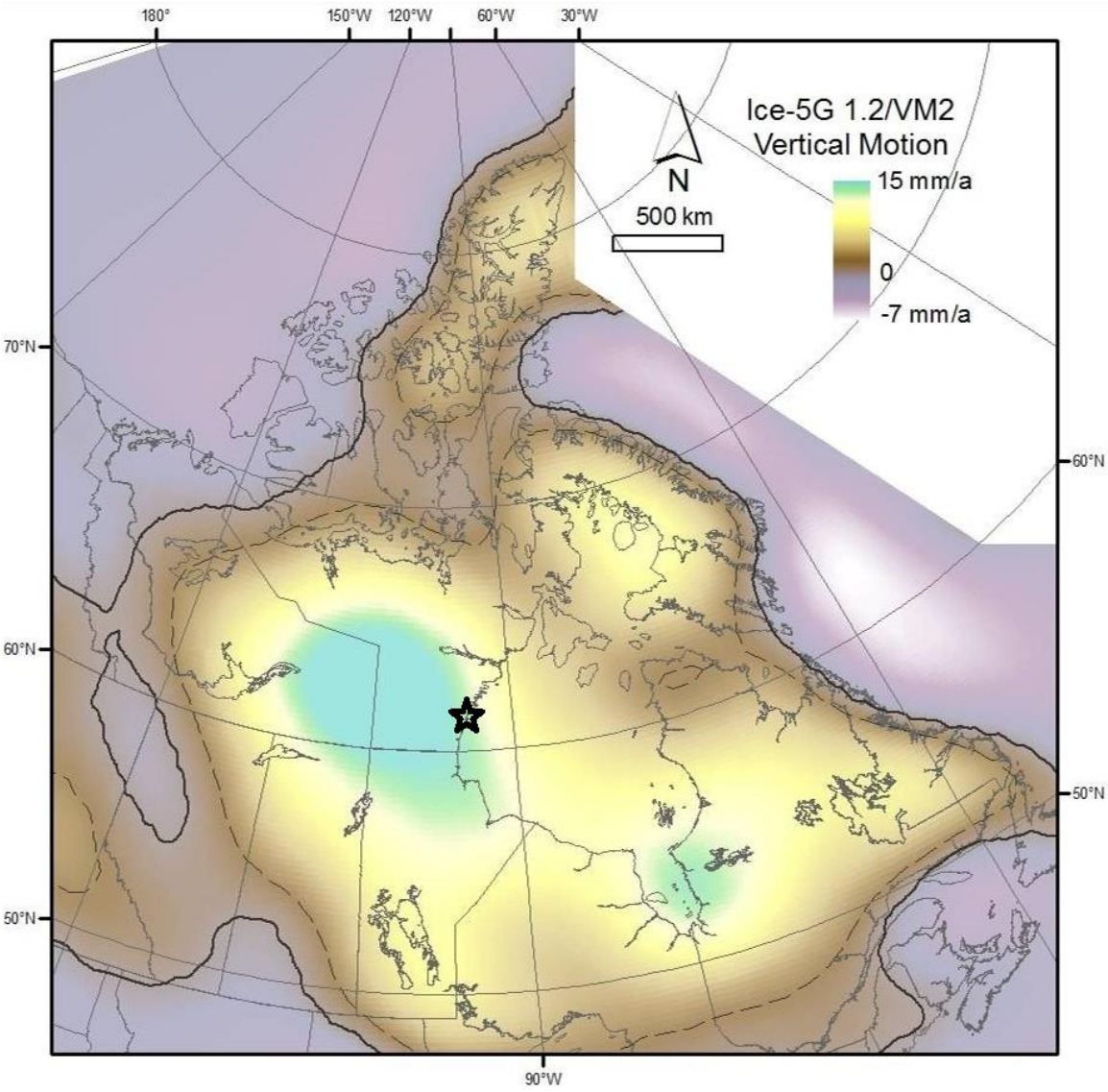

Figure 2.1: Rates of crustal uplift (average past 500 years, in mm yr−1) from glacial isostatic adjustment (GIA) predicted by the ICE-5G 1.2/VM2 model for the Canadian Arctic (Peltier, 2004). Solid line represents zero vertical motion due to GIA, broken line delineates uplift at 2 mm yr^{-1}. Star indicates location of Arviat, Nunavut. Courtesy: Gavin Manson, GSC-Atlantic, 2016.

The central Canadian Arctic continues to rebound due to GIA at a relatively rapid rate, to the extent that although global mean sea level has risen approximately 92 mm between 1960 and 2010 (Church et al., 2013), many areas in central Canada are still experiencing

rapid RSL fall. The rate of emergence is up to 10.00 mm/yr at Baker Lake NU, 11.86 mm/yr at Peawanick ON, and 12.77 mm/yr at Kuujuarapik QC; at Churchill MB, 260 km south of Arviat, the rate is 10.34 mm/yr (James et al., 2014). These rates stem from crustal uplift that is driven by GIA (Fig 2.1; Simon et al., 2014). As RSL falls, areas of previously submerged seafloor become exposed, a geological process called marine regression. Specifically, marine regression due to falling base (sea) level, rather than changes in sediment supply, is defined as 'forced regression' (Curray, 1964; Posamentier et al., 1992; Catuneanu, 2002).

Many parts of the central Canadian Arctic are expected to continue to experience forced regression through the next century, stemming from rapid GIA exceeding anticipated local sea-level rise (Fig. 2.1; James et al., 2015). Forced regression is synonymous with shoreline advance over sufficient time scales (Posamentier et al., 1992). As RSL falls, the high-water line (HWL) necessarily moves downslope and seaward, producing both vertical and horizontal shoreline migration. Simultaneously, novel sources of sediment may be activated through the migration of the wave base to previously deeper areas, promoting a dynamic sediment transport environment (Fraser et al., 2005; St. Hilaire-Gravel et al., 2010).

In places where glacial loading was greatest and most persistent, forced regression has played the largest relative role in recent landscape and coastal evolution (Dyke, 2004). In

Arctic Canada, the most rapid RSL fall is occurring along the coasts of Hudson Bay, and the resulting forced regression of the shoreline is expected to mitigate the impacts of global mean sea-level rise on a decadal timescale (James et al., 2014). However, few coastal studies have been undertaken in the region, even though several communities and Canada's principal Arctic seaport (Churchill, MB) are located along this coast.

Shoreline response is not necessarily simple or linear on human timescales, even in the face of rapid forced regression. These coasts still experience a suite of zonal (cold-climate) and azonal shore-zone processes (rate of RSL change, sea ice, wave climate, sediment source-sink dynamics, and basin characteristics) that shape the specific local shoreline response (Hart and Long, 1996; Lavoie et al., 2002). Shifting morphodynamics can result in non-linear evolutionary sequences as the coastal zone and relevant conditions shift through time as well (Cowell and Thom, 1994; Forbes et al., 1995). In certain circumstances, erosion has been observed in forced regressive environments, linked with factors such as fine-grained sediment shorelines, freeze-thaw processes, and energetic wave and storm surge activity (Ruz et al., 1998; Forbes et al., 2018). Even when forced regression of coarse sedimentary shorelines fuels general seaward shoreline migration, shifting patterns of erosion and deposition are seen on the local scale (St. Hilaire-Gravel et al., 2010). It is possible, and under the right conditions probable, that rates of sediment removal and shoreline erosion can outstrip the rate at which the shoreline migrates due to RSL fall.

The impacts of forced regression on the coastal environment therefore require further testing at local temporal and spatial scales suitable for community engineering and planning (Cowell and Thom, 1994; Forbes et al., 2014a). This information is particularly important for the many coastal communities in the Arctic that are responding to the effects of regional environmental change (Ford et al., 2010). This study addresses the knowledge gap in shoreline response to forced regression on human timescales through an inventory of coastal morphology within the municipal boundary of Arviat and a survey of historical shoreline change surrounding the townsite. The study documents the recent evolution of this coastal environment undergoing forced regression, and the high spatial variability of local short-term shoreline response.

2.2 Study area

The hamlet of Arviat (formerly known as Eskimo Point) is located at 61°09'N, 94°14'W, in the Kivalliq Region of Nunavut, on the western coast of Hudson Bay. A traditional meeting place for Caribou Inuit, the hamlet was formally established in the mid-20th century, with built-infrastructure concentrated on the northern section of 'Nuvuk', the unofficial but conventional local name for the prominent peninsula that extends east into Hudson Bay (Fig. 2.2). 'Nuvuk' remains to this day an ideal access point to the marine environment for travel and harvesting activities. The hamlet lies roughly 90 km north of the treeline and is underlain by continuous permafrost (Brown et al., 2001), a layer of ground that remains at or below 0°C for two or more years (van Everdingen, 1998).

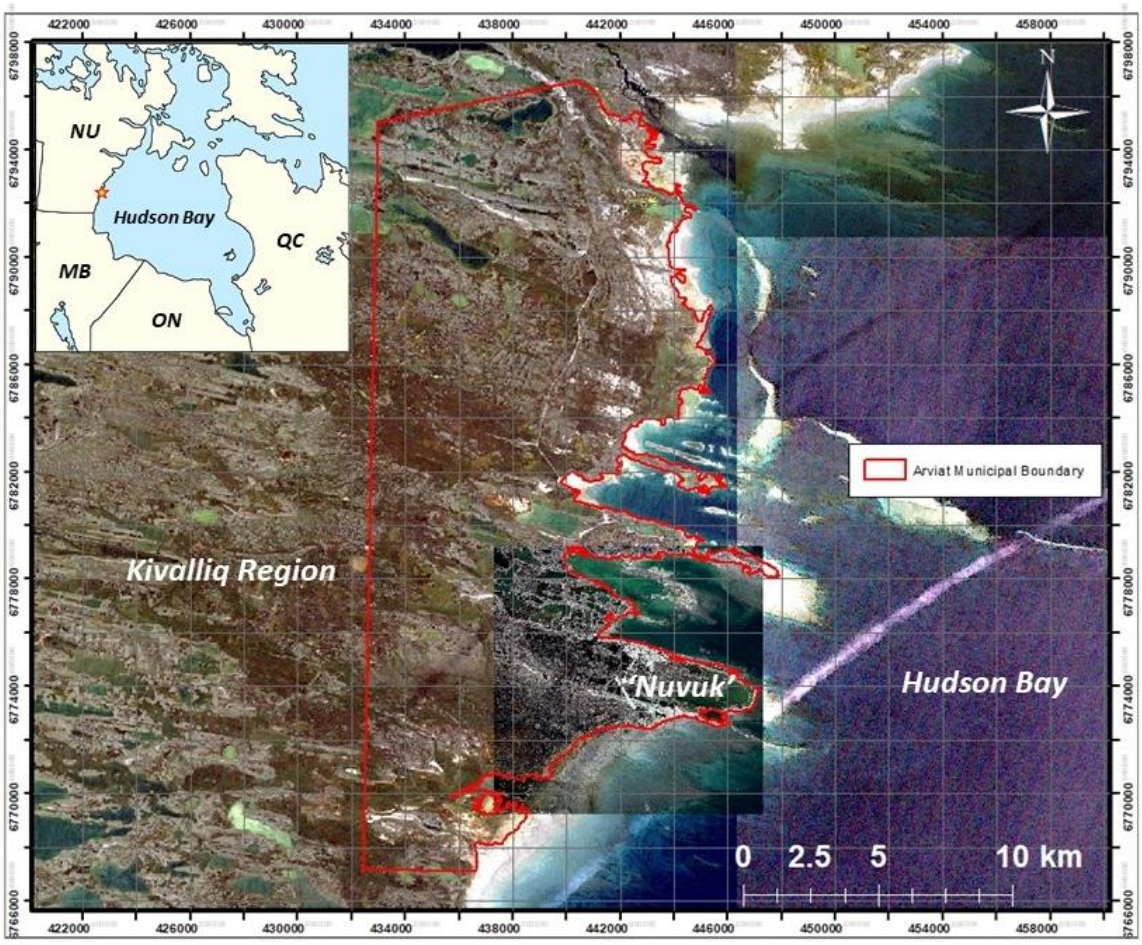

Figure 2.2: Hamlet of Arviat, Kivalliq Region, Nunavut, situated on a prominent point ('Nuvuk') extending east into Hudson Bay. Inset of Hudson Bay and surrounding area, with Arviat indicated by a star. Grey grid (Universal Transverse Mercator) provides georeference information and scale (2 km interval). Backdrop is orthorectified, 15-m resolution, panchromatic Landsat 7 images (2005). The 10 x 10 km area covering the immediate community is orthorectified, 0.5 m resolution, panchromatic WorldView-2 satellite imagery, courtesy of the Department of Community and Government Services, GN (contains material ©Digital Globe, 2011).

The community abuts a shallow bay to the north accessed by community members through many small, informal boat landings scattered along the hamlet beachfront. Infrastructure directly on the beachfront includes a large, central community dock and a

barge landing ramp at the eastern edge of the community. The barge landing is used for resupply by an annual sealift, which brings much of the community's non-perishable food, building materials, and other bulk goods. To the west of the community, two freshwater reservoirs sourced from nearby 'Wolf River' lie adjacent to the intertidal zone and along the principal road leading to the hinterland. There are also 42 community buildings, mostly private residences, along the hamlet waterfront facing the harbour to the north. Some of these buildings are almost adjacent to the foreshore/backshore boundary, on the edge of active coastal processes.

The Arviat shoreline is ice-locked for roughly 9 months of the year, although recent regional trends point to a delay of freeze-up and a lengthening open-water season (Scott and Marshall, 2010; Allard et al., 2014; Ford et al., 2016). It is a meso-tidal environment, semidiurnal with a 3.9 m spring tidal range (CHS, 2021). Climatological records for Arviat are sparse (1984-2007 for most variables). Records from Rankin Inlet to the north highlight the cold winters in the region, with average air temperatures from -25 to -38 °C between December and March, and mild summers, with average air temperatures in July and August approximately 11 °C (Environment Canada, 2018). Mean annual air temperature has increased at a rate of 0.12 °C/year from 1986 to 2012, with the greatest increases in the fall and early winter (Allard et al., 2014).

Arviat is underlain by the Canadian Shield, the ancient continental core of North America, specifically within the Hearne Domain of the Western Churchill Province. To the north, Neoarchean bedrock is exposed, mostly tonalite with minor elements of diorite (Tella et al., 2007). Within the Arviat municipal boundary bedrock is only exposed in isolated areas, mostly near the airport, where Proterozoic dark grey paragneiss with quartz lenses has been shaped by glacial processes into smoothed whaleback forms (Forbes et al., 2014a).

In the late Quaternary the regional geomorphology was dominated by continental ice sheets and related processes. Glacial ice sat atop 'Nuvuk' and the surrounding region for the majority of the last 100 ka. During the last glacial maximum (LGM), approximately 18 000 radiocarbon years before present (ka BP), local ice-sheet thickness is estimated to have been greater than 3 km, some of the thickest ice-cover experienced in North America during the Wisconsinan glaciation (Dyke et al., 2002). The last glacial flow, stemming from the nearby Keewatin Ice Divide, was toward the east, indicated by flutes and drumlins formed within the Maguse Lake Ice Stream (Aylsworth and Shilts, 1989; McMartin et al., 2021) and the Keewatin Ice Sheet had withdrawn entirely from the region by approximately 7.2 ka BP (8.1 ka calibrated; Dalton et al., 2020).

The depressed post-glacial landscape was immediately inundated by the Tyrrell Sea, a deglacial marine body that occupied modern Hudson Bay as well as much of the

surrounding land. Regional RSL at the onset of marine incursion is estimated to have been as much as 170 m higher than present, with the shoreline as far as 150 km inland of the modern coast (Dyke, 2004). Since the marine incursion, the crust has rebounded (uplifted) at a rate and extent commensurate with the deep crustal depression experienced during the LGM. Vertical adjustment continues to this day and into the future, with present-day crustal uplift rate at Arviat at 9.3 ±1.5 mm/yr (Simon et al., 2014). This modern rate extrapolates to 83.7 ±13.5 cm uplift between 2010 and 2100.

2.3 Materials and Methods

The following approaches were used to understand and illustrate coastal forms, configuration, and shoreline behaviour. Coastal characterization was undertaken to describe the form and material of the modern shoreline and to subdivide the coastal environment into quasi-homogenous reaches. Shoreline position change from 1960 to 2011 was documented and then analyzed within the context of RSL fall. Palaeoshoreline configuration and evolution over the past millennium of RSL fall was reconstructed using a digital elevation model.

Coastal classification was undertaken using the terminology and data-entry framework of the Coastal Information System (CIS), a linked relational database (Oracle®) and geographic information system (ESRI® ArcGIS) maintained by the Geological Survey of Canada (GSC; Sherin and Edwardson, 1996; Couture et al., 2015). Within this

framework, specific and relevant attributes, interpreted from remote sensing and in-situ data, were appended to one-dimensional segments of a continuous reference line representing the coastline. These attributes were used to characterize the form and material of the backshore (supratidal) and foreshore (intertidal) zones. The classification was applied at the scale of the municipal boundary, covering the highly indented coast from 8 km to the south to 20 km to the north of the townsite. Within a smaller focus area close to the community, (from the southern embayment, around the 'Nuvuk' peninsula, and along the Arviat waterfront to the head of the harbour), eight quasi-homogeneous shore segments were defined as a basis for more detailed geomorphological analysis (Figs. 2.3 and 2.4).

Shoreline change rates were calculated using the Digital Shoreline Analysis Software (DSAS) add-on to ArcGIS v10 (Thieler et al., 2009). Differences between the 1960 and 2011 shoreline position were determined from air photographs and satellite imagery using the two-dimensional (2D) high water line (HWL). The HWL was interpreted using a combination of the vegetation line, marine flora washup limits, and clastic beach crest indicators as necessary. This interpretation was cross referenced with in-situ measurements taken during field work. The indicators were mapped using geo-referenced 1960 air photographs (National Air Photo Library, flight line A17162, frames #3-10, 13–20, 25–31; RMS error range of 0.578–2.931 m) and a 2011 orthorectified, 0.5 m resolution, panchromatic WorldView-2 satellite image. The DSAS analysis generated 280 transects around the peninsula at 50 m spacing.

To obtain 2D, shore-normal profiles of the 'Nuvuk' shoreline, differential geographic positioning system (dGPS) surveys were completed from 10 to 14 August, 2014 using an SP80 GNSS Base/Rover System and Magellan ProMark 500 GPS receivers. The GPS transect locations were selected to target areas of change observed between historical air photographs and recent satellite imagery and to obtain representative data from all sedimentologically and morphologically distinct shoreline reaches. Shore-normal profiles were surveyed using discrete, 5-point averaged coordinates. Data points were taken at one to two metre intervals across sections of rapidly changing elevation (e.g., beach crests) and approximately every five metres across sections with relatively constant elevation (e.g., tidal flats). Shore-parallel beach berm and edge-of-vegetation transects were completed using continuous dGPS data logging collected on foot, for rapid data acquisition over hundreds of metres to kilometres. In total, 18 shore-normal transects were surveyed (Fig. 2.4) in addition to alongshore profiles in the lower foreshore and along the HWL.

The results from the shoreline change analysis and shore-normal survey profiles were combined to evaluate the net historical sediment removal or deposition at profile locations. The estimated RSL change over the 51-year period between 1960 and 2011 was taken from Simon et al. (2014). From measured 2011 HWL, the vertical RSL change was hindcast along the shore-normal profiles to determine the estimated historical HWL position attributable to RSL change alone. This captured the extent of horizontal shoreline position change directly attributable to vertical movement of HWL downslope, in other

words forced regression. This was then compared with the 1960 photogrammetric HWL to determine whether net sediment accretion or removal had occurred. Assuming negligible change in upper profile geometry, where the mapped 1960 shoreline was further inland than the RSL-projected shoreline, this indicates sediment deposition (i.e., the shore zone must have gained sediment volume for the 2011 shoreline to have progressed as far seaward as it has); where the mapped 1960 shoreline is seaward of its projected position, this indicates sediment removal (i.e., the shore zone must have lost sediment volume to have not progressed farther seaward).

Longer-term shore evolution under forced regression was approximated by sequential palaeo-shoreline mapping at 200-year intervals for the past 1000 years. This used a 2-m resolution digital elevation model (DEM) derived from interferometric synthetic aperture radar, courtesy 3vGeomatics® (Vancouver, BC), and the recently refined RSL curve for the region (Simon et al., 2014). Historic sea level height was taken from the RSL curve for each time slice and transposed onto the DEM. This mapping approach assumed an unchanging subaerial landscape post-emergence and was necessarily a simplification ignoring sediment transport processes.

2.4 Results

2.4.1 Coastal classification

The shoreline of the Arviat municipal boundary is ~130 km long and almost entirely unlithified. Its form and material are the result of an emergent littoral imprint on a formerly glaciated landscape, which has produced extensive tidal flats, slopes, and beaches composed of sand and gravel. This glacial legacy has also resulted in a highly indented shoreline morphology. The regional-scale shoreline orientation is N-S, following the rest of the west coast of Hudson Bay. However, the local shoreline is highly irregular (high fractal dimension), influenced by prominent esker ridges, local bedrock exposure, and highly variable shoreface gradients controlled by surficial geology and affecting wave refraction and attenuation (Fig. 2.3).

‘Nuvuk’ is a representative subset of the Arviat coastline, a prominent peninsula that projects eastward into Hudson Bay (Fig. 2.2). It is framed by two glaciofluvial eskers that generally run E-W, both joined and flanked by smaller glacial moraine ridges that generally run N-S. Where these ridges are absent, long stretches of active and relict tidal flats dominate. Where the shoreline intersects the glaciofluvial and glacial ridges, as in much of the northern, eastern and southern sections of the peninsula, gravel beaches predominate in the upper foreshore and backshore.

The foreshore and backshore zones within the Arviat municipal boundary were classified into 3 and 6 form categories, respectively (Fig. 2.3). The foreshore forms are beach, flat and outcrop. The backshore forms are anthropogenic, beach, cliff, dune, flat, and outcrop. All forms except outcrop are composed of unlithified materials. Unconsolidated foreshore and backshore materials range in grain size from silt to boulder, though sand and gravel dominate the shore zone within the municipal boundary.

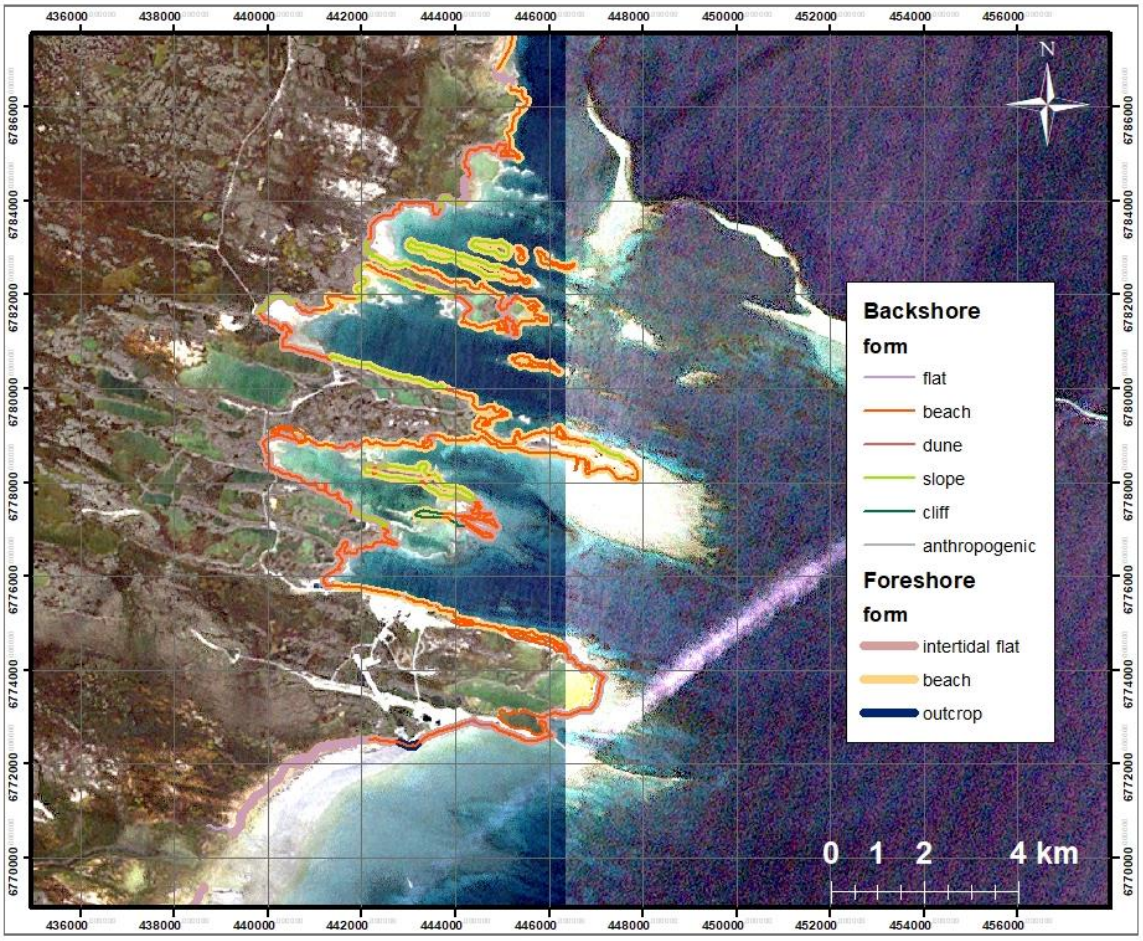

Figure 2.3: Coastal classification for the shoreline within the municipal boundary of Arviat. Note the strong indentation and highly variable orientation of the shoreline and accompanying small islands.

Beaches predominate in the backshore, except in the emergent flats to the south of 'Nuvuk' and at the heads of some of the small bays to the north. Where beaches are found along a relatively protected section of the foreshore, the backshore in some cases is mapped as a largely inactive slope. Slopes are generally found along the sides of former esker ridges that have emerged into the foreshore and backshore as small islands, or along E-W sections of the shoreline. There are some low scarps (wave-cut notches) in the

backshore, but these are not mapped at this scale. There is very limited cliff development, only found on the protected side of an emerged esker ridge island to the north of ‘Nuvuk’. Similarly, dune development is limited and focused on the large southern esker of ‘Nuvuk’.

Using the above classification, the ‘Nuvuk’ peninsula can be subdivided into eight segments with quasi-homogenous orientation, form, and materials (labelled A to H in Fig. 2.4).

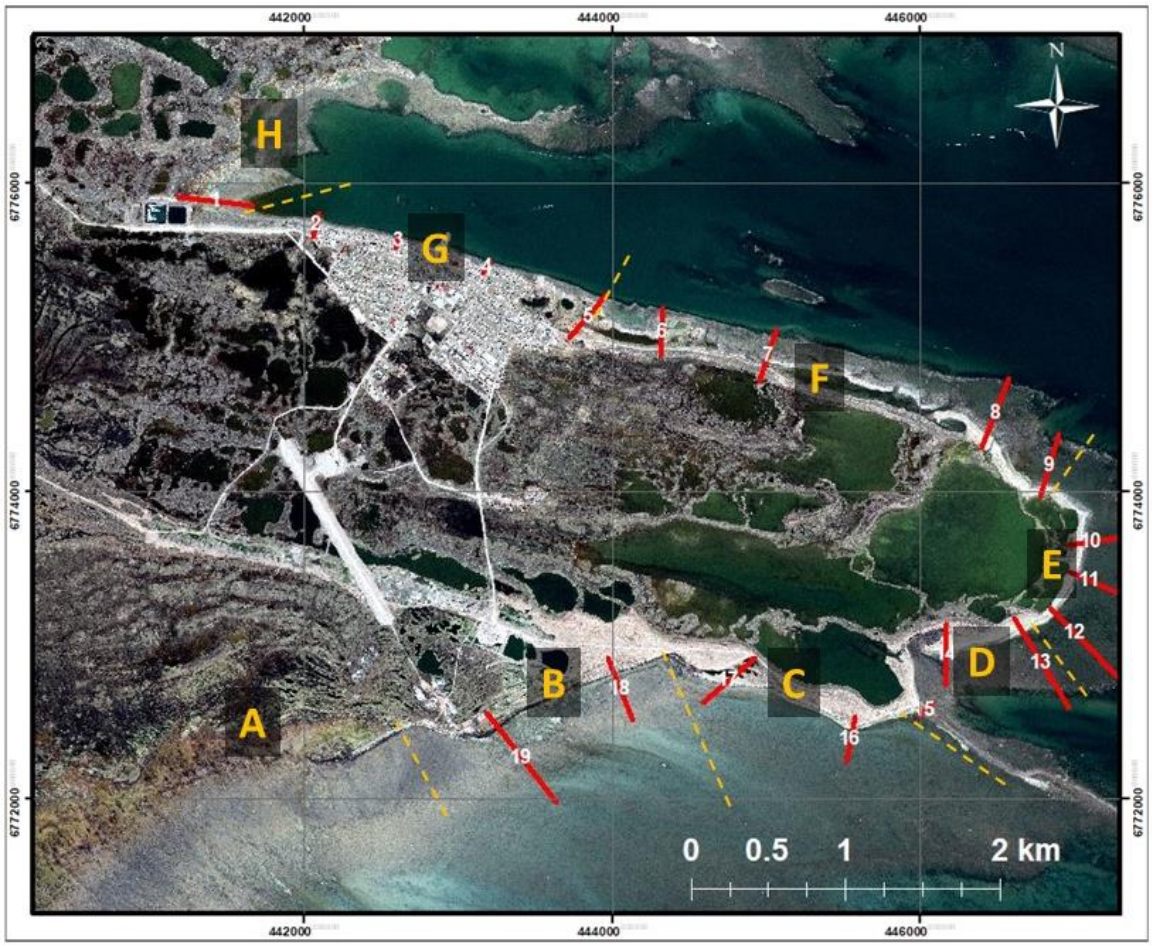

Figure 2.4: Quasi-homogenous shoreline segments around ‘Nuvuk’, defined according to orientation, form and material. Bold orange letters indicate the shoreline segments and are divided by dashed yellow lines. The red solid lines are the locations of dGPS coastal survey lines (contains material ©Digital Globe, 2011).

2.4.1.1 Segment A

Tidal flats, both active and abandoned by RSL change, dominate the shore zone to the south of ‘Nuvuk’. The backshore is an emerged tidal flat now covered in peat wetland. These flats continue south to a small creek and the southern municipal boundary. The drainage of this shallow slope is quite poor, owing to the incipient permafrost and fine-grained substrata. The foreshore-backshore boundary is marked by excess algae accumulation formed by high-tide wave action (Fig. 2.5). This segment lacks the well-defined beaches characteristic of the rest of the community shoreline, although there are some sandy bands closer to the eastern edge of the segment and a bedrock outcrop. The foreshore is an extensive active tidal flat, sloped <0.5° to the southeast and ranging from 2.5 to 4.5 km in width. This flat comprises most of the foreshore of segments B and C as well. The flat is predominately sand with a high concentration of cobble and small boulders at the surface, presumably attesting to active sea-ice transport. At the eastern end of the segment, there is a low sandy spit approximately 800 m long. This spit is at the western terminus of a longshore sediment transport corridor extending from the eastern point (east end of segment C). Evidence of previous iterations of similar spit growth, now in the backshore and often buried by organics, can be seen along the southern flank of the esker ridge inland to the west.

Figure 2.5: Southern section of ‘Nuvuk’ shoreline, facing southwest along the foreshore-backshore boundary of Segment A at low tide. To the right is a large build-up of dark algae marking the aforementioned boundary and to the left are the extensive tidal flats inundated twice daily.

2.4.1.2 Segment B

Moving east along the southern tidal flats, the shoreline connects with a whaleback bedrock outcrop and the southern esker ridge. Projecting off the re-worked esker and bedrock outcrops in the backshore are several relict beach ridges defined by cobble and boulder accumulation, as well as marine detritus and relict spits composed mostly of sand. At the outcrop, which forms a natural groyne for the shoreline, the foreshore-

backshore boundary begins to become defined by a swash-aligned beach <10 m in width and sloped 2.5-3.5° in the upper foreshore (Fig 2.7). Closer to the eastern end of the segment the beach expands to 15 m width (Fig. 2.6). The beach is backed in places by low scarps (<1 m high) ranging from active to semi-stabilized, otherwise it is backed by 2 to 8° slopes (Fig. 2.7). Near the bedrock outcrops the beach is composed of sand, with minor unsorted pebble, cobble, and small boulder elements (Fig. 2.6). Moving east, the beach becomes coarse gravel (cobble and boulder) with intermixed sandy-pebble gravel. There is a small sandy-pebble apron at the base of the beach in some areas (Fig. 2.6). In the foreshore, the tidal flats narrow to 0.9 to 1.5 km in width. The tidal flats are sloped 0.2° towards the southeast (Fig. 2.7). There is still significant algae deposition near the foreshore-backshore boundary, concentrated in concave sections of the shoreline, although not to the same extent as along segment A (Fig. 2.5).

Figure 2.6: Beach of segment B facing southeast at low tide. Note the sandy-pebble apron at the base of the beach, the accumulation of organics at the foreshore-backshore boundary, and the small (12 x 18 cm) yellow notebook for scale.

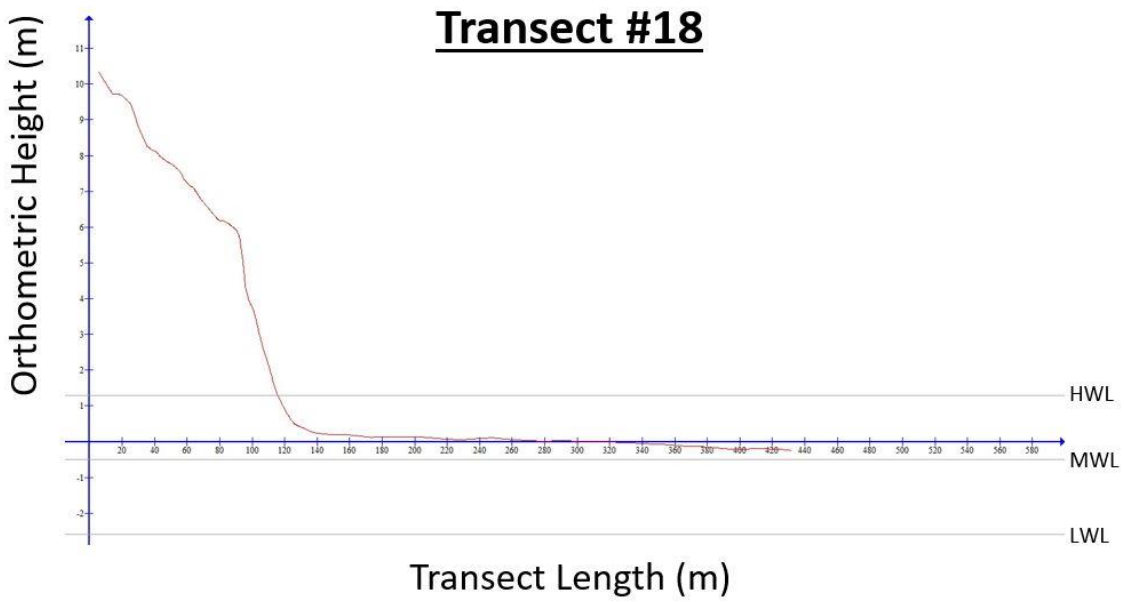

Figure 2.7: Transect #18 profile (VE=~20x). The beach backs onto the southern esker ridge, and is the highest backshore in the study area. The upper foreshore beach and lower foreshore flats are relatively uniform in slope throughout the segment.

2.4.1.3 Segment C

The easternmost end of the southern flats is where the backshore esker begins to directly parallel the shoreline (Fig. 2.4). The backshore is scarped throughout this segment, ranging from active sandy scarps <1 m high at the western end (Fig. 2.8, background) to semi-stabilized gravel scarps up to 4 m high at the eastern end and closest to the point (Fig. 2.9). As well, an eolian surficial unit caps the glaciofluvial framework in places. This unit is formed by wind reworking of local sand sources into dune ridges and ramps. Distinct pebbly sand relict beach ridges (former spits) and brackish ponds are present in

the immediate backshore along the western portion, lying between the crest of the esker ridge and the active shore zone.

The shore of Segment C is a drift-aligned beach backed by partially stabilized erosional scarps and an active, 430 m-long, pebbly sand spit (Fig. 2.4 in vicinity of transect #17). Well developed cross-shore sorting is evident in places. A sandy pebble apron is present at the base of the beach. At the western end of the segment the beach is 20 m wide and sandy. At the eastern end of the segment the beach is up to 40 m wide and the upper beach becomes gravel. The upper foreshore beach slope is ~6° while the flats slope at 0.3° to the southeast (Fig. 2.9). The segment terminates at a ~3 km-long, curved, and narrow bar projecting eastward into Hudson Bay. This bar is the extension of the framing southern esker ridge into the marine environment, as its crest emerges with RSL fall. It has limited sinuosity and is composed mostly of pebbly sand with isolated boulders. This bar also marks the northern end of the most extensive tidal flats around ‘Nuvuk’.

Figure 2.8: Southeastern section of ‘Nuvuk’ shoreline facing southwest towards the mainland at low tide. In the foreground is the boulder frame across the beach face of Segment C, littered at various wave run-up heights with marine detritus. To the right is the esker-dune complex that backs this section of the shoreline and to the left are the extensive tidal flats.

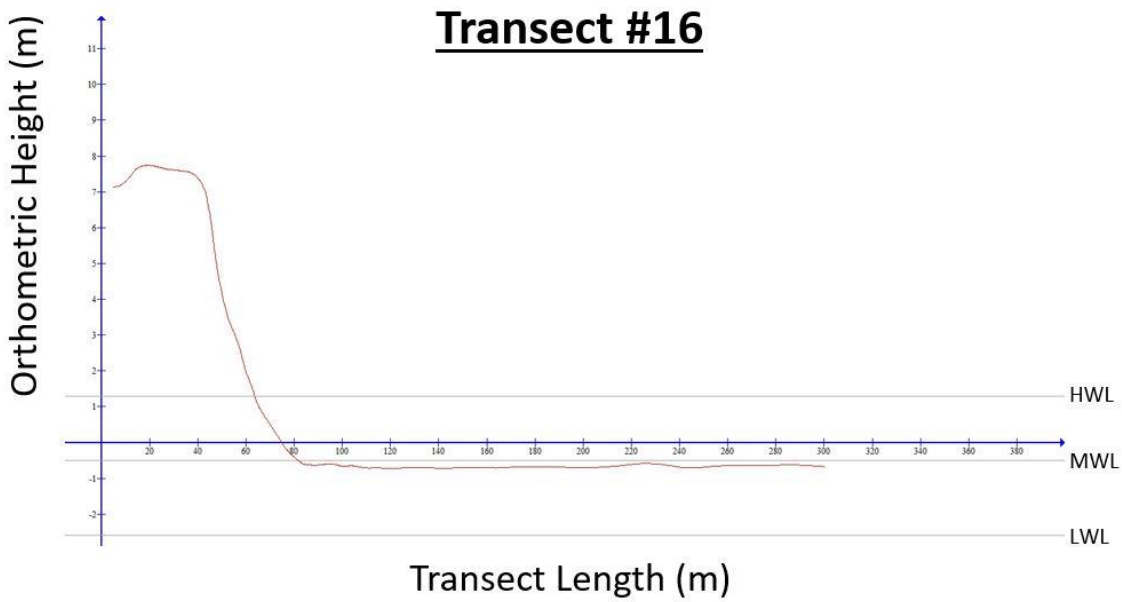

Figure 2.9: Transect #16 profile (VE=~15x). The backshore and upper foreshore are more steeply sloped along this segment relative to segment B. The height of the backshore diminishes moving from inland to the headland.

2.4.1.4 Segment D

North of the bar marking the boundary with segment C, opposing sandy spits are growing across the mouth of a tidal inlet (in process of transition to a lake; Fig. 2.4). The backshore here too is formed in wave and wind re-worked esker ridges. There is an estuarine channel in the centre of the segment, a 100 m-long pebbly sand and cobble spit growing northward, and a 175 m-long pebbly sand and cobble spit growing westward (Fig. 2.4). The tidal flats narrow to 470 m at the estuarine channel and the lower foreshore slopes 1.0° to the southeast (Fig. 2.11). The beach itself is 10 m wide (Fig. 2.11) with a

gentle slope (4°) and composed of poorly sorted cobble and small boulders within a sand and pebble matrix. There are algae deposits as well, though not to the same extent as in segments A-C (Fig. 2.10). Along the northern part of the segment there are active scarps <1 m high.

Figure 2.10: Segment D facing north approaching high tide. Note the remains of the ice foot in the background, lining the estuarine channel at the centre of the segment. The estuarine channel is almost abandoned by RSL fall, and the water bodies it links are transitioning to ponds and lakes.

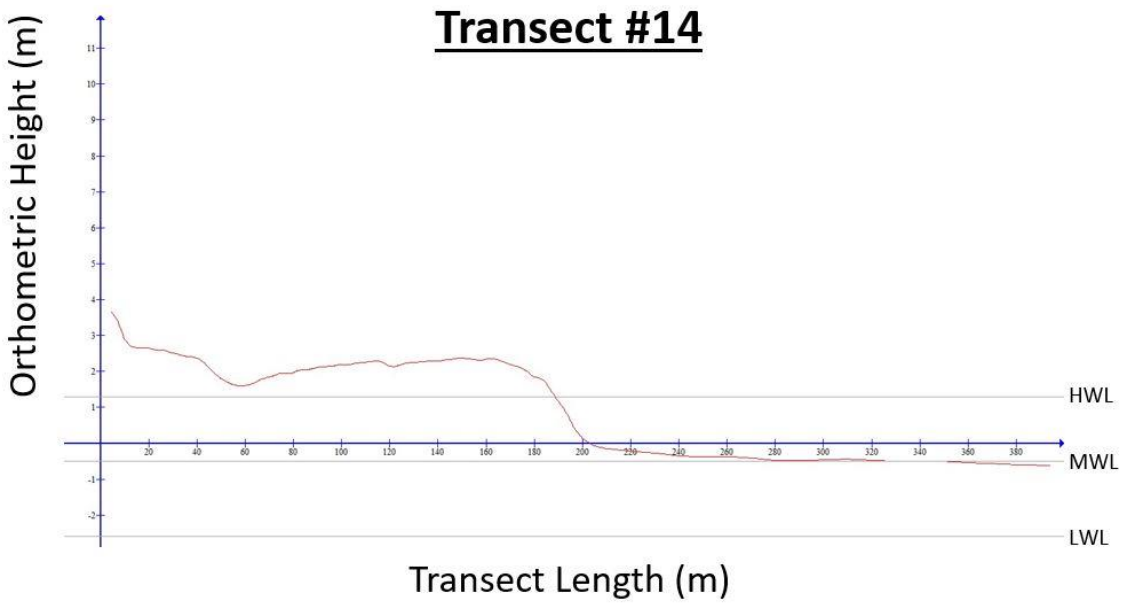

Figure 2.11: Transect #14 profile (VE=~15x). The 'hump' between 50 and 175 m along the length of the profile is the sandy spit prograding from the NE in a SW direction (Fig. 2.4).

2.4.1.5 Segment E

At the east-facing section of 'Nuvuk', an exposed gravel storm ridge dominates the backshore, partially scarped (Figs. 2.4 and 2.12). This segment experiences the highest rates of sediment removal and shoreline recession in the study area (Figs. 2.21 and 2.22). The erosional scarps are sandy, with intermixed cobbles and boulders (Fig. 2.12). The beach itself is 15 to 25 m in width (Fig. 2.13) and, in most places, cobble and boulder, with little to no sandy matrix (Fig. 2.12). The proportion of sand is variable across the beach and alongshore, with cobble predominating in places (Fig. 2.12). The largely gravel

beach slopes 5 to 6° to the east (Fig. 2.13). At the base of the beach the sandy matrix is more consistently present, with minor unsorted cobble and boulder elements extending into the tidal flats (Fig. 2.12). Minor algae bands in the upper foreshore mark varying run-up heights for wave action in recent months and years (Fig. 2.12). In the lower foreshore, the sand and cobble tidal terrace is between 0.2 and 1.0 km in width and is essentially flat, terminating abruptly and sloping into the nearshore (Fig. 2.13). The backshore slope along this section is between 4 and 18° (Fig. 2.13).

Figure 2.12: Eastern section of ‘Nuvuk’ shoreline, facing south. In the foreground is the erosional scarp characteristic of Segment E. To the left lies the relatively high angled beach face and to the right is the clastic ridge into which the scarp is cut. Note the marine algae tossed onto the ridge crest in the foreground.

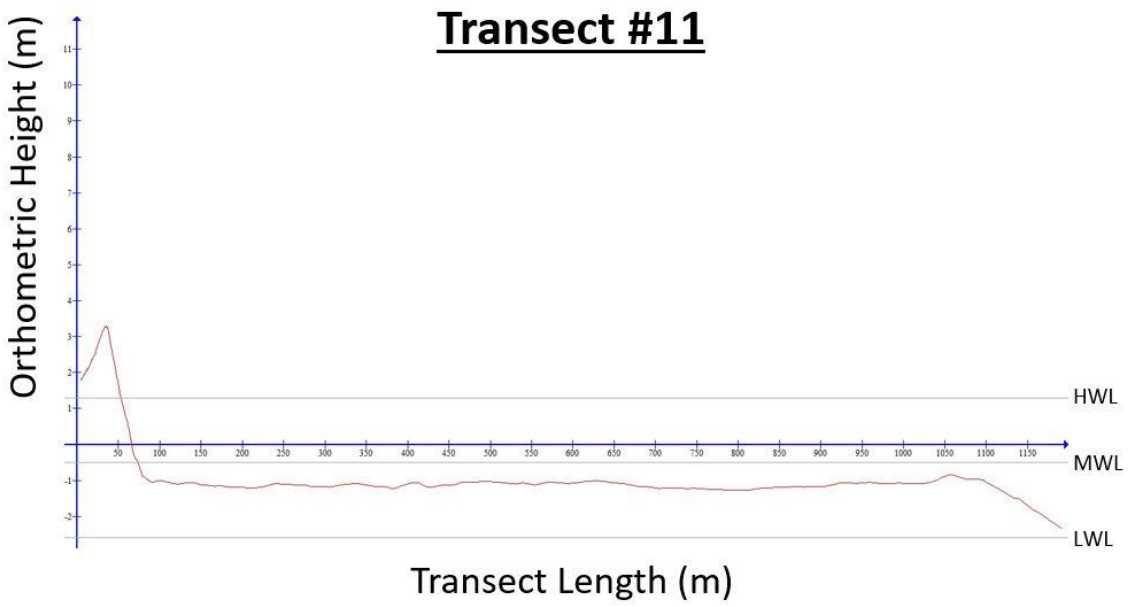

Figure 2.13: Transect #11 profile (VE=~40x). The relatively steep upper foreshore beachface drops to an extensive tidal flat of effectively uniform elevation. This flat terminates at a slight cobble and boulder ridge before sloping more steeply into the nearshore.

2.4.1.6 Segment F

The north-east facing portion of the 'Nuvuk' shoreline is also dominated by gravel beach (Fig. 2.14), but without the erosional scarps of Segment E (Fig. 2.12). This segment is linked in the backshore to the less prominent northern esker ridge, which shapes the shoreline's alignment and sedimentary character. Moving west along the segment towards segment G, the beach gives way to more sand and pebble-gravel, forming a drift-aligned beach with fewer cobbles and boulders (Fig. 2.14). The segment is more muted in relief and more irregular in planform relative to neighbouring segments E and G (Figs. 2.12,

2.14 and 2.16). The scarps of the headland are gone and replaced by cobble and boulder slopes in the backshore (Fig. 2.14). The wave run-up limit is intermittently marked by minor algae accumulations and hardy grasses (Fig. 2.14). The beach is 25 to 50 m in width and slopes 2 to 5° to the north (Fig. 2.15). There are three segments of a supratidal ridge found within the intertidal zone, the longest being 430 m in length (Fig. 2.25). Around and between the ridges are channels with minor spit development, although to a lesser degree than on the southern shore of 'Nuvuk' (Fig. 2.25). The tidal flats in the lower foreshore are essentially a terrace, like the headland of segment E (Fig. 2.14), and narrow to widths of 10 to 325 m (Fig. 2.15). They are incised in one location by a small fluvial channel that partly drains 'Nuvuk' during spring run-off and heavy precipitation (Fig. 2.25). The entire foreshore slopes 1 to 2° northwards (Fig. 2.15).

Figure 2.14: Northeastern section of ‘Nuvuk’ shoreline looking east along Segment F towards the headland. The informal road to the headland comes right to the foreshore-backshore boundary, as seen with the tire tracks. In the background one can see shifts from more coarse gravel beach to finer gravel beach in the embayment. Note as well the more muted relief relative to the headland and southern section of the coastline (Figs. 2.6, 2.8 and 2.12).

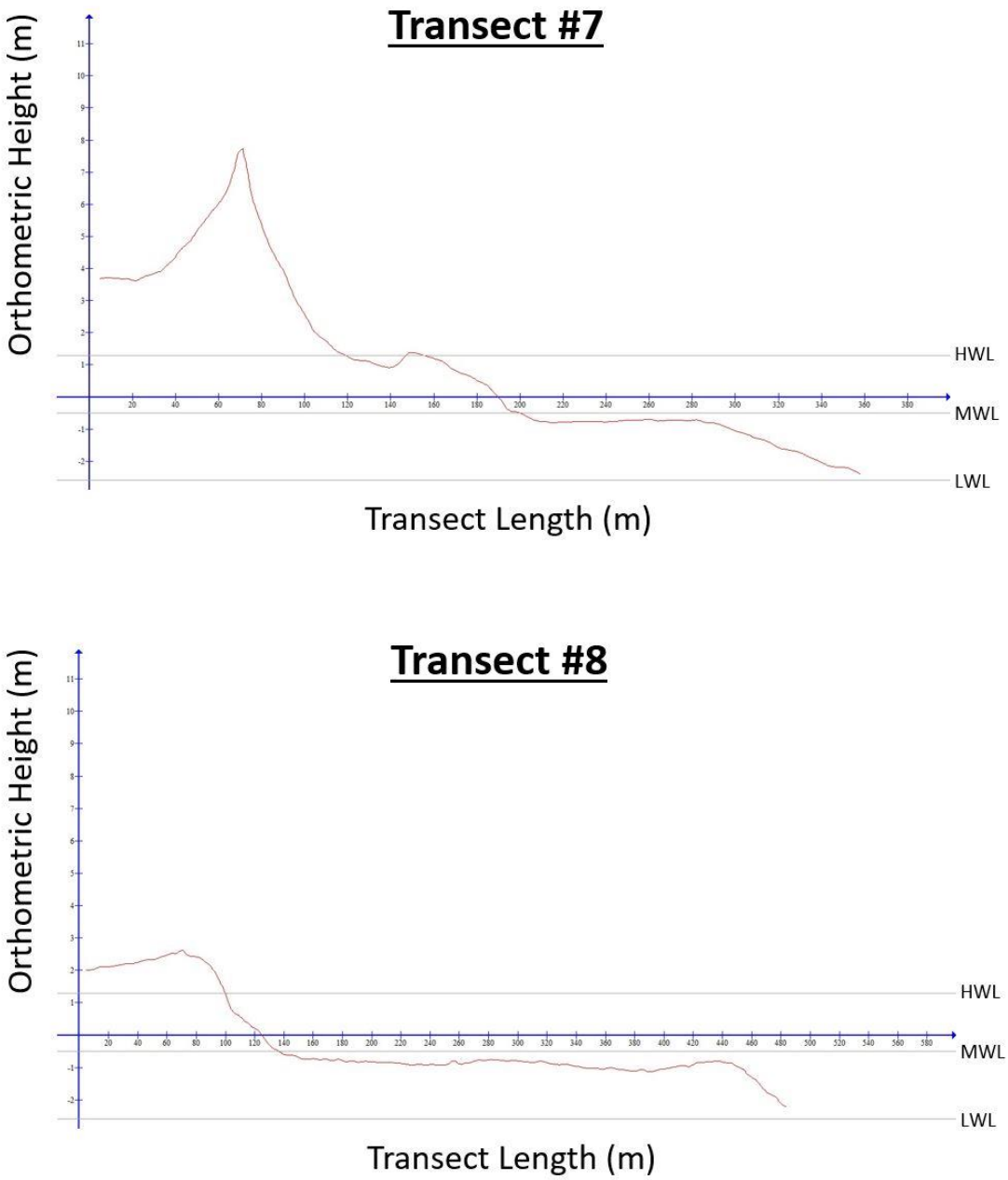

Figure 2.15: Transects #7 (VE=~15x) and #8 (VE=~20x). A minor foreshore crest is notable along transect #7. Transect #8 is more representative of the muted backshore elevation along the majority of segment F. As in segment E, the lower foreshore is essentially flat, before sloping into the nearshore at a breakpoint.

2.4.1.7 Segment G

The anthropogenic fill built-up around the esker ridge framework backs the community waterfront. The community was deliberately constructed along the section of 'Nuvuk' with the narrowest intertidal zone, allowing quick access to the marine environment for harvesting and travel. This section has several direct anthropogenic influences: a built-up community wharf, barge landing area, and many informal boat ramps where the larger cobbles and boulders have been displaced alongshore (Fig. 2.16). The foreshore-backshore boundary is slope-backed and marked by hardy vegetation and small storage sheds (Figs. 2.16 and 2.17). In some areas the community infrastructure is built right down to the high-tide line. The intertidal zone narrows, and the foreshore and backshore once again become coarser in character relative to the western end of segment F (Fig. 2.18). This coarse gravel beach slopes 2.5–7° to the north and is between 10 and 25 m in width, generally on the narrower end of that range (Fig. 2.18). In some areas the clast-supported gravel framework gives way to a sandy-pebble matrix (Fig. 2.16). West of the community dock, in places there is a minor low-tide flat at the base of the beach, where gravel sits in a sand matrix that has been worked into ripples by wave action (Fig. 2.17). In isolated embayments, an underlying shell-bearing marine mud is exposed. There is also evidence of alongshore transport of sediment as revealed by the removal and deposition of sediment on the western and eastern side of the community wharf, respectively (Fig. 2. 21), the wharf functioning as a groyne.

Figure 2.16: Northern community section of ‘Nuvuk’ shoreline facing west along Segment G at low tide. To the left are the hospital and several private residences. The beachface features many informal boat ramps, like the one in the immediate foreground, modified for easier boat access.

Figure 2.17: Further west along Segment G during the Fall season. Note the sandy terrace with wave ripples in the foreground and middle distance, exposed at low tide.

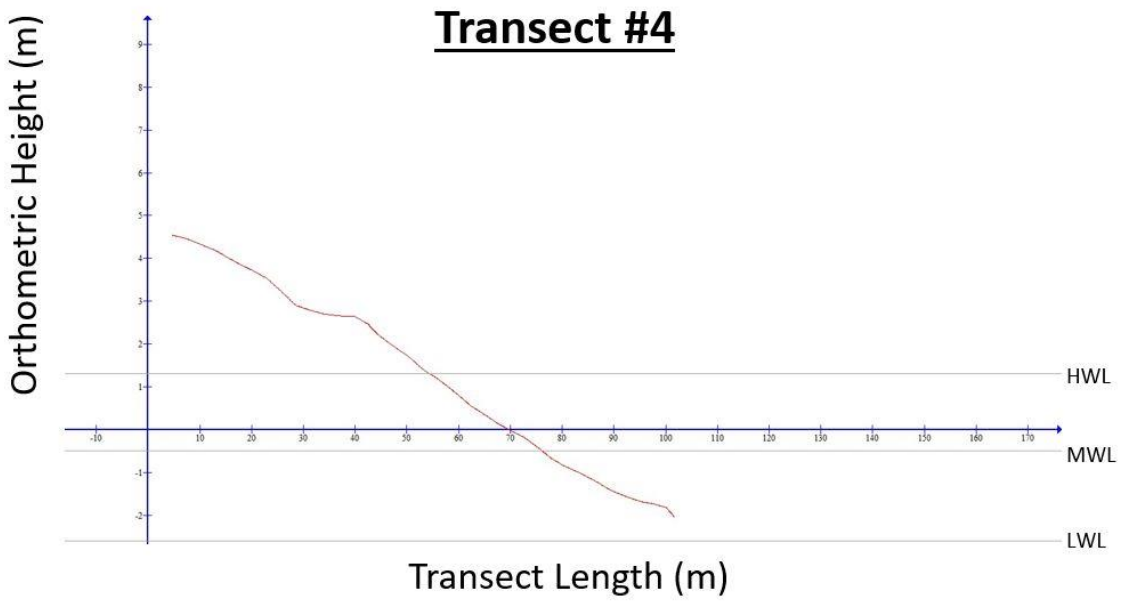

Figure 2.18: Transect #4 in profile (VE=~7x). The upper and foreshore slopes of the community segment are relatively uniform, allowing easier access to the bay to the north and the local marine environment.

2.4.1.8 Segment H

North of 'Nuvuk' at the head of the bay, the intertidal zone widens once again and a coarse gravel, swash-aligned beach predominates (Fig. 2.19). The backshore is a reworked glaciomarine complex that sits above 'Nuvuk' proper, rising as high as 15 m to the west. This glaciomarine complex is not scarped like the other eastern facing sections at the headland of 'Nuvuk' (Fig. 2.12). Instead, the backshore slopes gently 1° to the east and the foreshore-backshore boundary becomes relatively diffuse (Fig. 2.20). The sediments of the upper and lower foreshore are coarse gravel and poorly sorted (Fig.

2.19). The lower foreshore slope leading into the nearshore is roughly 300 m in width with a slope of 0.8° (Fig. 2.20).

Figure 2.19: Facing south along the foreshore-backshore boundary of Segment H approaching high tide. Note the cobble accumulation with limited interstitial material that is characteristic of the shoreface along Segment H. The entire segment slopes gently to the east.

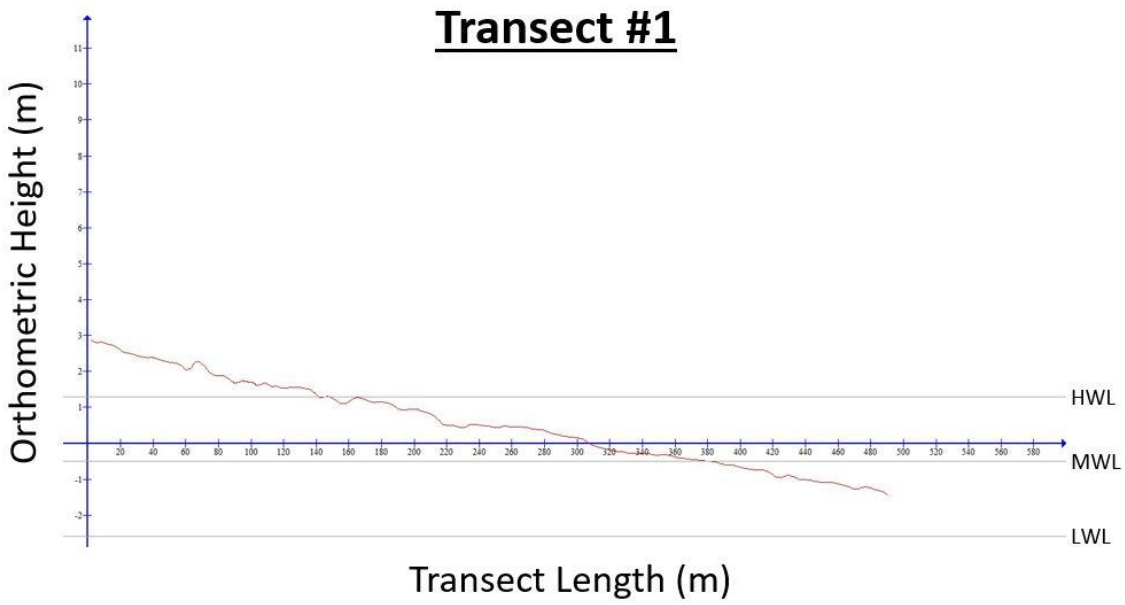

Figure 2.20: Transect #1 in profile (VE=~20x). The boulder-cobble slope face has an effectively uniform slope as it transitions from the backshore to the foreshore.

2.4.2 Shoreline change

Observed horizontal HWL change around 'Nuvuk' ranges from 62 m of retreat to 155 m of advance during the 51-year interval between 1960 and 2011 (Figs. 2.21 and 2.22). These net rates correspond to maximum mean rates of 1.2 m/yr retreat and 3.0 m/yr advance. The geometric mean shoreline advance is 15.1 m over the 51-year interval, or 0.30 m/yr (n=239 sections). The geometric mean shoreline retreat is 7.4 m over the 51-year interval, or 0.14 m/yr (n=41 sections).

Figure 2.21: DSAS shoreline change results. Extent of change in shoreline position is indicated by both the colour (red = retreat, green = advance) and the relative lengths of the coastal transects. Every 50th transect is labelled to correspond with Fig. 2.22. Transects in orange and red highlight the five areas exhibiting shoreline retreat, exceeding forced regression (contains material ©Digital Globe, 2011).

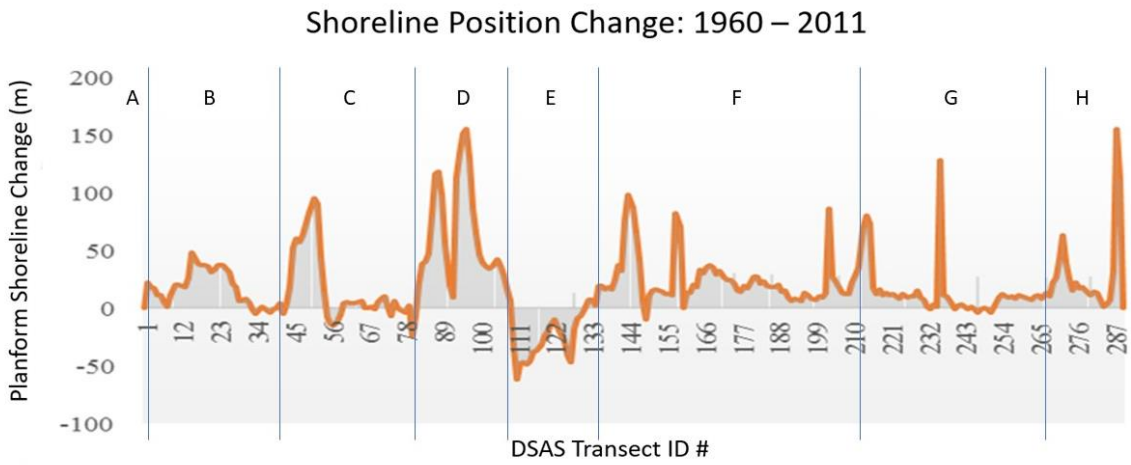

Figure 2.22: Shoreline position change. Positive change is seaward, negative change is landward. DSAS-generated transect numbers start at the south, follow the shoreline around 'Nuvuk', and end north of the community (Fig. 2.21).

There are five coastal reaches around 'Nuvuk' that are experiencing shoreline retreat (Figs. 2.21 and 2.22): 1) along the south-facing shore of 'Nuvuk', adjacent to developing spits; 2) along the convex, east-facing section of the 'Nuvuk' headland, where a relatively steep beach face is fronted by tidal flats between 0.2 and 1.0 km wide; 3) along the northeast shore at a single section east of a westward prograding spit; 4) discontinuous parts of the community waterfront, particularly west of the dock, where the intertidal zone is the narrowest in the study area; and 5) minor segments to the west and north of the community.

Shoreline retreat is most prevalent at the scarped gravel beach found at the headland of 'Nuvuk' (Segment E; Figs. 2.12 and 2.21). The rate of retreat is greatest at the two convex edges of the promontory (1.2 m/yr, Fig. 2.23). These sections have in effect been

‘smoothed’ over time by erosive forces, bringing their orientation closer to the shoreline around them. Along this section, measured backshore slope angles range from 12.7 to 18.6°, the steepest in the area (Fig. 2.13). This erosive action is taking place despite RSL fall and tidal flats up to 1 km wide that necessarily attenuate wave energy. The general trend of shoreline evolution along this segment is towards a swash alignment facing the dominant incoming wave energy from Hudson Bay. In contrast, sections of retreating shoreline along the southern and northern flanks of ‘Nuvuk’ are parts of drift-aligned beach systems, in which alongshore sediment transport is resulting in cell development and localized erosion. Incoming deep-water waves are refracted either side of the headland, creating the longshore currents and generating sediment transport westward along the flanks of ‘Nuvuk’.

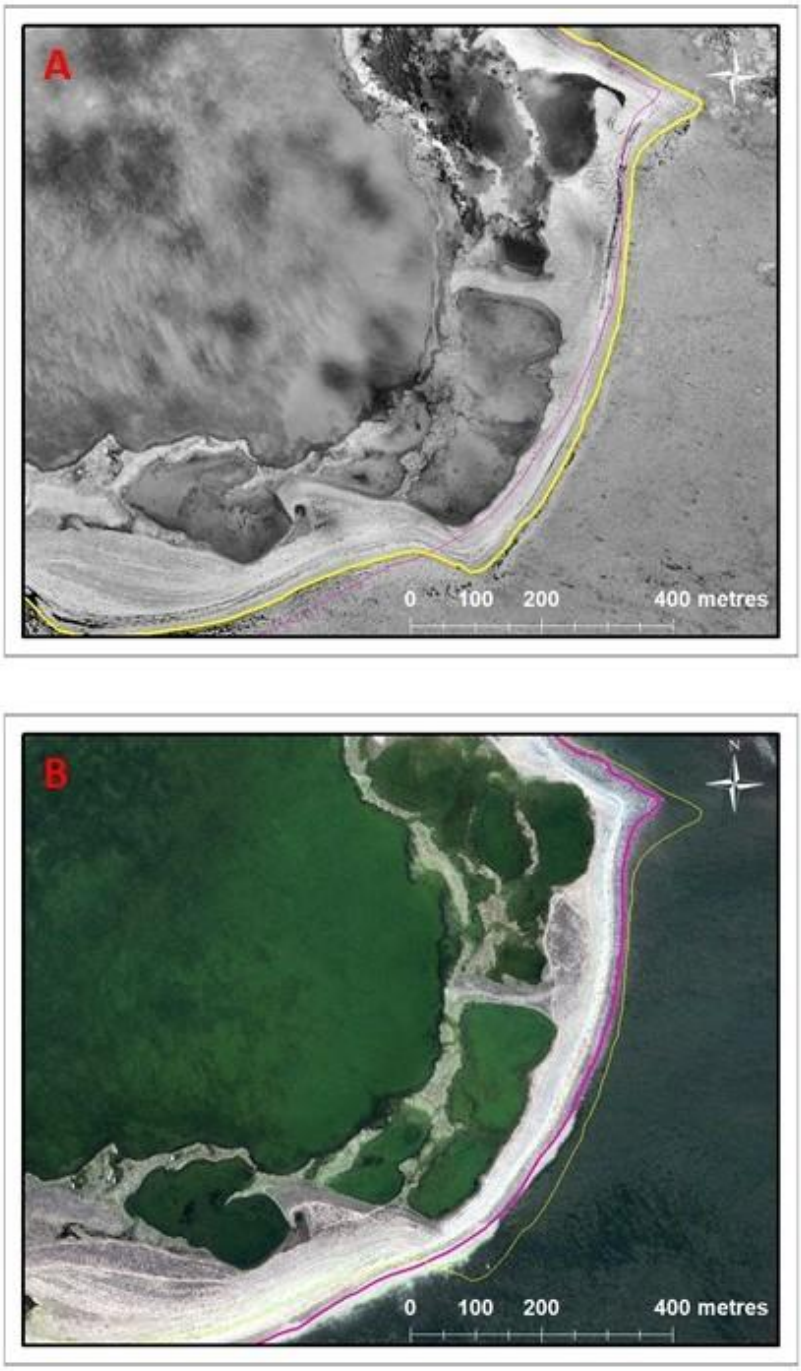

Figure 2.23: Shoreline retreat along the eastern shoreline of 'Nuvuk' (Segment E). A is the georeferenced air photograph of the shoreline in 1960. B is satellite imagery of the same shoreline reach in 2011. Note the 'smoothing' of the shoreline through erosive processes. The yellow line represents the 1960 interpreted HWL and the purple line represents the 2011 HWL (contains material ©Digital Globe, 2011).

Shoreline advance is greatest along the southern shore of ‘Nuvuk’ (3.0 m/yr), a drift-aligned section of progressive spit development and eventual abandonment to the backshore. Three small standing water bodies very close to high water level are separated by beach ridges that progressively grew and were sequentially abandoned by falling RSL (Fig. 2.24). These historic spits are all located at roughly the same height (Fig 2.25). Stable to retreating segments occur both up- and down-drift of the spits, reflecting the longshore development that feeds them. These shoreline evolution trends increase the shoreline sinuosity, in contrast to the trend of diminishing sinuosity at the headland.

Figure 2.24: Shoreline advance along the southern shoreline of 'Nuvuk' (Segment C). A is the georeferenced air photograph of the shoreline in 1960. B is satellite imagery of the same shoreline reach in 2011. Note the erosion taking place on either side of the prograding spit (contains material ©Digital Globe, 2011).

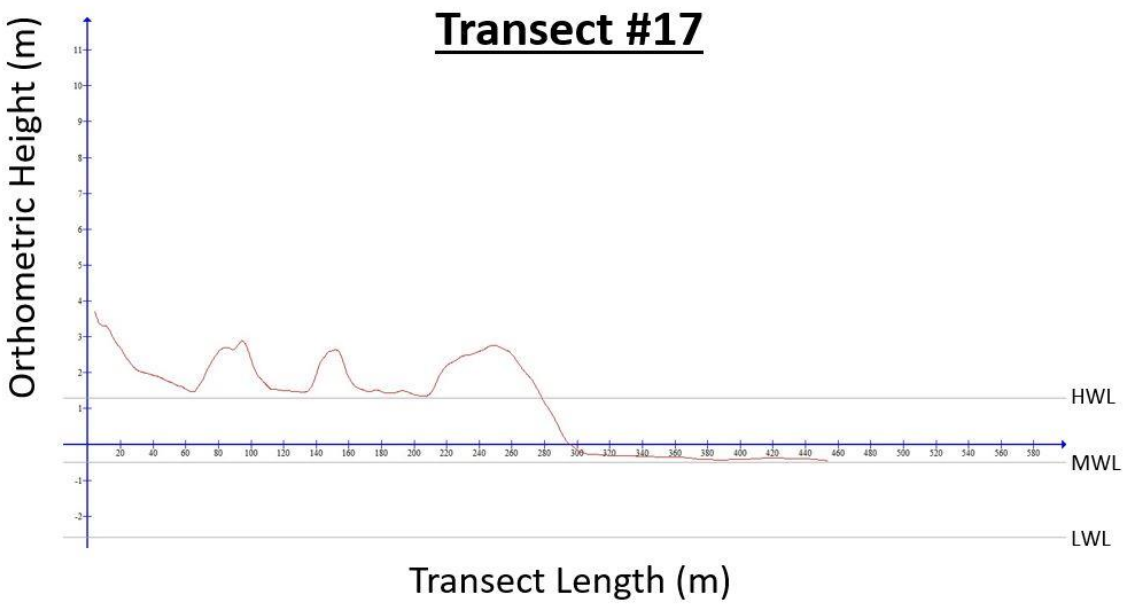

Figure 2.25: Transect #17 in profile (VE=~20x). The active spit crest is at the rightmost of the intermittent ridges highlighted here, two relict ridges are in the middle and the backshore esker flank slopes to the left of the profile.

The other environment in which shoreline evolution is most dynamic is where estuarine channels have evolved through RSL fall. The best example of these changes is along the northeastern section of 'Nuvuk' (Fig. 2.26). Here an estuary has infilled and drained completely, and another has had its opening narrow from both the east and west to the point where it is essentially a drainage channel rather than a tidal inlet. There is also evidence of shoreward migration of a supratidal ridge at the top of the frame (Fig. 2.26).

Figure 2.26: Estuarine infilling and landward beach-ridge migration along the northeastern shoreline of 'Nuvuk' (Segment F). Above is the georeferenced air photograph of the shoreline in 1960. Below is satellite imagery of the same shoreline reach in 2011. Note how the estuary is closing in from both sides of the channel (contains material ©Digital Globe, 2011).

Comparing measured and predicted historical HWL positions indicates where sediment deposition or erosion has occurred along the coastal transects independent of RSL change. Where the predicted positions are further inland than the historical positions, sediment deposition must have bridged the gap and accelerated shoreline movement seaward under falling RSL. Where predicted positions are further seaward than historical positions, sediment removal must have reduced the extent of shoreline advance or resulted in shoreline retreat.

Accelerated shoreline advance (10 sites), reduced seaward shoreline advance (3 sites), and landward shoreline retreat (5 sites) were observed at the surveyed profiles, based on shoreline migration relative to that expected by forced regression (Fig. 2.27). Two profiles abutting the community dock, four profiles along the northeastern section of 'Nuvuk', and four profiles around spits to the east and south of Nuvuk all experienced accelerated shoreline advance. Two profiles to the west of the community and one profile to the east experienced shoreline advance but at a reduced rate than one would expect from RSL change alone, pointing to historical net erosion. Finally, three eastern profiles and two profiles near developing spits to the south of Nuvuk experienced shoreline retreat.

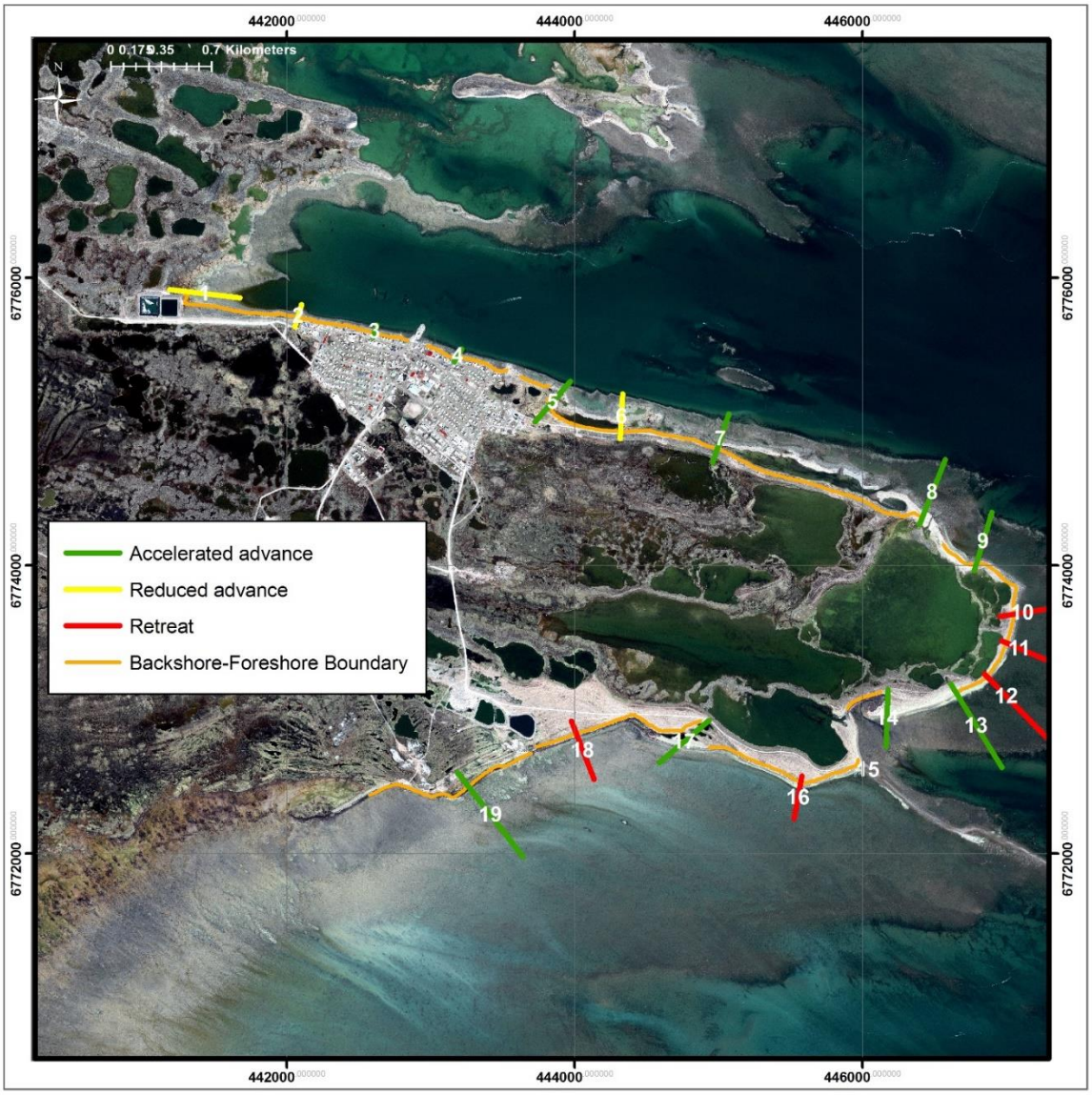

Figure 2.27: dGPS coastal transects and net sediment movement analysis results. The colouring of the shore-normal transects represent the profiles where sediment has been either added (accelerated shoreline advance) or removed (reduced shoreline advance and retreat) between 1960 and 2011 (contains material ©Digital Globe, 2011).

2.4.3 Palaeo-shoreline mapping

Palaeoshoreline mapping results detail a complex legacy of recent emergence of Arviat and the surrounding landscape from Hudson Bay (Fig. 2.28). The modern coastal environment is a product of both (1) progressive emergence of low-gradient inner-shelf slopes and E-W oriented esker ridges and (2) step-wise emergence of moraine ridges and the areas behind them. The modern terrestrial environment is naturally a partial product of the same processes. Wave reworking has modified the sedimentary character of terrestrial landforms and, in some areas, created new landforms or veneers around the glacial framework. Modern freshwater bodies are also formed through the transition from the marine to the terrestrial environment. What were initially saline or brackish estuaries and lagoons progressively emerged to become the freshwater ponds and lakes of the modern landscape. As the landscape has drained after emergence, many of these basins have transitioned from perennial inundation to seasonal inundation as the water table and expanding permafrost layer in the subsurface adjusted over time.

Using the DEM described above and the RSL history for Arviat determined by Simon et al. (2014), the approximate past shoreline can be determined based on fine-scale elevation contours, demonstrating cumulative emergence. Pre-development 1960 air photographs were used to supplement DEM data in areas of anthropogenic influence. The resulting ‘hindcast’ shorelines at 200-year intervals over the past millennium are illustrated below.

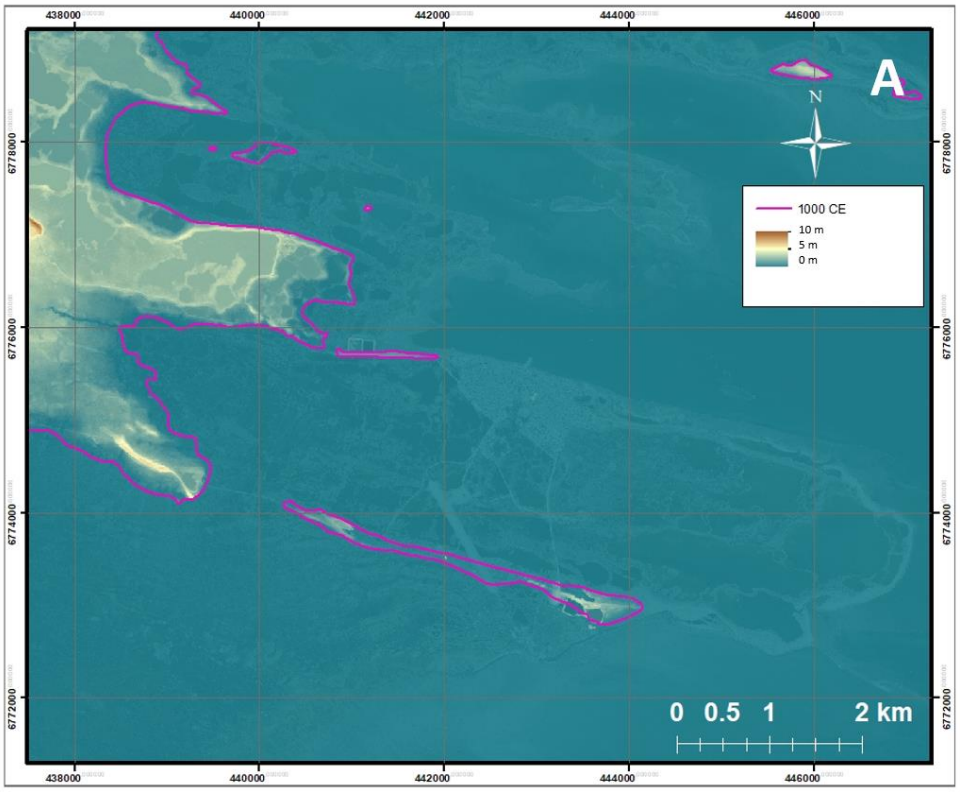
A
N
1000 CE
10 m
5 m
0 m
0 0.5 1 2 km
438000
440000
442000
444000
446000
6778000
6776000
6774000
6772000

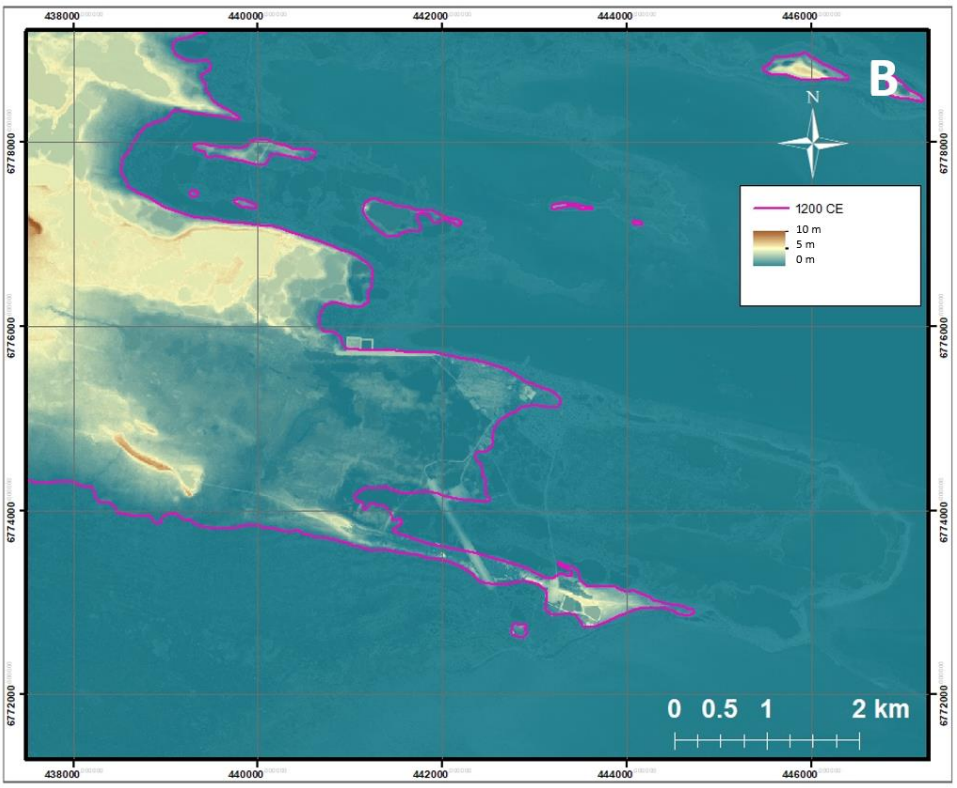
B
N
1200 CE
10 m
5 m
0 m
0 0.5 1 2 km
438000
440000
442000
444000
446000
6778000
6776000
6774000
6772000

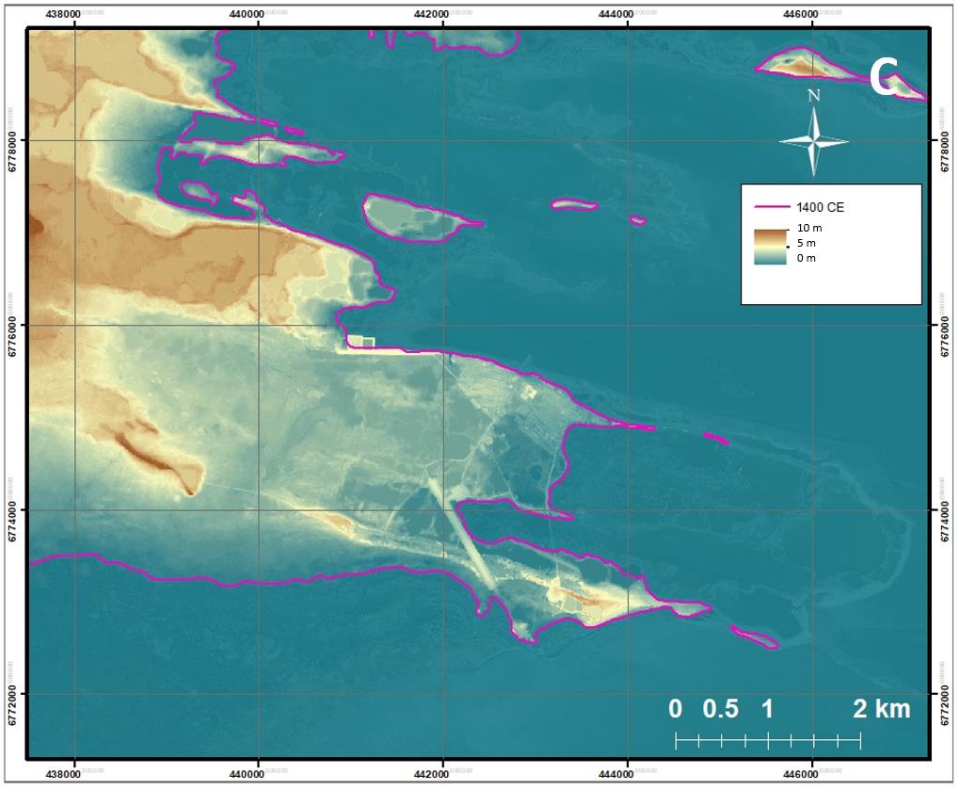
C
N
1400 CE
10 m
5 m
0 m
0 0.5 1 2 km
438000
440000
442000
444000
446000
6778000
6776000
6774000
6772000

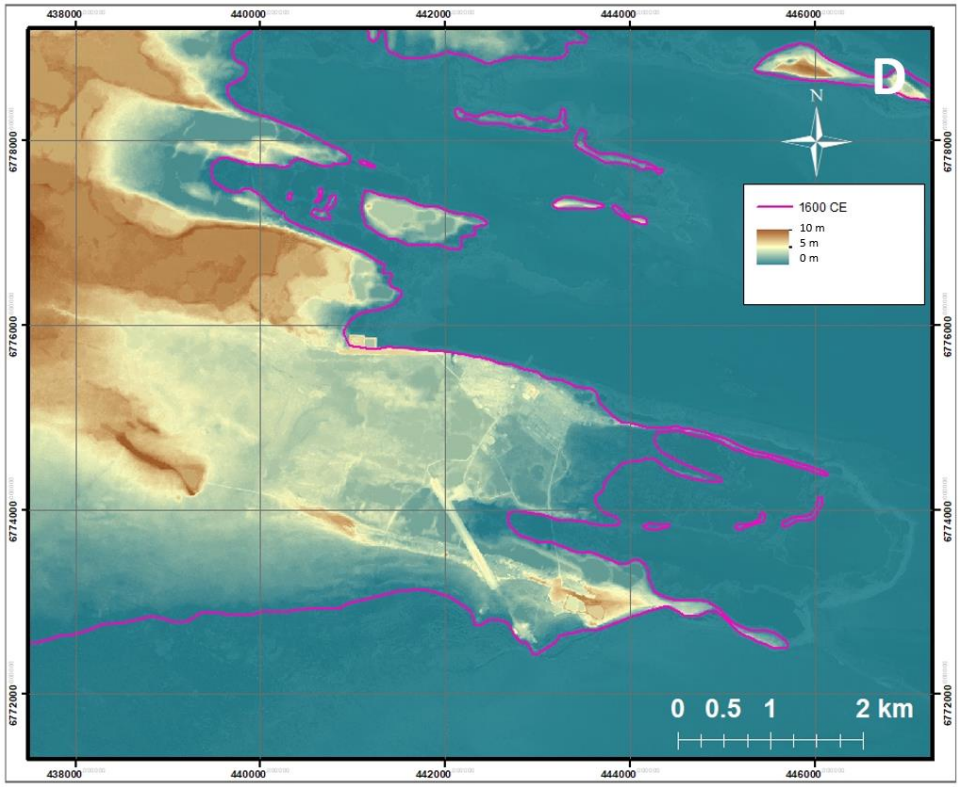
D
N
1600 CE
10 m
5 m
0 m
0 0.5 1 2 km
438000
440000
442000
444000
446000
6778000
6776000
6774000
6772000

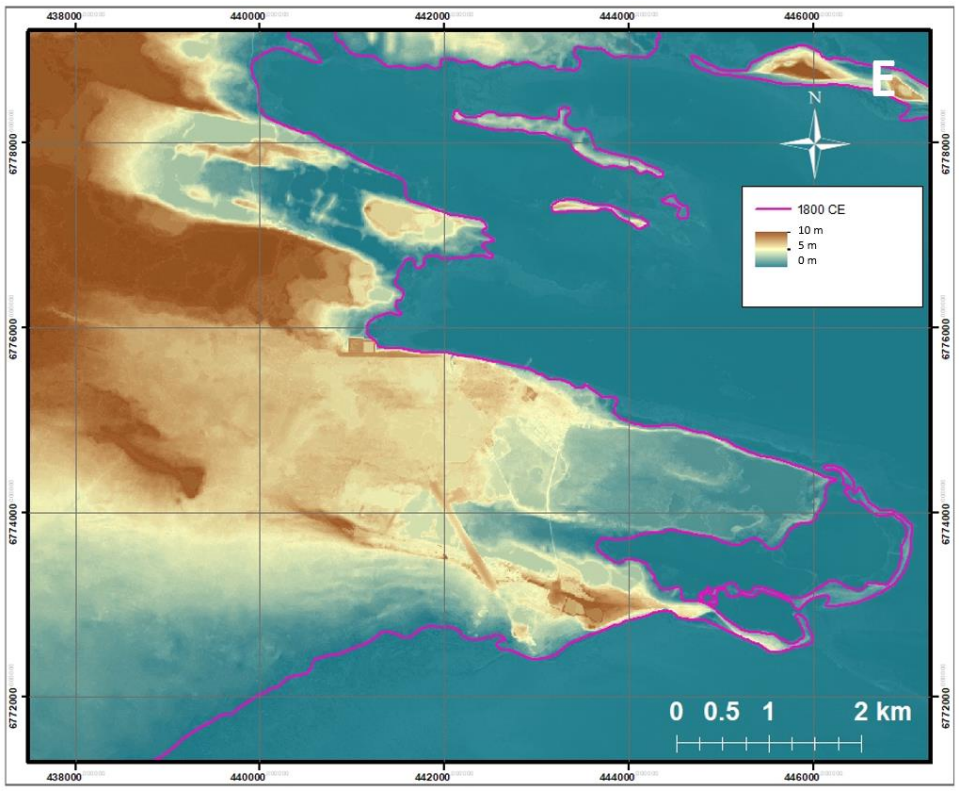
E
N
1800 CE
10 m
5 m
0 m
0 0.5 1 2 km
438000
440000
442000
444000
446000
6778000
6776000
6774000
6772000

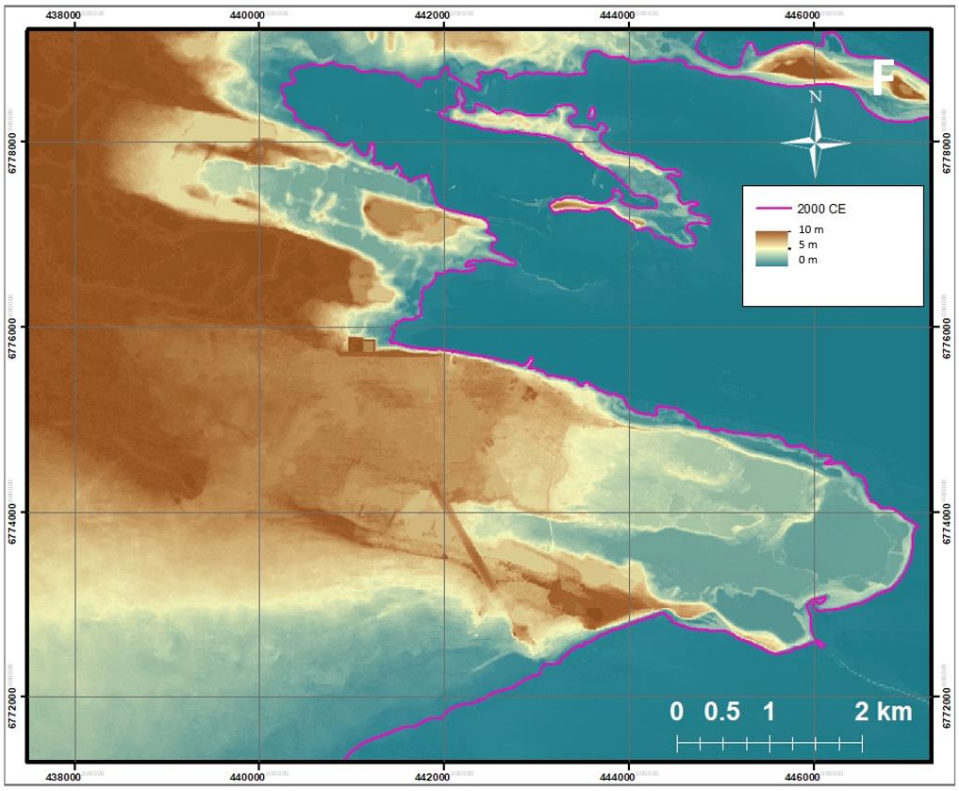
F
N
2000 CE
10 m
5 m
0 m
0 0.5 1 2 km
438000
440000
442000
444000
446000
6778000
6776000
6774000
6772000

Figure 2.28: Palaeoshoreline mapping from 1 ka to present at 200-year intervals (contains material ©3vGeomatics). The purple line in each panel denotes the contemporary MWL. Historical shorelines positions coinciding with areas of extensive anthropogenic modification, such as the airport and water reservoirs, were mapped using air photographs which predated anthropogenic development (contains material ©Digital Globe, 2011).

At 1 ka (Fig. 2.28A), approximately the year 1000 CE, most of 'Nuvuk' is submerged save for the highest section of the southern esker and a thin stretch of the northern esker. Tidal flats extend to the south of the southern esker and between the two eskers, with a series of lakes and ponds to the northwest, constrained by moraine ridges. One lone prominent island exists to the north within the study area, with several smaller islands just beginning to emerge. It is unknown how high the southern esker once rose above the modern landscape; much of it has been (and continues to be) excavated for aggregate. This anthropogenic imprint creates numerous landscape artefacts in the palaeogeography.

Moving 200 years closer to present, at about 1200 CE (Fig. 2.28B), 'Nuvuk' is starting to emerge. An extensive flat west of the modern townsite has now emerged and is flanked by the two dominant E-W eskers, although it is likely flooded intermittently. The site now occupied by the community and associated infrastructure begins to emerge. More small islands begin to shoal in the bay to the north of 'Nuvuk'. Coastal slopes are emerging, both between the northern and southern eskers as well as to the north. It is difficult to be precise about the location of the shoreline around the townsite at this time, due to the

anthropogenic re-working of the area during development. The modern townsite pad has been built up extensively using anthropogenic fill, leaving relief-positive artefacts in the DEM.

At about 1400 CE (Fig. 2.28C), the present townsite is likely almost completely emerged, although much of it is unsheltered and still prone to periodic marine flooding. Further south, the gap within the southern esker where tidal currents used to flow has completely emerged at this stage and the eastern section of the southern esker has transitioned from a shore-normal island to a long ridge extending into the bay. The islands to the north of 'Nuvuk' continue to grow and the northern tidal flats are interspersed with emergent ridges, further channelling flow and modifying wave refraction.

By about 1600 CE (Fig. 2.28D), the northern and southern eskers framing 'Nuvuk' have almost completely emerged, forming extended spits that mirror each other in orientation. The tidal flats of present day 'Nuvuk' are further confined between the two eskers due to transverse moraine ridge emergence. As well, the flats continue to expand progressively from the base of the southern esker along the western edge and southwards. All modern islands north of the community have emerged at this stage.

At about 1800 CE (Fig. 2.28E), the southeastern section of Nuvuk is the only remaining area still below high-water level and the landscape looks much the same as it does today,

save for the community infrastructure and aggregate extraction. Islands and lagoon complexes frame the submerged area to the east and southeast, attaching to the two eskers. At present, these former islands, in part, form the modern shoreline of 'Nuvuk', and the lagoons have become brackish lakes, in the process of transitioning to freshwater lakes (Fig 2.28F).

These palaeoshoreline mapping results are corroborated by a well-developed wave washover lobe, observed and sampled in 2009 (sample site 21 of Simon et al., 2014; mapped in Forbes et al., 2014a). This washover lobe contained marine algal material washed over the beach crest at about 9 m current elevation (Fig. 2.29), suggesting that RSL stood roughly 7 to 8 m above present sea level. The algal fragments had calibrated ^{14}C 2σ age ranges of (691-905) and (722-934) cal. years BP (median ages of 800 and 837 cal. yrs BP, respectively). Thus they place the active storm ridge at this point along the southern esker crest at approximately 1200 CE (Fig. 2.28B).

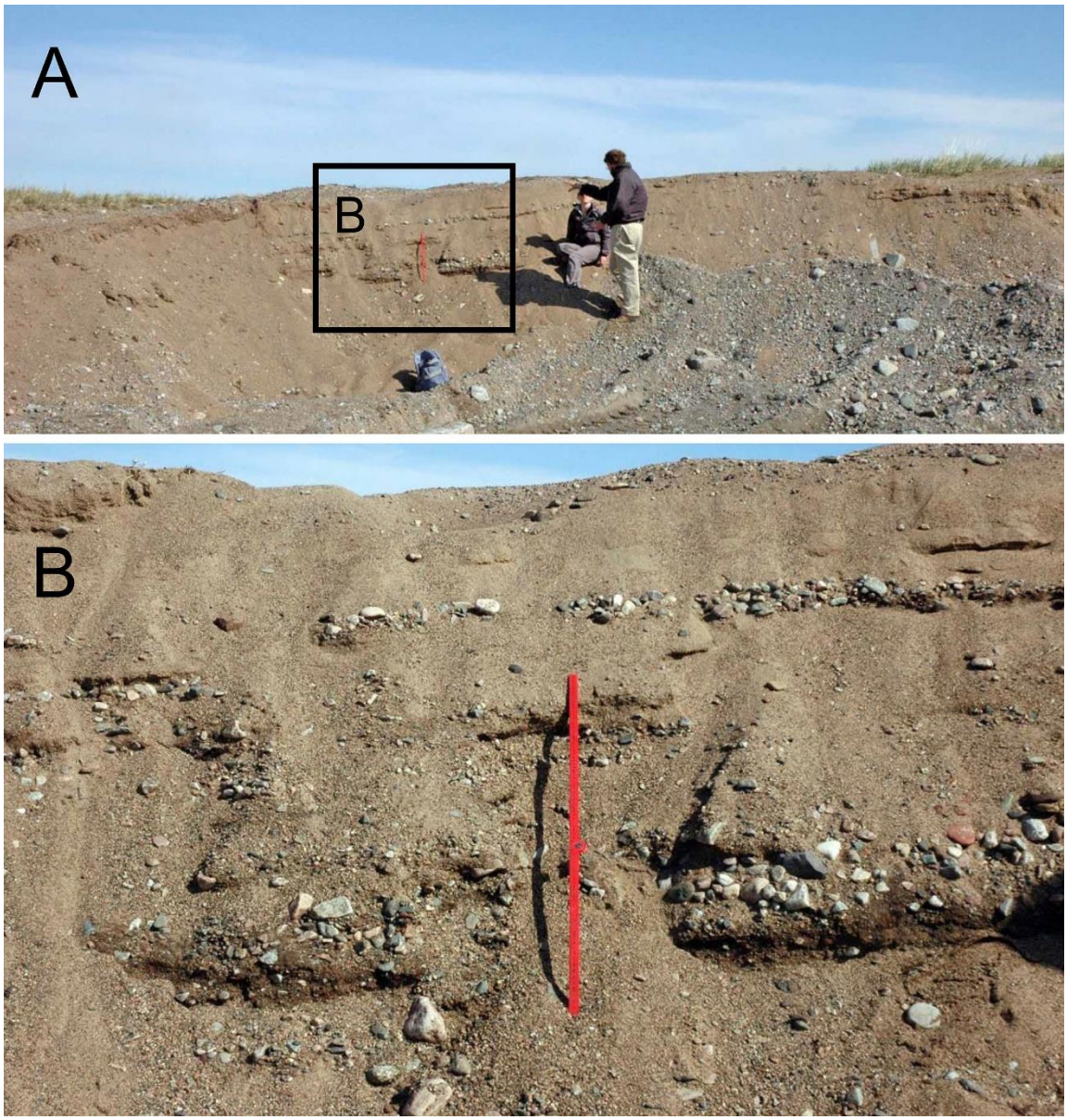

Figure 2.29: Washover (backbarrier) deposit ~9 m above sea level on the crest of the southern esker ridge, site 21 of Simons et al. (2014). Washover flow was from right to left and it deposited gently-sloping stratified sand and gravel with incorporated marine algae with median age of about 0.8 cal ka BP. Box in panel A shows location of panel B; exposed length of ruler ~0.8 m (photo courtesy D. Forbes).

2.5 Discussion

Given sufficient time, universal seaward shoreline advance is expected in any forced regression environment (Posamentier et al., 1992). It is largely due to our understanding of the principles of forced regression that much of the Arctic coastal zone is hypothesized to be at relatively low risk of marine hazard exposure under climate change conditions (Shaw et al., 1998b; Lemmen and Warren, 2016; Manson et al., 2019), as seaward shore advance reduces coastal sensitivity to erosion and storm events. Generally, the shoreline around Arviat has undergone such an advance since 1000 CE and earlier, and over the decades since 1960 (Figs 2.21, 2.22 and 2.28).

However, given that the local shoreline is almost entirely unconsolidated (Fig. 2.3), it is not surprising that coastal dynamics also play a significant role in shore-zone evolution. There are areas where shoreline advance is either under-predicted by RSL fall or the trend of advance is reversed (Figs. 2.23 and 2.27). This necessarily means that coastal evolution is occurring, in part, due to sediment mobilization, transport and deposition on a sufficient scale to reverse forced regressive shoreline trends.

Shoreline retreat in Arctic coastal environments can be the result of several variables. These include not only emergence/submergence trends, but also changing sediment supply from fluvial, cliff, dune or nearshore sites, increased wind and wave energy, shifting wave and wind incident angles, and reduced sea ice (Are et al., 2008; Bird, 2011;

St-Hilaire-Gravel et al., 2010, 2012). On submergent coasts with permafrost and excess ground ice, thermal degradation processes are sensitive to increasing air, ground, and sea-surface temperatures (e.g., Gunther et al., 2015; Fritz et al., 2017; Jones et al., 2018). On emergent coasts, the inception of permafrost in the subsurface of the shore-zone emerging from the marine environment is an additional factor affecting surface elevation and stability (e.g., Hansell et al., 1983; Boisson et al., 2020).

Given the spatially variable shoreline responses along the Arviat community shoreline over the study period, longshore sediment transport and sediment source-sink relationships are interpreted as an additional forcing agent of general shoreline change, superimposed on forced regression. Because the RSL change is locally constant, sediment transport and source-sink relationships are considered the primary forcing agent of local divergence in shoreline response. Sediment is being entrained and transported both from areas where erosion is taking place and from areas of shoreline advance where the rate is lower than that predicted by RSL fall (e.g., Fig. 2.23). Sediment is being deposited in areas where the rate of shoreline advance exceeds that predicted by RSL (e.g., Figs 2.24 and 2.26). These divergent trends are strongly influenced by shoreline configuration, exposure, and alignment relative to wind, wave, and ice forcing. Additional variability may result from onshore sediment pathways, such as estuarine channels, wind transport, wave overtopping, and ice push, which can vary over relatively short distances (Reimnitz et al., 1990; Taylor and Frobel 2006).

Within this interpretive framework, the most prominent sediment source in the Arviat area is the eastward facing headland of 'Nuvuk' (segment E, Figs. 2.12 and 2.13). Wave runup at this headland is forming an erosional scarp and mobilizing sediment to the north and south alongshore (Fig. 2.23), where it is deposited in nearby sediment sinks: on the beachface, along the down-drift tails of spits, and in estuarine channels (e.g., segments D and F). Interestingly, there are only minor reductions in headland width at the erosive headland. This is likely due to the overtopping of the gravel storm ridge into the brackish lake to the west, and wave- and ice-processes pushing sand and gravel sediment onshore, migrating the entire headland ridge landward as opposed to strictly removing sediment from the segment and transporting it alongshore.

The degree of erosion along this east-facing section of 'Nuvuk' is linked primarily to the degree to which the shoreline is convex and exposed to incoming refracted waves from Hudson Bay. The greater the convex angle, the greater the degree of refraction focusing wave energy on the headland. With the ongoing increase in the length of the open-water season (Ford et al., 2016; Forbes et al., 2018), overall wave energy in western Hudson Bay can be expected to increase, promoting further erosion and landward shoreline migration in segment E, including the observed hotspots at the corners (Fig. 2.11).

Beyond the active wave-driven sediment transport taking place at the eastern end, various minor source-sink relationships are playing out along the drift-aligned southern section of

‘Nuvuk’. Where spit development is most active (Fig. 2.24), shifts from areas of sediment removal to areas of sediment deposition are a result of morphodynamic feedback related to longshore transport variability (e.g., Carter and Orford, 1991; Forbes et al., 1995; St-Hilaire-Gravel et al., 2012; Stéphan et al., 2018). During the same period that the spit was growing, it was cannibalizing its proximal section updrift, and material was also being removed downdrift as it approached the inflection point at the transition from segments C to B. In these areas the removal of material was sufficient to induce shoreline retreat (Fig. 2.24). These trends are in keeping with the temporal and alongshore variability in sediment transport and associated cell development (Carter and Orford, 1991). Slow variation in shoreline configuration as RSL continues to fall will lead to changes in the loci of sediment deposition, as has occurred in the past with the formation of three spit ridges (Fig. 2.24).

In some areas where the shoreline is discontinuous, coastal evolution seems to be more heavily influenced by forced regression. Most prominent are areas of the foreshore where estuarine channels have infilled with sediment and the shoreline has generally advanced seaward (e.g., segments D and F). If the enclosure of these channels was strictly unidirectional, they could be attributed to alongshore dynamics in the same way the spits are. However, since there is instead evidence of enclosure from both sides between 1960 and 2011 (e.g., Fig. 2.26), it is a process by which gradual shoreline abandonment through forced regression undoubtedly plays a major role. As the base level falls and the

sill elevation increases, the volume of water and sediment moving through the channel decreases and with it the impacts of alongshore currents on the shoreline change as well.

Projecting shoreline behaviour into the future, the hypothesis remains that most of the shoreline will continue to advance seaward due to forced regression. However, we must consider the possibility that present sediment source-sink relationships are incongruous with different timescales of shoreline evolution in a forced regression environment. The loss of estuarine channels to the backshore, activation/deactivation of sediment sources and sinks due to the vertically migrating wave base, and the terraced nature of the local shore zone will all play a role in forcing divergent and potentially acute changes in shore zone evolution.

For example, terraced tidal flats to the east and northeast of ‘Nuvuk’ will eventually be abandoned to the terrestrial environment. Most of these flats lie no more than 1.5 m below HWL at present and will become a part of the terrestrial environment if present trends persist (James et al., 2021). This would set up a new set of shoreline dynamics and effect dramatic changes in shoreline configuration. However, without a change in external factors, such as wave climate, this new shoreline would still be expected to follow observed patterns of erosion, centred around convex and eastward facing sections as well as south-facing cliff sections on the southeast shore of ‘Nuvuk’ (Figs. 2.8 and 2.12), and deposition centred around spit development north and south of ‘Nuvuk’ (Figs. 2.24 and

2.26). The abandonment of these terraced tidal flats will fuel the most dramatic change in local shoreline position on a human time scale.

Another, more subtle way in which shoreline dynamics may be affected moving forward is through the loss of sediment availability in the foreshore and nearshore, particularly if the rate of RSL fall diminishes or even reverses due to climate-driven global mean sea-level rise (James et al., 2014). Should the rate of emergence of previously submerged glacigenic sediment sources decrease, the sedimentary budget of the shoreline may decrease in turn and be necessarily recouped from the terrestrial environment. This process is already observable at the macro scale. Within Hudson Bay, inputs from rivers, subaerial coastal erosion, marine primary production, and atmospheric deposition only represent a third of known input into the basin (Kuzyk et al., 2009). The remainder is posited to be largely sourced from the migration of the coastal zone into the basin, continuously activating new sediment sources. It is thus useful to think of at least a portion of sediment sources in the sedimentary budget of a forced regression environment as stemming from the progressive activation of nearshore deposits (Fairbridge, 1961; St-Hilaire-Gravel et al., 2010). Then, when sediment is activated in the nearshore and migrates along vertical sediment pathways (into deeper water), it is eventually reactivated as the wave base subsequently lowers. This progressive combing of the shoreline seaward leads to sediment sinks gradually becoming sediment sources before they are either abandoned to the terrestrial environment or migrate along the vertical sediment pathway again (Ballantyne, 2002; St-Hilaire-Gravel et al., 2010).

This leads to the question of how much a slowdown of sediment activation through base level fall and wave base vertical migration would impact assumed trends of shoreline advance. Global mean sea level rise is predicted to reduce the rate of RSL fall in forced regression environments on a time scale relevant to engineering and community planning (James et al., 2014). This will cause a decrease in the rate of activation of nearshore glacigenic sediment sources, which could reduce net input into the coastal system. It remains to be seen how much effect this predicted slowdown in base level fall will have on local coastal sedimentary budgets, shoreline change and associated coastal hazards. An increase in the number and breadth of erosive reaches would not be unexpected.

These assumptions are consistent with principles of paraglacial geomorphology, the study of landforms and processes that are a legacy of glacial and deglacial sediment production (Forbes and Syvitski, 1994). The defining feature of paraglacial geomorphology is a timeline of early postglacial sediment abundance, followed by progressively diminishing sediment supply over spans of 10^1-10^4 years (Forbes, 2011b). As time from deglaciation increases, the system loses its paraglacial character through reworking of the glacigenic landforms and their available sediment by nonglacial processes. In a coastal paraglacial environment these processes are mostly marine. The timing and quantity of sediment availability in coastal paraglacial environments is determined by the disposition of glacigenic landforms relative to the coastline and by the relative exposure of these sediments to wave action through RSL change and shoreline change (Forbes and Syvitski, 1994).

The activation of new terrestrial glacigenic sediment sources with rising sea level in transgressive settings has been extensively investigated and accounts for a significant proportion of coastal sediment supply in many formerly glaciated areas (e.g., Forbes, 2011b; Orford et al., 2002). In contrast, the coastal paraglacial signal in a forced regressive context, wherein new glacigenic sources are located seaward and gradually become activated as they emerge above wave base, has received very little attention. This is one of the first studies to document the activation of large emergent glacigenic sediment sources to form a paraglacial coastal system under forced regression (see also Boisson and Allard, 2020).

In this context, the palaeoshoreline analysis presented in this study is particularly instructive (Fig. 2.28). As RSL has fallen, coastal sediment sources have been activated along the flanks of the local esker ridges for the past 1000 years, forming high-stand beaches with the same sediment size range, from sand to boulder, as seen along the coast today. These coarse gravel beaches are preserved on the slopes of high points along the esker ridge and terminal spits have repeatedly formed at progressively lower elevations at the downdrift end of successive longshore transport corridors on the southern esker flank (segment A). The intermediate beach deposits developed over this time have been reactivated, reworked, or buried under windblown sand.

As the rate of falling RSL has decreased over time, the rate of activation of new glacigenic sources may have diminished, promoting cannibalization and erosion. In the future, rising global mean sea level will continue to decrease and potentially reverse the rate of RSL fall in modern forced regression environments. This process will in turn result in a loss in available sediment, and has the potential to reduce the rate of shoreline advance where it is already occurring, shift areas in a state of shoreline advance to one of shoreline retreat, and increase the rate of shoreline retreat in areas already experiencing it.

These relationships may be clouded by the evolution of the continuous permafrost within the recently emerged marine sediments, although the potential for growth or subsequent degradation of excess ice in the coarse sediments of the Arviat municipality is limited. However, finer-grained deposits found primarily in the tidal flats and emergent flats between the esker ridges have a higher potential for permafrost aggradation (Hansell et al., 1983), near-surface ground ice development, and eventual susceptibility to a warming climate. Although the substrata of the Arviat area are unstudied, shell-bearing marine muds are exposed on the northern shore of the peninsula along the Arviat waterfront and these are susceptible to permafrost and ground-ice accumulation as they emerge. Similar deposits, exposed by channel incision below the bridge at the west end of town, have failed by slumping during heavy rainfall in the past (Forbes et al., 2014a). This confirms that some substrata present in the area do represent a potential geotechnical hazard. Combined with decreasing sea ice duration and extent, degrading permafrost in long-

emerged sediments may increase coastal susceptibility to high-energy storm wave events, and these events themselves may be increasing (Zhang et al., 2004).

Changes in the open-water season have the potential to increase wave energy independent of any changes to local storm climate. There has been a recent regional delay in freeze-up timing and a corresponding increase in the length of the open-water season (Scott and Marshall, 2010; Allard et al., 2014; Ford et al., 2016). Should these trends continue, more net wave energy will reach the shoreline and fuel further shoreline change. Erosive trends will be strengthened in areas such as the 'Nuvuk' headland, with potential repercussions downdrift along both sides of the peninsula.

2.6 Conclusions

The Arviat shoreline is, at present, largely undergoing advance at a geometric mean rate of 0.30 m/yr and maximum mean rate of 3.0 m/yr. However localised erosion is occurring, decreasing the rate of mean rate of shore advance above. In places erosion is even overwhelming forced regression conditions to cause local retreat (Fig. 2.27), at a geometric mean rate of 0.14 m/yr and maximum mean rate of 1.2 m/yr. Fortunately, the impacts on community infrastructure at present are limited. An expected decrease in the rate of forced regression (to an extent as yet uncertain; James et al., 2014, 2021), and climate-driven changes in marine forcing, could, however, exacerbate erosion in the areas already experiencing a degree of shoreline retreat.

The results of this study demonstrate that coastal dynamics within the Arviat region of western Hudson Bay are sufficiently energetic to counteract the expected effects of RSL fall in some reaches. Localized mobilization, transport, and deposition of sediment in the coastal zone are playing a significant role in the coastal evolution of the shoreline surrounding Arviat.

- The principal forcing agent for shoreline change around Arviat is forced regression of the shoreline.
- Longshore sediment transport and sediment source-sink relationships are an additional forcing agent of general shoreline change and the principal forcing agent of divergent shoreline change, superimposed on (and in isolated areas outstripping) forced regression.
- The largest sediment source for divergent shoreline evolution in the Arviat area is the eastward facing headland of ‘Nuvuk’, specifically the sands and gravels remobilized from erosion of the two emerging eskers.
- More limited source-sink pathways are a result of the development and evolution of drift-aligned beach systems along the northern and southern headland flanks.
- The local shore-zone systems and sediment sources may be abandoned by RSL fall in the near future and new ones will take their place, just as previous shore zones and sources have been abandoned and replaced.

- Palaeoshoreline reconstruction gives a preliminary understanding of expected changes to present shoreline configuration under RSL conditions.

2.7 References

Allard, M., Manson, G.K., & Mate, D.J. (2014). Reconnaissance assessment of landscape hazards and potential impacts of future climate change in Whale Cove, southern Nunavut. *Summary of Activities 2013,* Canada-Nunavut Geoscience Office, 171–182.

Are, F., Reimnitz, E., Grigoriev, M., Hubberten, H.W., & Rachold, V. (2008). The influence of cryogenic processes on the erosional Arctic shoreface. *Journal of Coastal Research*, 24(1), 110-121.

Asplin, M.G., Galley, R., Barber, D.G., & Prinsenberg, S. (2012). Fracture of summer perennial sea ice by ocean swell as a result of Arctic storms. *Journal of Geophysical Research: Oceans*, 117(C6).

Aylsworth, J. M., & Shilts, W. W. (1989). Bedforms of the Keewatin ice sheet, Canada. *Sedimentary Geology,* 62(2–4), 407-428.

Ballantyne, C.K. (2002). Paraglacial geomorphology. *Quaternary Science Reviews*, 21(18), 1935-2017.

Bird, E. (2011). *Coastal geomorphology: an introduction*. John Wiley & Sons.

Boisson, A. & Allard, M. (2020). Morphological and evolutionary patterns of emerging Arctic coastal landscapes: the case of northwestern Nunavik (Quebec, Canada). *Arctic Science*, 6, 488-508, https://doi.org/10.1139/as-2020-0002.

Boisson, A., Allard, M. & Sarrazin, D. (2020). Permafrost aggradation along the emerging eastern coast of Hudson Bay, Nunavik (northern Québec, Canada). *Permafrost and Periglacial Processes*, 31(1), 128-140, https://doi.org/10.1002/ppp.2033.

Brown, J., Ferrians, O.J., Jr., Heginbottom, J.A. & Melnikov, E.S. (2001). Circum-Arctic map of permafrost and ground ice conditions. National Snow and Ice Data Center, digital media, URL - gsg.uottawa.ca/data/open/svgmetadata/circum-arctic.pdf

Canadian Hydrographic Service (2021). Canadian Tide and Current Tables v. 4: Arctic and Hudson Bay. Fisheries and Oceans Canada, Ottawa, 92 p.

Carter, R.W.G., & Orford, J.D. (1991). The sedimentary organisation and behaviour of drift-aligned gravel barriers. In: N.C. Kraus, K.J. Gingerich, and D.L. Kreibel, (eds.), Coastal Sediments 91, Seattle, WA, American Society of Civil Engineers, New York, pp.

Catuneanu, O. (2002). Sequence stratigraphy of clastic systems: concepts, merits, and pitfalls. *Journal of African Earth Sciences*, 35(1), 1-43.

Church, J.A., Clark, P.U., Cazenave, A., Gregory, J.M., Jevrejeva, S., Levermann, A., Merrifield, M.A., Milne, M.A., Nerem, R.S., Nunn, P.D., Payne, A.J., Pfeffer,

W.T., Stammer, D., & Unnikrishnan, A.S. (2013). Sea level change. *Climate change*, pp. 1137-1216.

Comiso, J.C., Parkinson, C.L., Gersten, R., & Stock, L. (2008). Accelerated decline in the Arctic sea ice cover. *Geophysical Research Letters*, 35(1), LO1703.

Couture, N.J., Forbes, D.L., Fraser, P.R., Frobel, D., Jenner, K.A., Manson, G.K., Solomon, S.M., Szlavko, B., and Taylor, R.B., (2015). A Coastal Information System for the Southeastern Beaufort Sea, Yukon and Northwest Territories. Geological Survey of Canada, Open File 7778, 1 .zip file. doi:10.4095/295975

Cowell, P.J., & Thom, B.G. (1994). Morphodynamics of coastal evolution. In: R.W.G. Carter and C.D. Woodroffe (eds.) *Coastal Evolution. Late Quaternary shoreline morphodynamics*. Cambridge University Press, Cambridge, pp. 33-86.

Curray, J.R. (1964). Transgressions and regressions. In: R.L. Miller (ed.) *Papers in Marine Geology:* New York, Macmillan, pp. 175-203.

Dalton, A.S., Margold, M., Stokes, C.R., Tarasov, L., Dyke, A.S., Adams, R.S., Allard, S., Arends, H.E., Atkinson, N., Attig, J.W., Barnett, P.J., Barnett, R.L., Batterson, M., Bernatchez, P., Borns, H.W., Breckenridge, A., Briner, J.P., Brouard, E., Campbell, J.E., Carlson, A.E., Clague, J.J., Curry, B.B., Daigneault, R., Dubé-Loubert, H., Easterbrook, D.J., Franzi, D.A., Friedrich, H.G., Funder, S., Gauthier, M.S., Gowan, A.S., Harris, K.L., Hétu, B., Hooyer, T.S., Jennings, C.E., Johnson, M.D., Kehew, A.E., Kelley, S.E., Kerr, D., King, E.L., Kjeldsen, K.K., Knaeble, A.L., Lajeunesse, P., Lakeman, T.R., Lamothe, M., Larson, P., Lavoie, M., Loope,

H.M., Lowell, T.V., Lusardi, B.A., Manz, L., McMartin, I., Nixon, F.C., Occhietti, S., Parkhill, M.A., Piper, D.J.W., Pronk, A.G., Richard, P.J.H., Ridge, J.C.R., Ross, M., Roy, M., Seaman, A., Shaw, J., Stea, R.R., Teller, J.T., Thompson, W.B., Thorleifson, L.H., Utting, D.J., & Wright Jr, H. E. (2020). An updated radiocarbon-based ice margin chronology for the last deglaciation of the North American Ice Sheet Complex. *Quaternary Science Reviews*, 234, 106223.

Dyke, A.S. (2004). An outline of North American deglaciation with emphasis on central and northern Canada. In Gibbard, P.L. & Ehlers, P. (eds.) *Quaternary Glaciations: Extent and Chronology*, Amsterdam, Boston, pp. 373-424.

Dyke, A.S., Andrews, J.T., Clark, P.U., England, J.H., Miller, G.H., Shaw, J., & Veillette, J.J. (2002). The Laurentide and Innuitian ice sheets during the last glacial maximum. *Quaternary Science Reviews*, 21(1–3), 9-31.

Environment Canada (2018). Canadian climate normals (1981-2010); Environment Canada, URL <https://climate.weather.gc.ca/climate_normals/index_e.html > Accessed 24 Apr 2021.

Fairbridge, R.W. (1961). Eustatic changes in sea level. *Physics and Chemistry of the Earth*, 4, 99-185.

Forbes, D.L. (editor). (2011a). State of the Arctic Coast 2010 – Scientific Review and Outlook. International Arctic Science Committee, Land-Ocean Interactions in the Coastal Zone, Arctic Monitoring and Assessment Programme, International

Permafrost Association. Helmholtz- Zentrum, Geesthacht, Germany, 178 p. http://arcticcoasts.org

Forbes, D.L. (2011b) Glaciated Coasts. In: Wolanski E. and McLusky D.S. (eds.) *Treatise on Estuarine and Coastal Science*, Vol 3, pp. 223–243. Waltham: Academic Press.

Forbes, D.L., & Syvitski, J.P.M., (1994). Paraglacial coasts. In: Carter, R.W.G., Woodroffe, C.D. (eds.), *Coastal Evolution. Late Quaternary Shoreline Morphodynamics*, Cambridge University Press, Cambridge, pp. 373–424.

Forbes, D.L., Orford, J.D., Carter, R.W.G., Shaw, J., & Jennings, S.C. (1995). Morphodynamic evolution, self-organisation, and instability of coarse-clastic barriers on paraglacial coasts. *Marine Geology*, 126(1), 63-85.

Forbes, D.L., Bell, T., James, T.S., & Simon, K.M. (2014). Reconnaissance assessment of landscape hazards and potential impacts of future climate change in Arviat, southern Nunavut. *Summary of Activities 2013*, Canada-Nunavut Geoscience Office, pp. 183–192.

Forbes, D.L., Bell, T., Manson, G.K., Couture, N.J., Cowan, B., Deering, R.L., Hatcher, S.V., Misiuk, B. and St-Hilaire-Gravel, D. (2018). Coastal environments and drivers. In: Bell, T. and Brown, T.M. (editors). *From Science to Policy in the Eastern Canadian Arctic: an Integrated Regional Impact Study (IRIS) of Climate Change and Modernization*. ArcticNet, Québec, 210-249

(http://www.arcticnet.ulaval.ca/pdf/media/29170_IRIS_East_full%20report_web.pdf).

Ford, J.D., Bell, T., & St-Hilaire-Gravel, D. (2010). Vulnerability of community infrastructure to climate change in Nunavut: a case study from Arctic Bay. In Community Adaptation and Vulnerability in Arctic Regions (G.K. Hovelsrud & Barry Smit, Eds.). Springer, Dordrecht, 107-130.

Ford, J.D., Bell, T., & Couture, N.J. (2016). Perspectives on Canada's North Coast region. in Canada's Marine Coasts in a Changing Climate, (D.S. Lemmen, F.J. Warren, T.S. James and C.S.L. Mercer Clarke, Eds.); Government of Canada, Ottawa, ON, 153-206.

Fraser, C., Hill, P., & Allard, M. (2005). Morphology and facies architecture of a falling sea level strandplain, Umiujaq, Hudson Bay, Canada. *Sedimentology,* 52(1), 141-160.

Fritz, M., Vonk, J.E. & Lantuit, H. (2017). Collapsing Arctic coastlines. *Nature Climate Change*, 7(1), 6-7, https://doi.org/10.1038/nclimate3188.

Gunther, F., Overduin, P.P., Yakshina I.A., Opel, T., Baranskaya, A.V., & Grigoriev, M.N. (2015). Observing Muostakh disappear: permafrosdt thaw subsidence and erosion of a ground-ice-rich island in response to Arctic summer warming and sea ice reduction, *The Cryosphere*, 9(1), 151-178, https://doi.org/10.5194/tc-9-151-2015.

Hart, B.S., & Long, B.F. (1996). Forced regressions and lowstand deltas: Holocene Canadian examples. *Journal of Sedimentary Research*, 66(4).

Hansell, R.I.C., Scott, P.A., Staniforth, R. & Svoboda, J. (1983). Permafrost development in the intertidal zone at Churchill, Manitoba: a possible mechanism for accelerated beach uplift. *Arctic*, 36(2), 196-203.

James, T.S., Henton, J.A., Leonard, L.J., Darlington, A., Forbes, D.L., & Craymer, M., (2014). Relative Sea level Projections in Canada and the Adjacent Mainland United States; Geological Survey of Canada, Open File 7737, 72 p. doi:10.4095/295574

James, T.S., Henton, J.A., Leonard, L.J., Darlington, A., Forbes, D.L., & Craymer, M., (2015). Tabulated values of relative sea-level projections in Canada and the adjacent mainland United States. Geological Survey of Canada, Open File 7942, 81 p. doi: 10.4095/297048

James, T.S., Robin, C., Henton, J.A. and Craymer, M. (2021). Relative sea-level projections for Canada based on the IPCC Fifth Assessment Report and the NAD83v70VG national crustal velocity model. Geological Survey of Canada, Open File 8764, 1 zip file, https://doi.org/10.4095/327878

Jones, B.M., Farquharson, L.M., Baughman, C.A., Buzard, R.M., Arp, C.D., Grosse, G., Bull D.L, Günther, F., Nitze, I., Urban, F., Kasper, J.L., Frederick, J.M., Thomas, M., Jones, C., Mota, A., Dallimore, S., Tweedie, C., Maio, C., Mann, D.H., Richmond, B., Gibbs, A., Xiao, M., Sachs, T., Iwahanam, G., Kanevskiy, M., &

Romanovksy, V.E. (2018). A decade of remotely sensed observations highlight complex processes linked to coastal permafrost bluff erosion in the Artic. *Environmental Research Letters*, 13(11), 115001, https://doi.org/10.1088/1748-9326/aae471

Kuzyk, Z.A., Macdonald, R.W., Johannessen, S.C., Gobeil, C. & Stern, G.A., (2009). Towards a sediment and organic carbon budget for Hudson Bay. *Marine Geology*, 264(3-4): 190-208.

Lantuit, H., & Pollard, W. H. (2008). Fifty years of coastal erosion and retrogressive thaw slump activity on Herschel Island, southern Beaufort Sea, Yukon Territory, Canada. *Geomorphology*, 95(1), 84-102.

Lantuit, H., Overduin, P.P., Couture, N., Wetterich, S., Aré, F., Atkinson, D., Brown, J., Cherkashov, G., Drozdov, D., Forbes, D.L., Graves-Gaylord, A., Grigoriev, M., Hubberten, H.W., Jordan, J., Jorgensen. T., Ødegård, R.S., Ogorodov, S., Pollard, W.H., Rachold, V., Sedenko, S., Solomon, S., Steenhuisen, F., Streletskaya, I & Vasiliev, A. (2012). The Arctic Coastal Dynamics database: A new classification scheme and statistics on Arctic permafrost coastlines. *Estuaries and Coasts*, 35(2), 383-400.

Lavoie, C., Allard, M., & Hill, P. R. (2002). Holocene deltaic sedimentation along an emerging coast: Nastapoka River delta, eastern Hudson Bay, Quebec. *Canadian Journal of Earth Sciences*, 39(4), 505-518.

Lemmen, D.S. & Warren, F.J. (2016). Synthesis. In Lemmen, D. S., Warren, F. J., James, T. S. & Mercer Clarke, C. S. L. (eds.) *Canada's Marine Coasts in a Changing Climate*, Government of Canada, Ottawa, ON, 17-26.

Manson, G.K., Couture, N.J., & James, T.S., (2019). CanCoast Version 2.0: data and indices to describe the sensitivity of Canada's marine coasts to changing climate. Geological Survey of Canada, Open File 8551, 1 .zip file. https://doi.org/10.4095/314669

Mason, O.K. (2010). Beach ridge geomorphology at Cape Grinnell, northern Greenland: a less icy Arctic in the mid-Holocene. *Geografisk Tidsskrift/ Danish Journal of Geography*, 110(2), 337-355.

McMartin, I., Godbout, P.M., Campbell, J.E., Tremblay, T., & Behnia, P. (2021). A new map of glacigenic features and glacial landsystems in central mainland Nunavut, Canada. *Boreas*, 50(1), 51-75.

Mitrovica, J.X., Gomez, N., Morrow, E., Hay, C., Latychev, K., & Tamisiea, M.E. (2011). On the robustness of predictions of sea level fingerprints. *Geophysical Journal International*, 187(2), 729-742.

Møller, J.J., Yevzerov, V.Y., Kolka, V.V., & Corner, G.D. (2002). Holocene raised-beach ridges and sea-ice-pushed boulders on the Kola Peninsula, northwest Russia: indicators of climatic change. *The Holocene*, 12(2), 169-176.

Orford, J.D., Forbes D.L., & Jennings, S.C. (2002). Organisational controls, typologies and time scales of paraglacial gravel-dominated coastal systems. *Geomorphology*, 48, 51-85.

Peltier, W.R., (2004). Global Glacial Isostasy and the Surface of the Ice-Age Earth: The ICE-5G (VM2) Model and GRACE. *Annual Review of Earth and Planetary Sciences*, 32(1), 111-149.

Posamentier, H.W., Allen, G.P., James, D.P., & Tesson, M. (1992). Forced regressions in a sequence stratigraphic framework: concepts, examples, and exploration significance (1). *AAPG Bulletin*, 76(11), 1687-1709.

Reimnitz, E., Barnes, P.W., & Harper, J.R. (1990). A review of beach nourishment from ice transport of shoreface materials, Beaufort Sea, Alaska. *Journal of Coastal Research*, 6(2), 439-469.

Robin, C.M.I., Craymer, M., Ferland, R., James, T.S., Lapelle, E., Piraszewski, M., & Zhao, Y. (2020). NAD83v70VG: A new national crustal velocity model for Canada. Geomatics Canada, Open File 0062, 1. zip file. https://doi.org/10.4095/327592

Ruz, M.H., Allard, M., Michaud, Y., & Hequette, A. (1998). Sedimentology and evolution of subarctic tidal flats along a rapidly emerging coast, eastern Hudson Bay, Canada. *Journal of Coastal Research*, 1242-1254.

Sanjaume, E. & Tolgensbakk, J. (2009). Beach ridges from the Varanger Peninsula (Arctic Norwegian coast): characteristics and significance. *Geomorphology* 104(1-2), 82-92.

Scott, J. & Marshall, G. (2010). A step-change in the date of sea-ice breakup in western Hudson Bay. *Arctic*. 63(2), 155-164.

Shaw, J., Taylor, R.B. Forbes, D.L., Ruz, M-H., & Solomon, S. (1998a). Sensitivity of the Coasts of Canada to Sea-Level Rise. Geological Survey of Canada, Bulletin 505, 79 p. +map.

Shaw, J., Taylor, R.B., Solomon, S., Christian, H.A., & Forbes, D.L. (1998b). Potential impacts of global sea-level rise on Canadian coasts. *The Canadian Geographer/Le Géographe canadien*, 42(4), 365-379.

Sherin, A.G., & Edwardson, K.A. (1996). A coastal information system for the Atlantic Provinces of Canada. *Marine Technology Society. Marine Technology Society Journal*, 30(4), 20-27.

Simon, K.M., James, T.S., Forbes, D.L., Telka, A.M., Dyke, A.S., & Henton, J.A. (2014). A relative sea-level history for Arviat, Nunavut, and implications for Laurentide Ice Sheet thickness west of Hudson Bay. *Quaternary Research*, 82(1), 185-197.

St-Hilaire-Gravel, D., Bell, T., & Forbes, D.L. (2010). Raised gravel beaches as proxy indicators of past sea-ice and wave conditions, Lowther Island, Canadian Arctic Archipelago. *Arctic*, 63(2), 213-226.

St-Hilaire-Gravel, D., Forbes, D.L., & Bell, T. (2012). Multitemporal analysis of a gravel-dominated coastline in the central Canadian Arctic Archipelago. *Journal of Coastal Research*, 28(2), 421-441.

Stéphan, P., Suarez, S., Fishaut, B., Autret, R., Blaise, E., Houson, J., Ammann, J., & Grandjean, P. (2018). Monitoring the medium-term retreat of a gravel spit barrier and management strategies, Sillon de Talbert (North Brittany, France). *Ocean & Coastal Management*, 158, 64-82, https://doi.org/10.1016/j.ocecoaman.2018.03.030

Tella, S., Paul, D., Berman, R.G., Davis, W.J., Peterson, T.D., Pehrsson, S.J. & Kerswill, J.A. 2007: Bedrock geology compilation and regional synthesis of parts of the Hearne and Rae domains, Western Churchill Province, Nunavut- Manitoba; Geological Survey of Canada, Open File 5441, scale 1:550 000.

Thieler, E.R., Himmelstoss, E.A., Zichichi, J.L., & Ergul, A. (2009). *The Digital Shoreline Analysis System (DSAS) version 4.0-an ArcGIS extension for calculating shoreline change* (No. 2008-1278). US Geological Survey.

Van Everdingen, R.O. (1998). *Multi-language glossary of permafrost and related ground-ice terms*. Arctic Institute of North America, University of Calgary.

Wright, L.D. & Thom, B.G. (1977). Coastal depositional landforms: a morphodynamic approach. *Progress in Physical Geography*, 1(3), 412-459.

Zhang, X., Walsh, J.E., Zhang, J., Bhatt, U.S., & Ikeda, M. (2004). Climatology and interannual variability of Arctic cyclone activity: 1948–2002. *Journal of Climate*, 17(12), 2300-2317.

CHAPTER 3: CONCLUSION

3.1 Summary

The goal of this study was to improve scientific understanding of the forms, materials, and shoreline evolution of an emergent Arctic coastal paraglacial system (Forbes et al., 2014). Given that the principles of forced regression are understood as the key forcing agent counteracting shoreline retreat and coastal hazard exposure in the central Canadian Arctic, this study stands out as one of the first contributions to an understudied field in a poorly documented region (Shaw et al., 1998; Lemmen and Warren, 2016). While forced regression principles may be relevant over sufficiently large temporal and spatial scales, this does not necessarily mean that they hold up at scales relevant for human use (Posamentier et al., 1992; Wright and Tom, 1994).

To accomplish this study goal, field and remotely sensed data were acquired and analyzed within the municipal boundary of Arviat, Nunavut, part of an emergent glacial sedimentary plain in the central Canadian Arctic. The foreshore and backshore within the municipal boundary were characterized and historical shoreline change around the community was analyzed. Within the study area, shoreline advance predominated over shoreline retreat, as predicted by the forced regression conditions of the environment. However, coastal dynamics have also been sufficiently energetic to reduce the rate of shoreline advance, or even reverse these trends in favour of shoreline retreat along select reaches of the shoreline.

The principal forcing agent for shoreline change within this region is forced regression, as predicted by the distribution of glacio-isostatic rebound and evidenced by the widespread occurrence of raised beach deposits west of the modern Hudson Bay shoreline (Shaw et al., 1998; Dyke 2004; Simon et al., 2014). The steady base level fall experienced by the Arviat coastal environment is presently mitigating the effects of an increasingly energetic wave climate inferred from the lengthening of the open water season and increasing open water fetch (Forbes 2011; Allard et al., 2014). As such, the immediate risk to the community and its infrastructure imposed by coastal hazards is relatively low (Forbes et al., 2014). However, there are reaches of concern where shoreline retreat and reduced shoreline advance are occurring. As the open water season continues to expand, wave action will have more time with which to mobilize sediment along the shoreline and storm events will have more opportunities where the shoreline is unprotected by seasonal ice cover (Zhang et al., 2004).

As well, expected changes to the rate of forced regression within this century because of accelerating global sea-level rise will impact local RSL and shoreline evolution trends (James et al., 2021). Changes to RSL will influence the availability of sediment sources in the foreshore and nearshore. Where once these sediment sources were consistently activated by falling RSL, a decreasing rate of activation of these sources will have effects on the sedimentary budget of the coastal environment. Slowing RSL fall will not necessarily decrease sediment availability, depending on local conditions, as this process will also expose available sediment sources to wave energy for longer periods of time, in

turn prolonging the process of morphodynamic adjustment along these reaches (Cowell and Thom, 1994).

The results of this study demonstrate that coastal dynamics along this section of western Hudson Bay are presently sufficiently energetic to counteract the results of forced regression along some reaches, despite one of the most rapid rates of glacioisostatic rebound in the world (James et al., 2021). Localized mobilization, transport and deposition of sediment in the coastal zone are still playing a significant role in the coastal evolution of the shoreline surrounding Arviat. A reversal in local and regional RSL trends resulting from the most extreme climate scenarios and sea-level projections (James et al., 2014) would result in dramatic changes in the shoreline response in western Hudson Bay.

With respect to impacts on Arviat's coastal infrastructure driven by shoreline adjustment, the expected short-term impacts are relatively minor. There is an observation tower located at the eastern headland that may be undercut by shoreline erosion, but infrastructure around the community proper remains at low risk at present. Limited silt-sand exposures have grain-size distributions consistent with glaciomarine offshore samples taken from the modern terrestrial environment (Forbes et al., 2014). So at least some of the coarser sand and gravel beach material present is a veneer overlying at least some finer grained substrata. More prolonged exposure to wave action due to slowing forced regression (exacerbated by climate change and reduced sea ice) could

disproportionately impact shoreline trends and cause a more rapid change to an erosive state in reaches containing these finer-grained strata. Without improved knowledge of the local sedimentary stratigraphy, these potential hazard exposures are presently undefined. If, on the other hand, RSL fall continues apace, shoaling in the bay and surrounding coastal environment could pose a hazard to marine traffic in the area (Tsuji et al., 2009). This would have the potential to affect the entire community through adverse impacts on subsistence lifestyles and navigational hazards for the annual sea lift, which resupplies most of the community's bulk goods for the year.

3.2 Future Directions

The findings from this study could be supported and built upon in several ways. It is worth remembering that although the relationships outlined may seem straightforward, they are limited by the two-time slices for which we have data and observations. It is entirely reasonable and probable that the coastal dynamics of the Arviat region have shifted through space and time, in response to variables such as seasonal changes, storm activity, anthropogenic activity, and the morphodynamic evolution of the shoreline (Carter and Woodroffe 1994; Forbes, 2011). In the coming years there will be increased extent and duration of open water, which will increase open water fetch for storm winds and thus will increase the frequency and energy of surface waves, with direct implications for sediment reworking and coastal stability (Forbes, 2011).

The temporal range of data acquisition and analysis could be broadened. Repetition of the in situ and remote sensing surveys completed in this study would improve understanding of coastal evolutionary trends and variability. Transect reoccupation before and after storm events would improve understanding of shoreline response to acute, high-energy events with the potential to move large amounts of sediment over short periods of time (St. Hilaire-Gravel et al., 2012). As well, re-mapping the planform shoreline position using future satellite imagery would provide a clearer picture of the consistency of past trends and help clarify our capacity to accurately predict future shoreline change.

The acquisition of nearshore bathymetric and sedimentary data in the coastal zone of Arviat would provide a more complete understanding of active coastal processes and sediment transport pathways. Nearshore morphology plays an important role in conditioning morphodynamic processes generated in the offshore by waves and currents (Cowell and Thom, 1994). Such data could be obtained through shallow acoustic seabed mapping technologies or bathymetric LiDAR, producing data which could also have significant cross-over value for regional benthic ecology studies (Brown et al., 2011). As well, stratigraphic studies could help confirm the applicability of forced regression coastal allostratigraphy models, based upon the existence of discontinuities between stratigraphic sequences, generated on the eastern shore of Hudson Bay, marked by coarse-grained upper shoreface deposits that gradually trend to finer grained shoreface deposits downslope (Fraser et al., 2005). The specific local response may be constrained by

decreasing accommodation space, which is occurring as a result of RSL fall and is a partial product of the emerging seabed morphology.

Observing changes in local sea level would determine whether eustatic sea level rise is keeping pace with or outstripping glacioisostatic rebound for Arviat and the western Hudson Bay region (James et al., 2021). Were this to occur, dramatic changes in shoreline behaviour would likely result, with a shift from generally advancing to retreating shorelines (Forbes et al., 2014) and large-scale shifts in coastal evolutionary trends would not be unexpected.

Coastal environments with highly indented shorelines may have particularly divergent shoreline responses over relatively short distances, due to greater variability in longshore sediment transport and in shoreline exposure. Further study of glacial coastlines such as Arviat, with ice-flow parallel and perpendicular landforms left in close proximity, would improve our understanding of the degree to which divergent paraglacial shoreline change depends on this fractal dimension.

The results from this study effectively complement scientific understanding of the current and future exposure sensitivities to coastal hazards in forced regression environments (Ford et al., 2010). The proper identification and characterization of the nature of exposure-sensitivities can in turn help identify effective adaptations in the face of a

changing environment. Researchers and community planners cannot dismiss the potential for shoreline erosion in forced regression environments out of hand.

3.3 Concluding Remarks

Although the principles of forced regression remain a valid starting point for understanding the evolution of emergent paraglacial environments, coastal dynamics can be sufficiently energetic to counteract the expected results under the appropriate circumstances. Coastal environments that are unconsolidated, undergoing rapid RSL change and that have been recently exposed to morphodynamic coastal evolutionary feedback may undergo more rapid shoreline adjustment than areas of RSL stability.

Sediment mobilization, transport and deposition are important components of coastal evolution despite rapid RSL fall and stand to make a greater contribution to shoreline evolution as rates of regional and local RSL fall diminish or potentially reverse in the coming century. Further study is necessary to confirm observed trends, and to better understand the ways in which the evolution of emergent paraglacial coastal environments will be modified moving forward.

3.4 References

Allard, M., Manson, G.K., & Mate, D.J. (2014). Reconnaissance assessment of landscape hazards and potential impacts of future climate change in Whale Cove, southern Nunavut. *Summary of Activities 2013,* Canada-Nunavut Geoscience Office, 171–182.

Brown, C.J., Smith, S.J., Lawton, P., & Anderson, J.T. (2011). Benthic habitat mapping: A review of progress towards improved understanding of the spatial ecology of the seafloor using acoustic techniques. *Estuarine, Coastal and Shelf Science*, 92(3), 502-520.

Carter, R.W.G. & Woodroffe, C.D. (1994). Coastal evolution: an introduction. In: R.W.G. Carter and C.D. Woodroffe (eds) *Coastal Evolution. Late Quaternary shoreline morphodynamics*. Cambridge University Press, Cambridge.

Cowell, P.J., & Thom, B.G. (1994). Morphodynamics of coastal evolution. In: R.W.G. Carter and C.D. Woodroffe (eds.) *Coastal Evolution. Late Quaternary shoreline morphodynamics*. Cambridge University Press, Cambridge.

Dyke, A.S. (2004). An outline of North American deglaciation with emphasis on central and northern Canada. In Gibbard, P.L. & Ehlers, P. (eds.) *Quaternary Glaciations: Extent and Chronology,* Amsterdam, Boston, pp. 373-424.

Forbes, D.L. (editor). (2011). State of the Arctic Coast 2010 – Scientific Review and Outlook. International Arctic Science Committee, Land-Ocean Interactions in the Coastal Zone, Arctic Monitoring and Assessment Programme, International

Permafrost Association. Helmholtz- Zentrum, Geesthacht, Germany, 178 p. http://arcticcoasts.org

Forbes, D.L., Bell, T., James, T.S., & Simon, K.M. (2014). Reconnaissance assessment of landscape hazards and potential impacts of future climate change in Arviat, southern Nunavut. *Summary of Activities 2013*, Canada-Nunavut Geoscience Office, pp. 183–192.

Ford, J.D., Bell, T., & St-Hilaire-Gravel, D. (2010). Vulnerability of community infrastructure to climate change in Nunavut: a case study from Arctic Bay. In Community Adaptation and Vulnerability in Arctic Regions (G.K. Hovelsrud & Barry Smit, Eds.). Springer, Dordrecht, 107-130.

Fraser, C., Hill, P., & Allard, M. (2005). Morphology and facies architecture of a falling sea level strandplain, Umiujaq, Hudson Bay, Canada. *Sedimentology,* 52(1), 141-160.

James, T.S., Henton, J.A., Leonard, L.J., Darlington, A., Forbes, D.L., & Craymer, M., (2014). Relative Sea level Projections in Canada and the Adjacent Mainland United States; Geological Survey of Canada, Open File 7737, 72 p. doi:10.4095/295574

James, T.S., Robin, C., Henton, J.A. and Craymer, M. (2021). Relative sea-level projections for Canada based on the IPCC Fifth Assessment Report and the NAD83v70VG national crustal velocity model. Geological Survey of Canada, Open File 8764, 1 zip file, https://doi.org/10.4095/327878

Lemmen, D.S. & Warren, F.J. (2016). Synthesis. In Lemmen, D. S., Warren, F. J., James, T. S. & Mercer Clarke, C. S. L. (eds.) *Canada's Marine Coasts in a Changing Climate*, Government of Canada, Ottawa, ON, 17-26.

Posamentier, H.W., Allen, G.P., James, D.P., & Tesson, M. (1992). Forced regressions in a sequence stratigraphic framework: concepts, examples, and exploration significance (1). *AAPG Bulletin*, 76(11), 1687-1709.

Shaw, J., Taylor, R.B., Solomon, S., Christian, H.A., & Forbes, D.L. (1998). Potential impacts of global sea-level rise on Canadian coasts. *The Canadian Geographer/Le Géographe canadien*, 42(4), 365-379.

St-Hilaire-Gravel, D., Forbes, D.L., & Bell, T. (2012). Multitemporal analysis of a gravel-dominated coastline in the central Canadian Arctic Archipelago. *Journal of Coastal Research*, 28(2), 421-441.

Tsuji, L.J., Gomez, N., Mitrovica, J.X., & Kendall, R. (2009). Post-glacial isostatic adjustment and global warming in subarctic Canada: implications for islands of the James Bay region. *Arctic*, 62(4), 458-467.

Wright, L.D. & Thom, B.G. (1977). Coastal depositional landforms: a morphodynamic approach. *Progress in Physical Geography*, 1(3), 412-459.

Zhang, X., Walsh, J.E., Zhang, J., Bhatt, U.S., & Ikeda, M. (2004). Climatology and interannual variability of Arctic cyclone activity: 1948–2002. *Journal of Climate*, 17(12), 2300-2317.

APPENDIX A: COASTAL TRANSECTS AND ANALYSIS

Figure A.1: Coastal transects of Arviat (contains material ©Digital Globe, 2011).

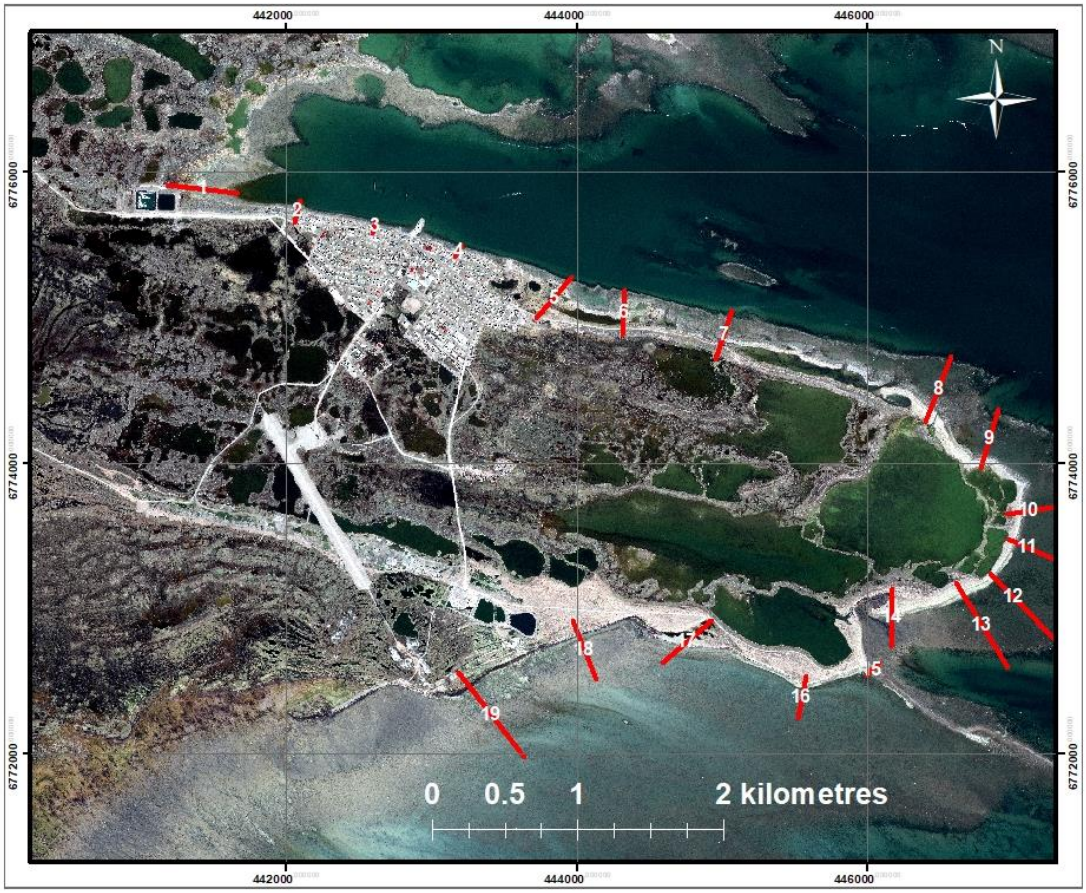

Transect #1

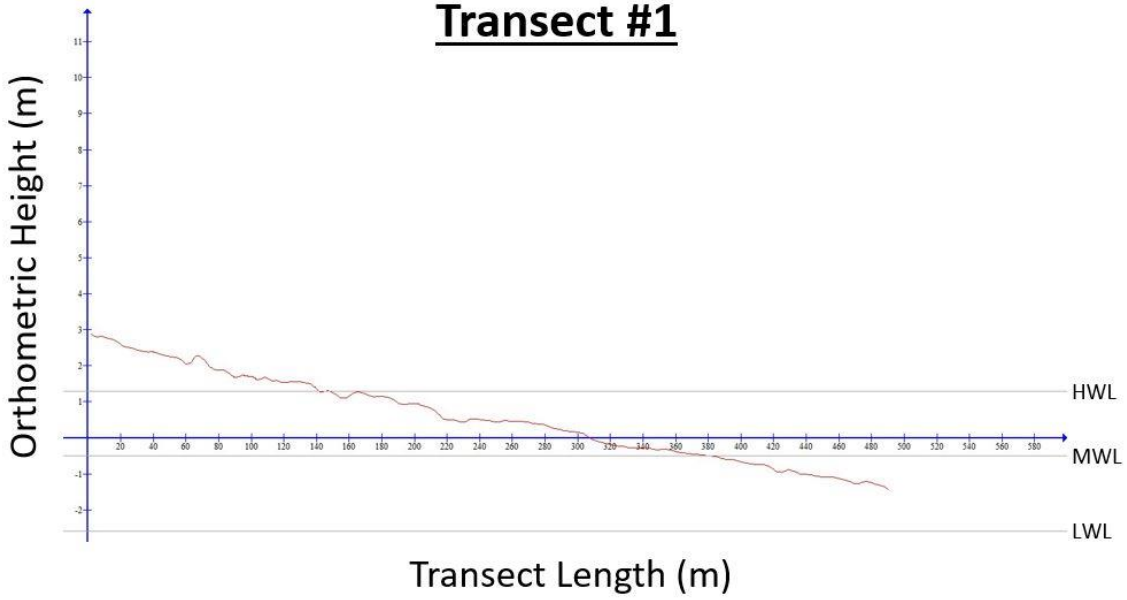

Transect #2

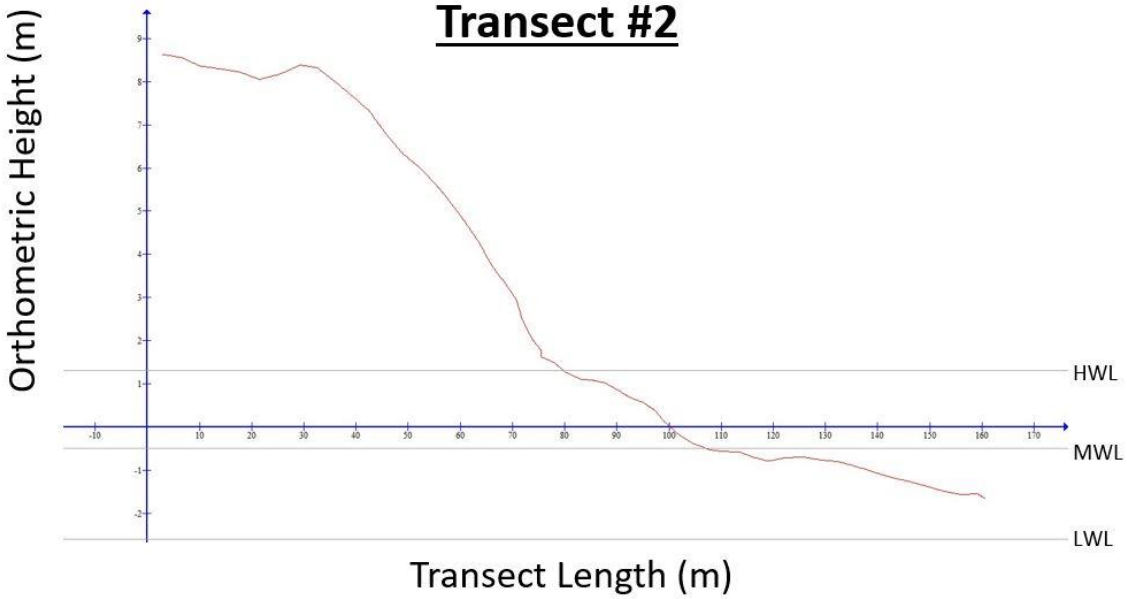

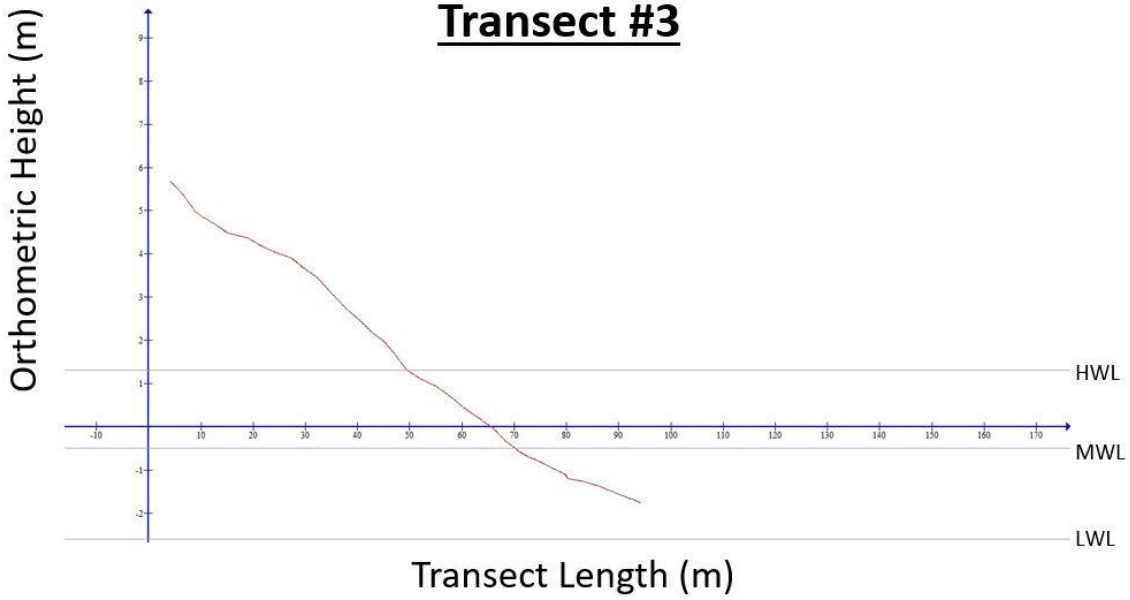
Transect #3
Orthometric Height (m)
HWL
MWL
LWL
Transect Length (m)

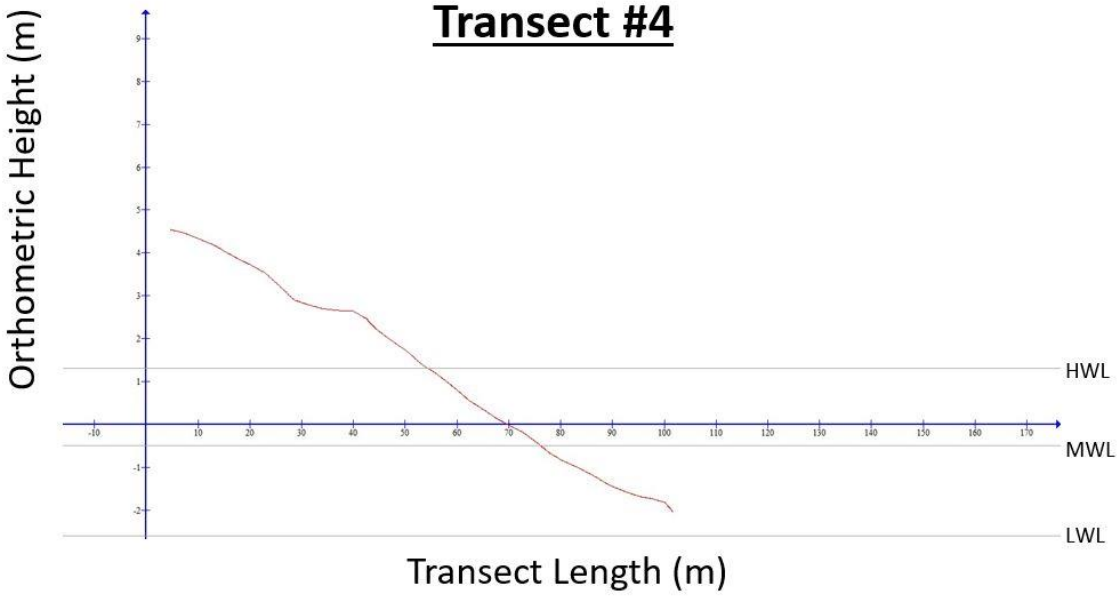
Transect #4
Orthometric Height (m)
HWL
MWL
LWL
Transect Length (m)

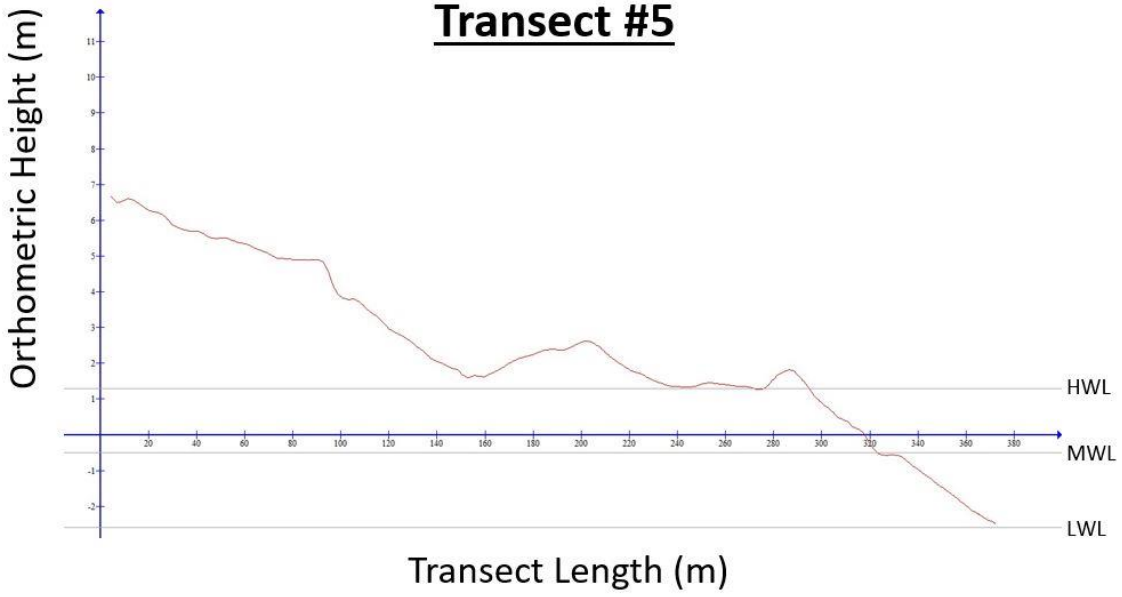
Transect #5
Orthometric Height (m)
HWL
MWL
LWL
Transect Length (m)

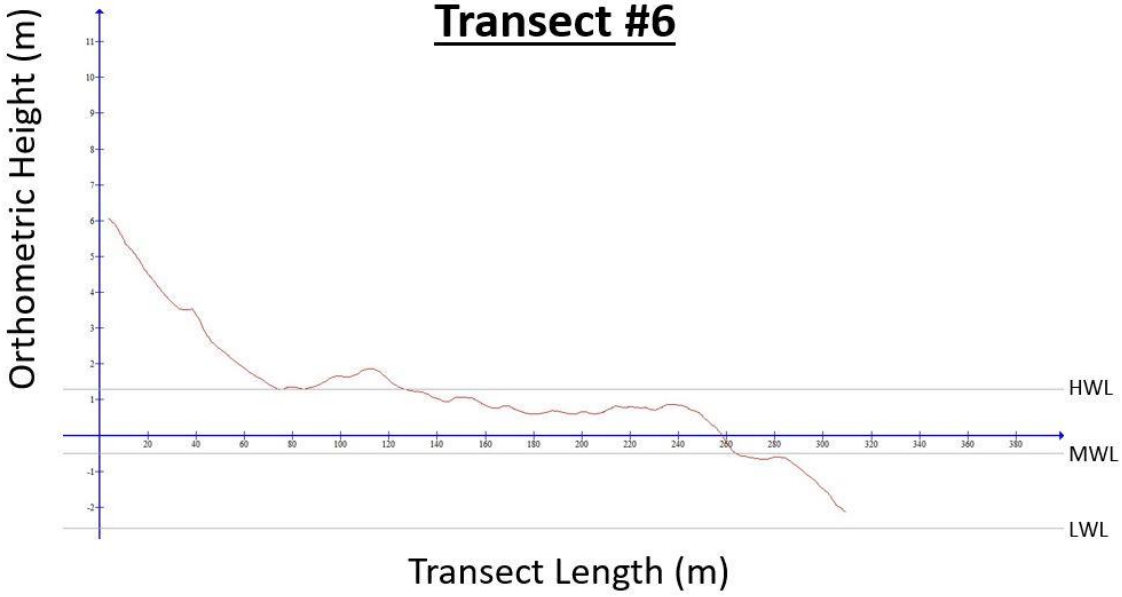
Transect #6
Orthometric Height (m)
HWL
MWL
LWL
Transect Length (m)

Transect #7

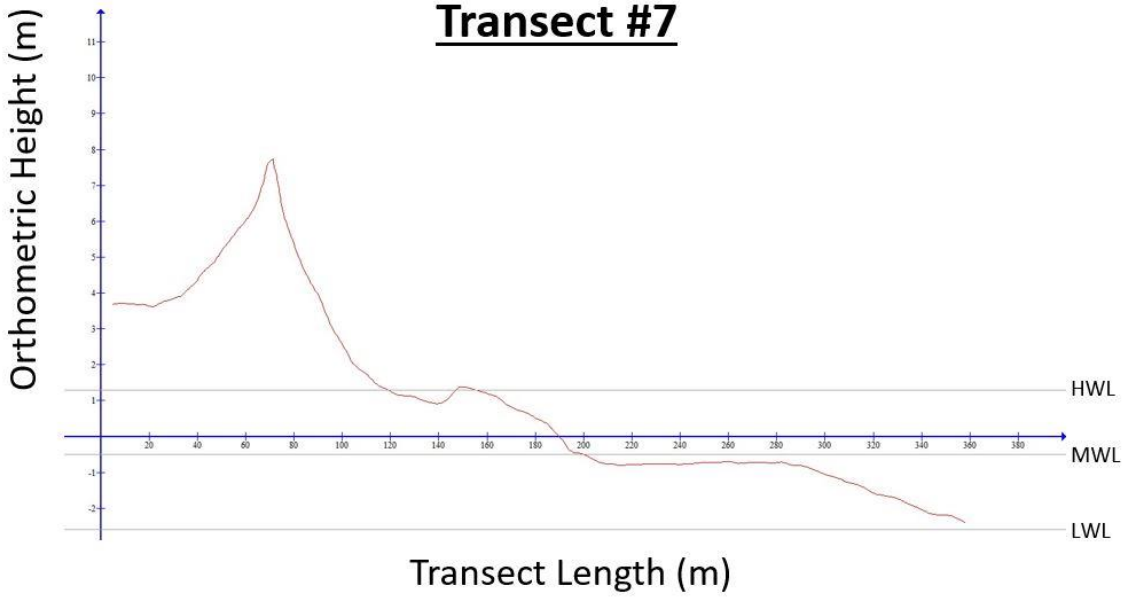

Transect #8

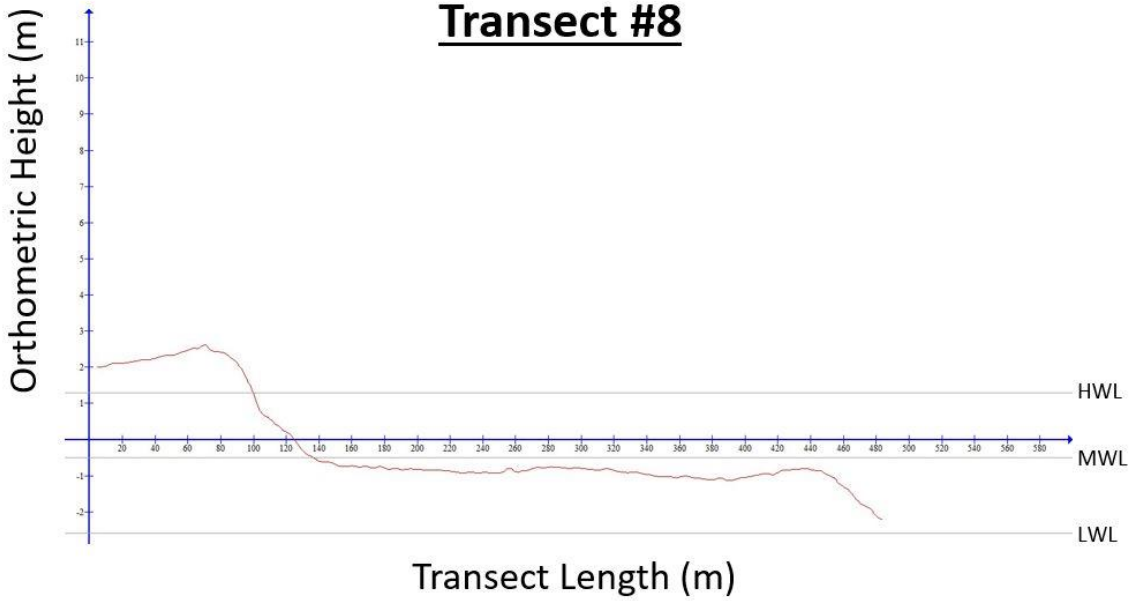

Transect #9

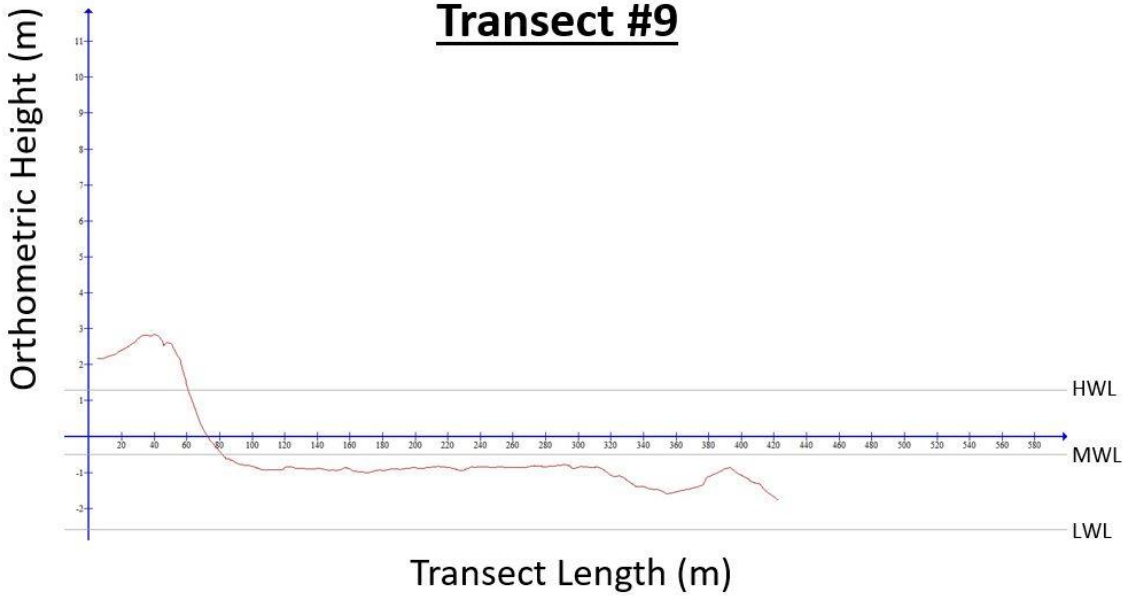

Transect #10

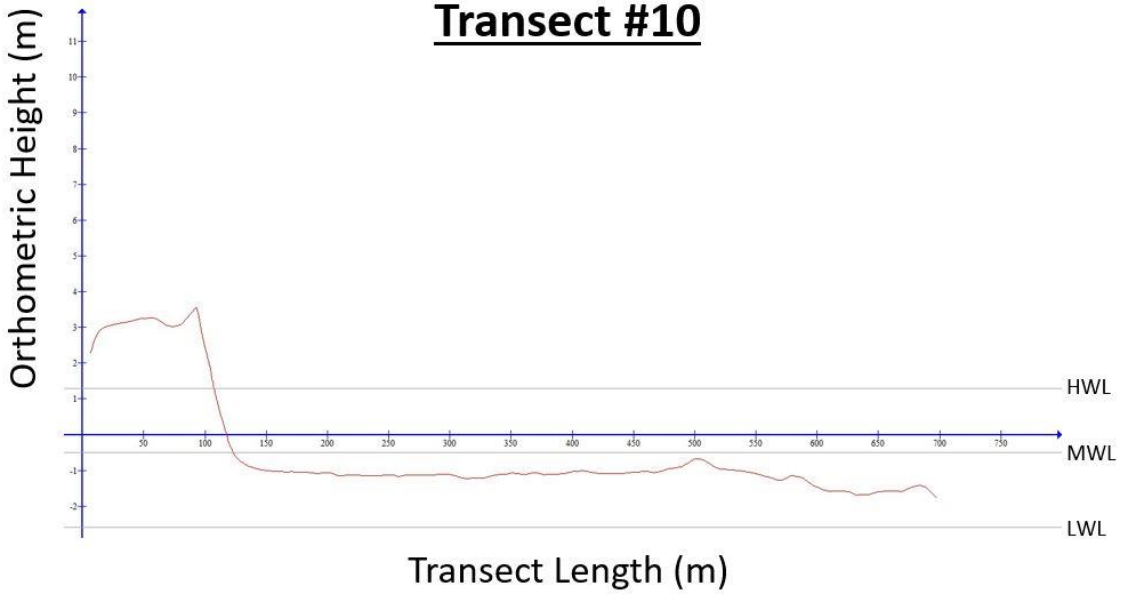

Transect #11

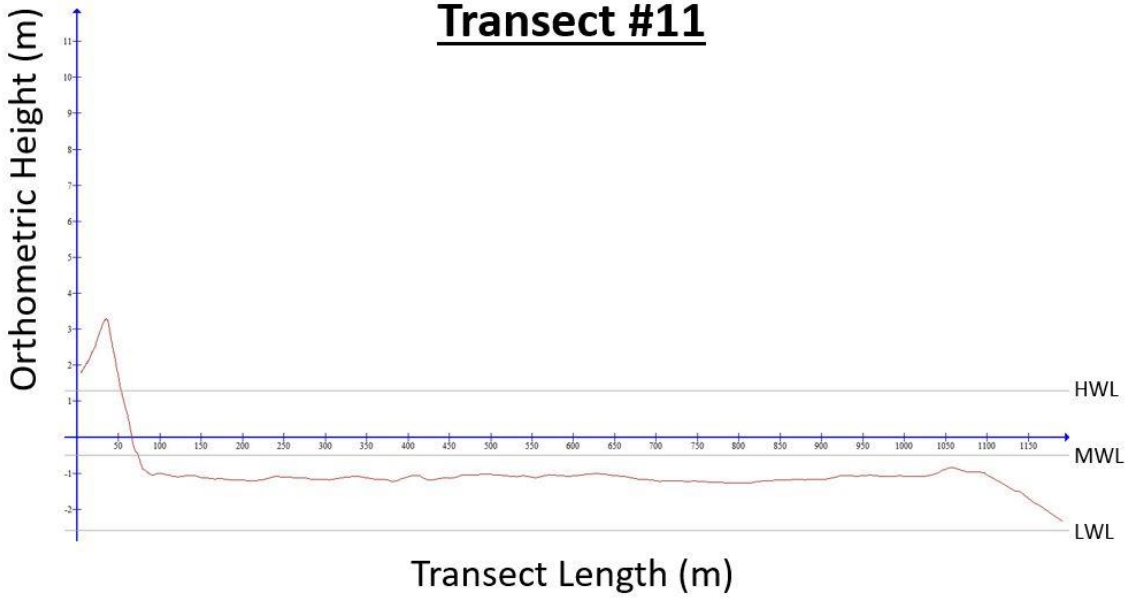

Transect #12

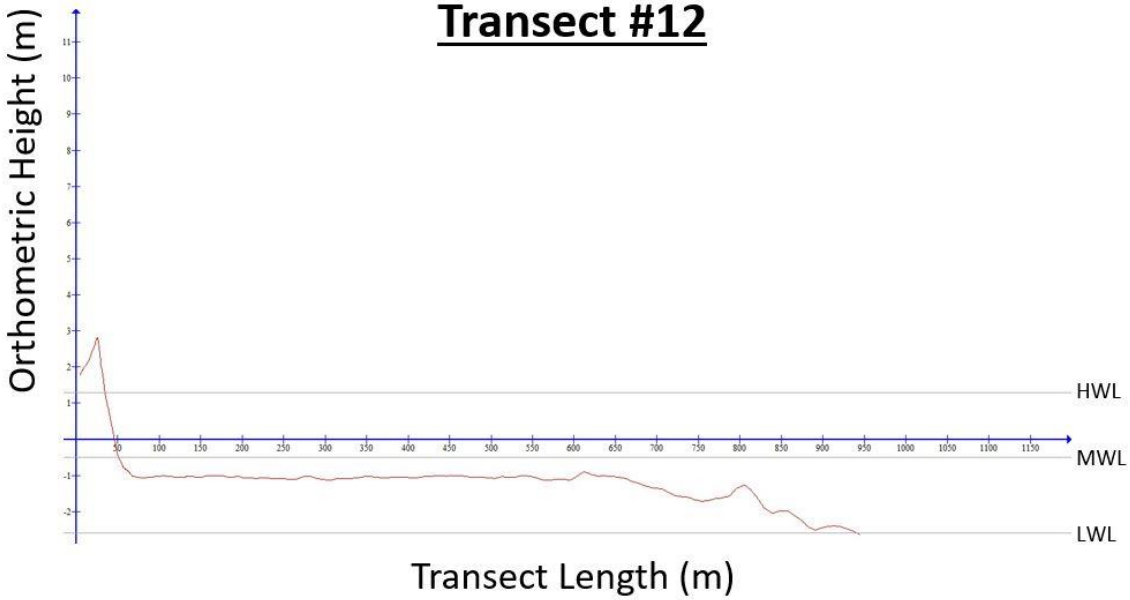

Transect #13

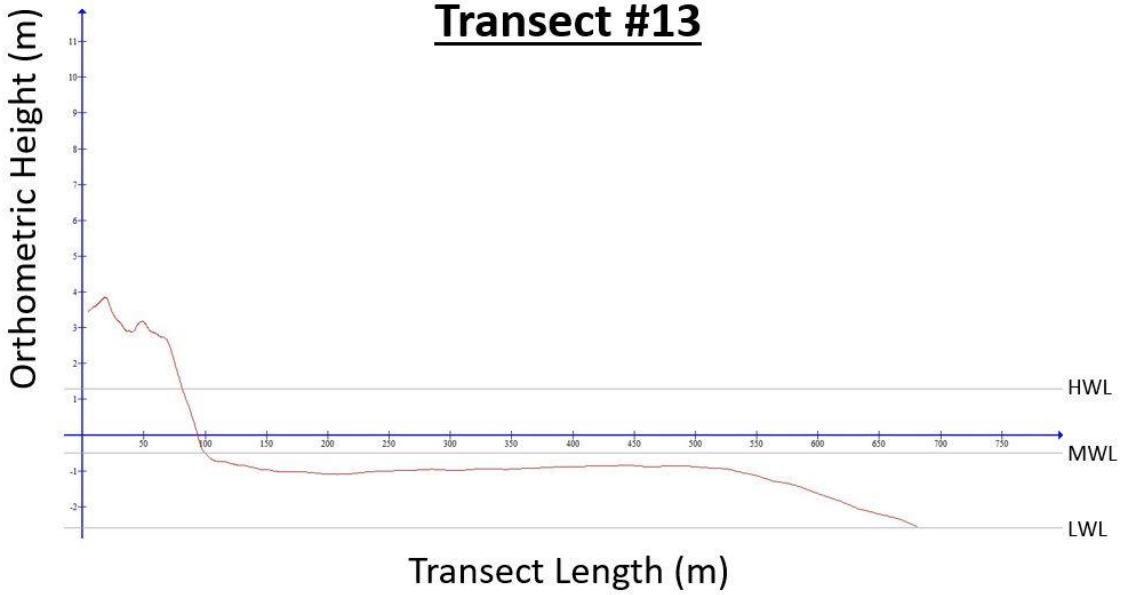

Transect #14

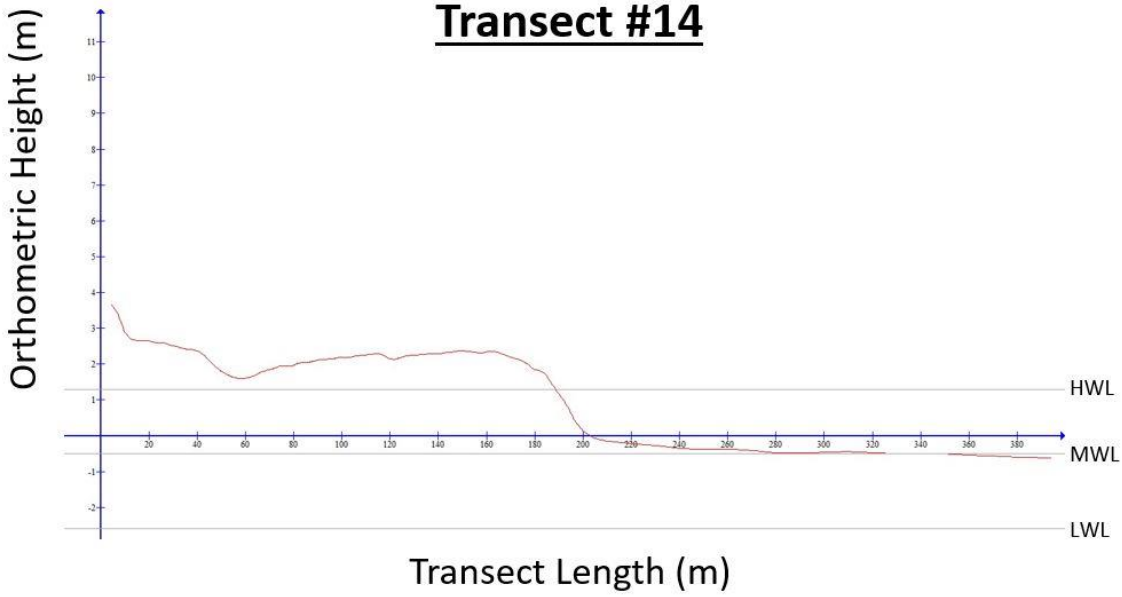

Transect #15

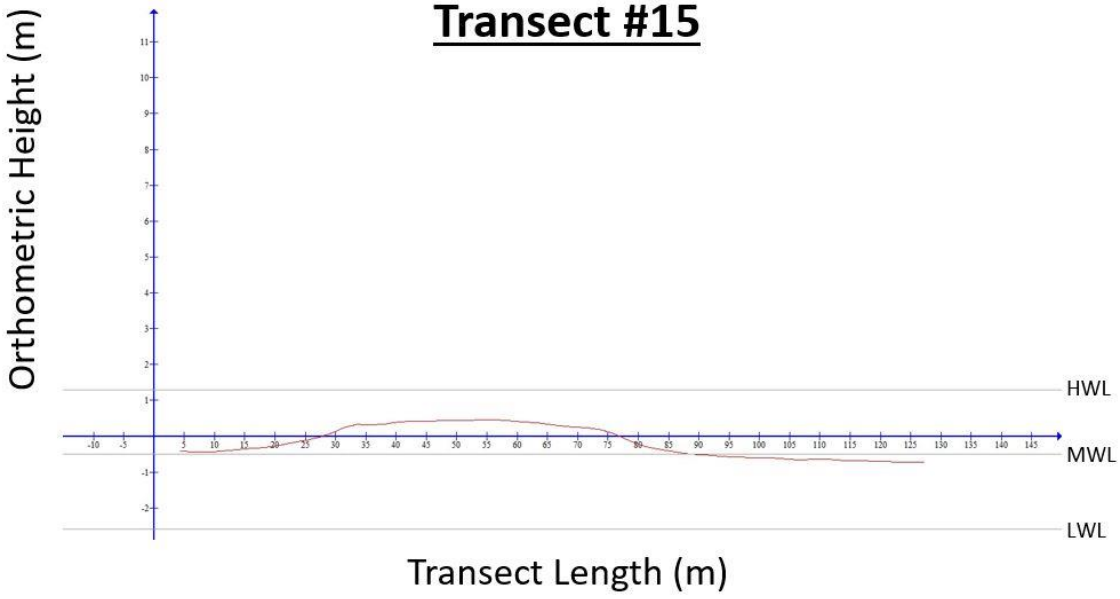

Transect #16

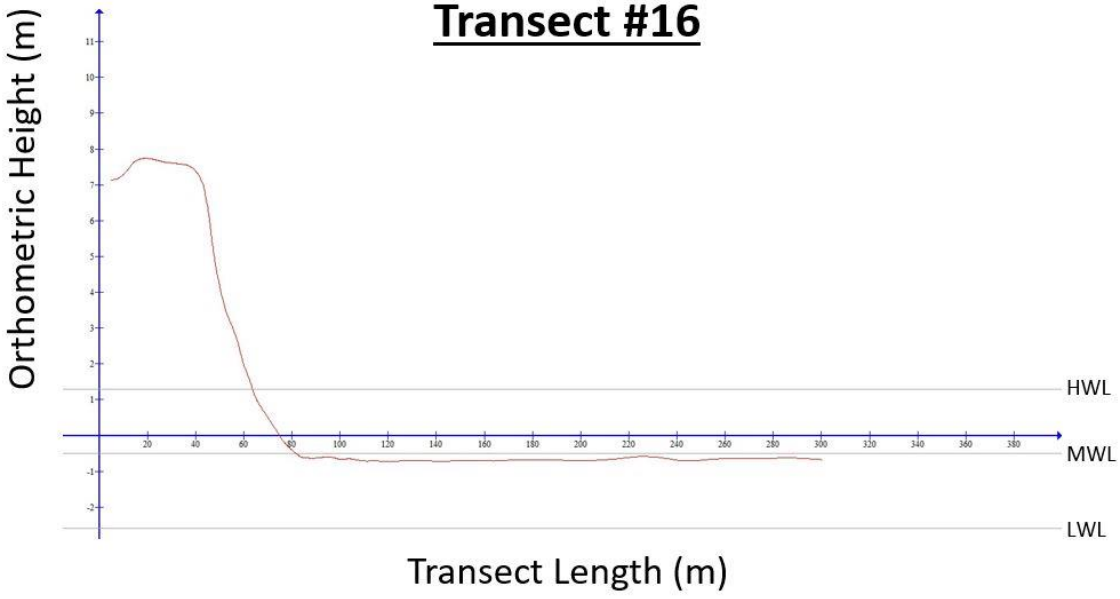

Transect #17

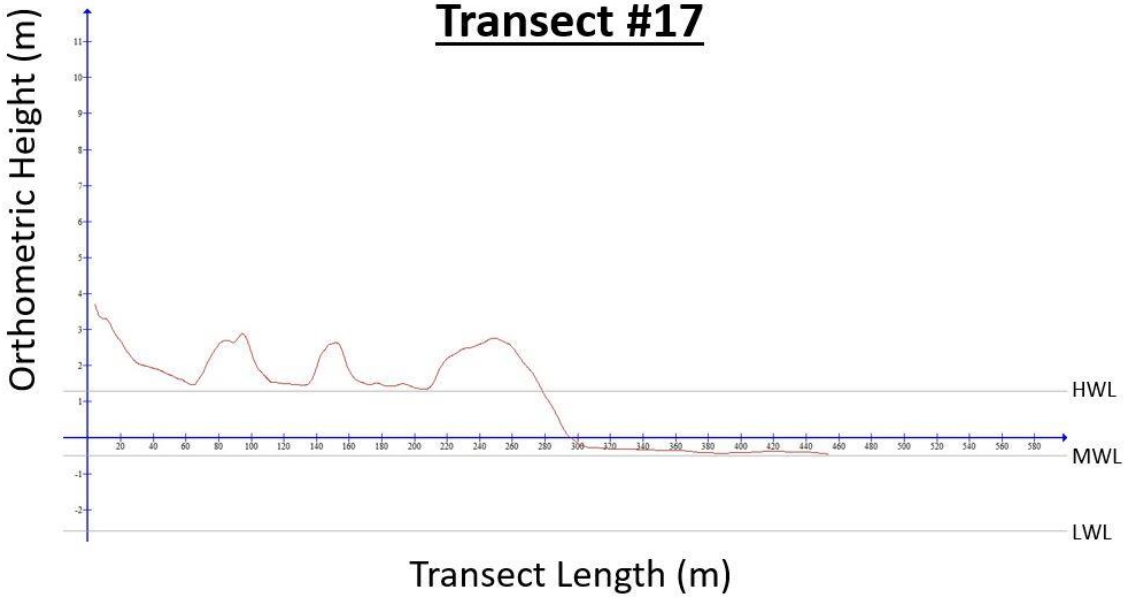

Transect #18

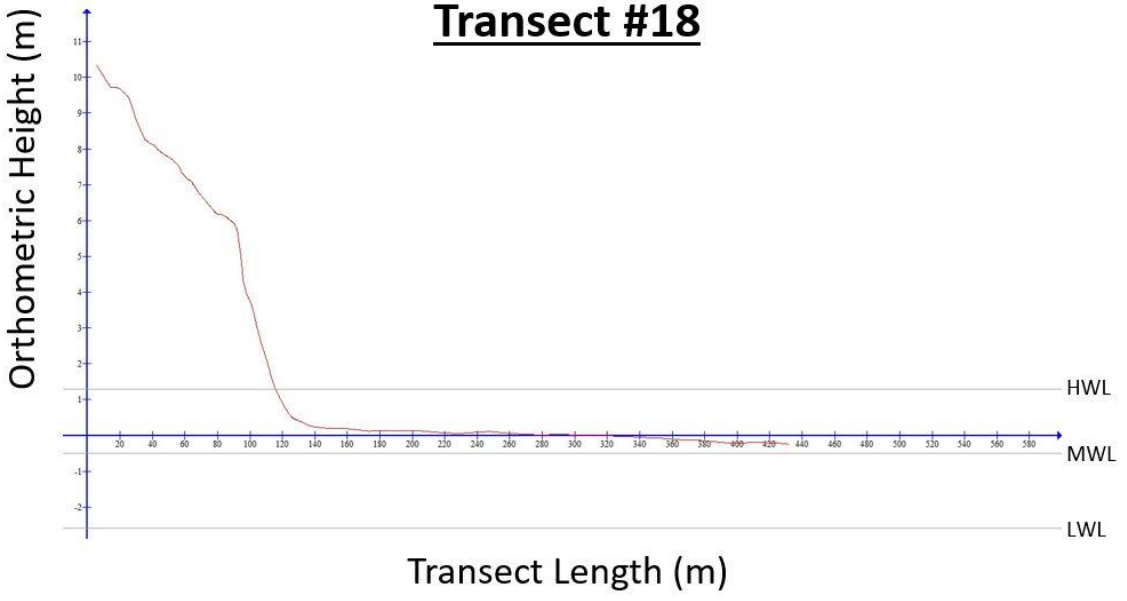

Transect #19

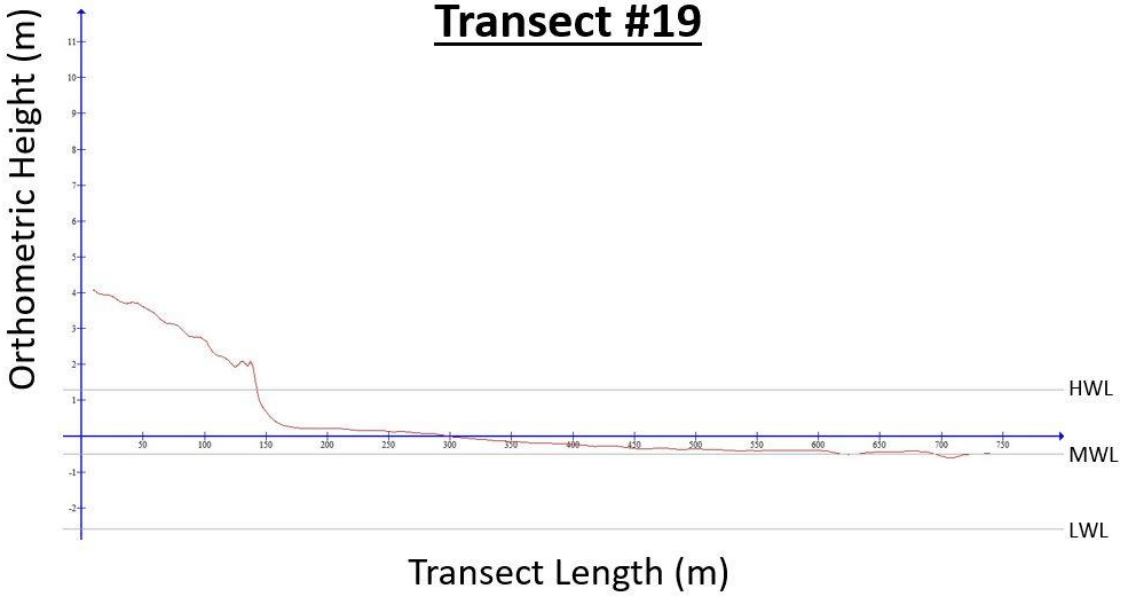

Table A.1: Backshore and foreshore values along shore normal coastal transects

Transect ID	Backshore slope angle	Total foreshore slope angle	Beach length (m)	Upper foreshore slope	Lower foreshore slope
01	1.1°	0.8°	n/a	0.5°	0.5°
02	15.8°	3.8°	30	3.7°	0.9°
03	9.3°	6.7°	20	2.6°	2.6°
04	6.2°	7.2°	20	4.1°	4.1°
05	2.3°	4.9°	n/a	n/a	n/a
06	6.7°	1.9°	n/a	n/a	n/a
07	13.4°	1.8°	50	2.3°	0° before slope break into ns
08	4.7°	0.9°	40	2.8°	0° before slope break into ns
09	8.8°	0.9°	25	4.6°	0° before slope break into ns
10	18.6°	0.5°	25	5.3°	Flat before slight lip and slow break into ns
11	12.7°	0.3°	15	6.0°	Flat before break into ns
12	16.8°	0.4°	25	5.3°	Flat before slope break into ns
13	4.2°	0.7°	25	5.1°	Flat before slope break into the ns
14	3.8°	0.9°	n/a	n/a	n/a
16	18.1°	0.6°	20	5.6°	n/a
17	5.2°	1.0°	n/a	n/a	n/a
18	8.0°	0.5°	15	3.5°	0.2°
19	2.0°	0.3°	n/a	2.8°	<0.1°

Table A.2: Comparing observed planform shoreline change to predicted changes along coastal transects

Transect ID	Predicted planform shoreline change (+41.85 cm water level; Simon et al., 2014)	Observed planform shoreline change (from DSAS)	Difference (observed change – predicted change)	Shoreline position change relative to expectation
01	+ 72.98 m	+ 36.44 m	- 36.54 m	Red'd advance
02	+ 3.26 m	+ 2.53 m	- 0.73 m	Red'd advance
03	+ 1.51 m	+ 3.31 m	+ 1.8 m	Acc'd advance
04	+ 4.48 m	+ 10.72 m	+ 6.24 m	Acc'd advance
05	+ 69.15 m	+ 76.97 m	+ 7.82 m	Acc'd advance
06	+ 62.19 m	+ 23.92 m	- 38.27 m	Red'd advance
07	+ 7.02 m	+ 15.54 m	+ 8.52 m	Acc'd advance
08	+ 8.62 m	+ 40.75 m	+ 32.13 m	Acc'd advance
09	+ 1.75 m	+ 15.76 m	+ 14.01 m	Acc'd advance
10	+ 2.35 m	- 18.33 m	- 20.68 m	Retreat
11	+ 3.48 m	- 27.43 m	- 30.91 m	Retreat
12	+ 0.90 m	- 51.35 m	- 52.25 m	Retreat
13	+ 3.12 m	+ 28.77 m	+ 25.65 m	Acc'd advance
14	+ 3.51 m	+ 134.95 m	+ 131.44 m	Acc'd advance
16	+ 2.98 m	- 0.66 m	- 3.64 m	Retreat
17	+ 5.39 m	+ 118.81 m	+ 113.42 m	Acc'd advance
18	+ 4.05 m	- 3.71 m	- 7.76 m	Retreat
19	+ 2.68 m	+ 41.14 m	+ 38.46 m	Acc'd advance